

June 17 2011

CBN 11-2

USAGE OF LIQUID METALS IN POSITRON PRODUCTION SYSTEM OF ILC

Alexander Mikhailichenko

Cornell University, CLASSE, Ithaca, NY 14853

Presented at **FRIB, Michigan State University, East Lansing,**
May 23, 2011

Abstract

The positron production system of ILC uses the hard undulator radiation ($\sim 20\text{MeV}$) carrying power up to 200 kW for irradiation of $\sim 0.5X_0$ -thick target. We describe the target made of liquid Bismuth-Lead alloy in comparison with the spinning W or Ti target. For the focusing of positrons we suggested a compact lens where the Liquid Lithium used as a conductor and a coolant. Liquid Lithium (or Bi/Pb) alloy used as a coolant of Graphite in a gamma beam absorber. Some crucial elements of the system such as pumps, windows, nozzles, and dynamics of liquid Lithium flow in a lens are described also. Highly efficient positron collection system with liquid Lithium lens allows relaxed parameters of the undulator and target.

PLAN

1. HOW TO OBTAIN POSITRONS

Conventional positron source.

Undulator-based polarized-positron source

Positron source for ILC

2. UNDULATOR

3. TARGET

W, Ti wheel target

Liquid Lead/Bismuth target

Cooling schemes

4. LITHIUM LENS

Design

Lithium flow

Pumps, etc

5. COLLIMATORS AND THE PHOTON DUMP

6. PRIMARY ACCELERATING STRUCTURE

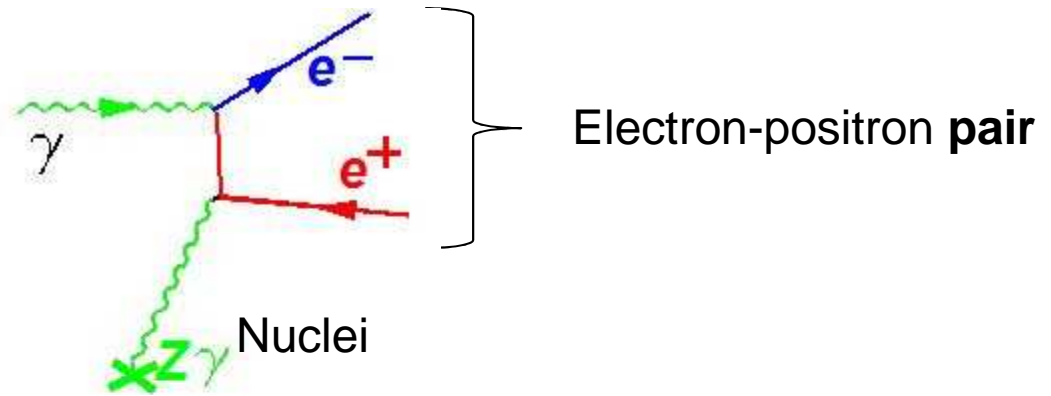
7. EXPERIMENT E-166 AT SLAC

8. PERSPECTIVES

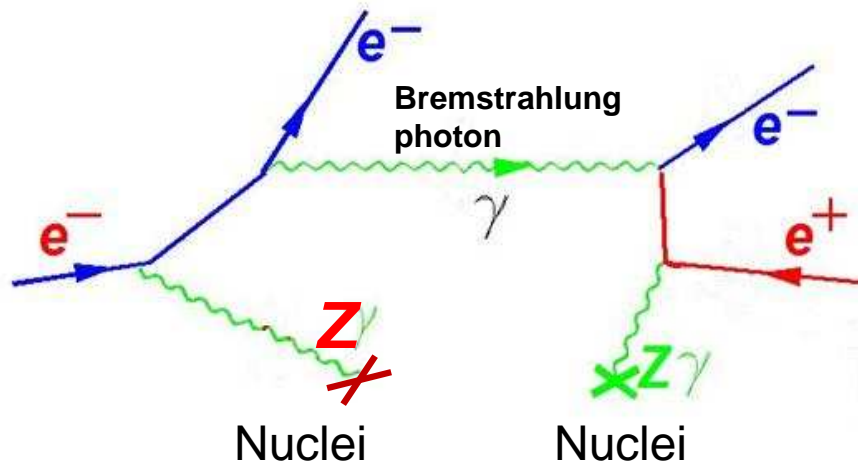
9. SUMMARY

1. HOW TO OBTAIN POSITRONS

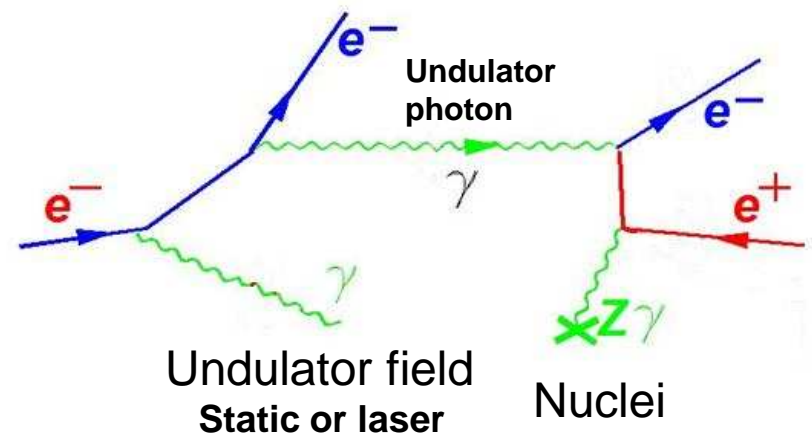
The only way to create a positron



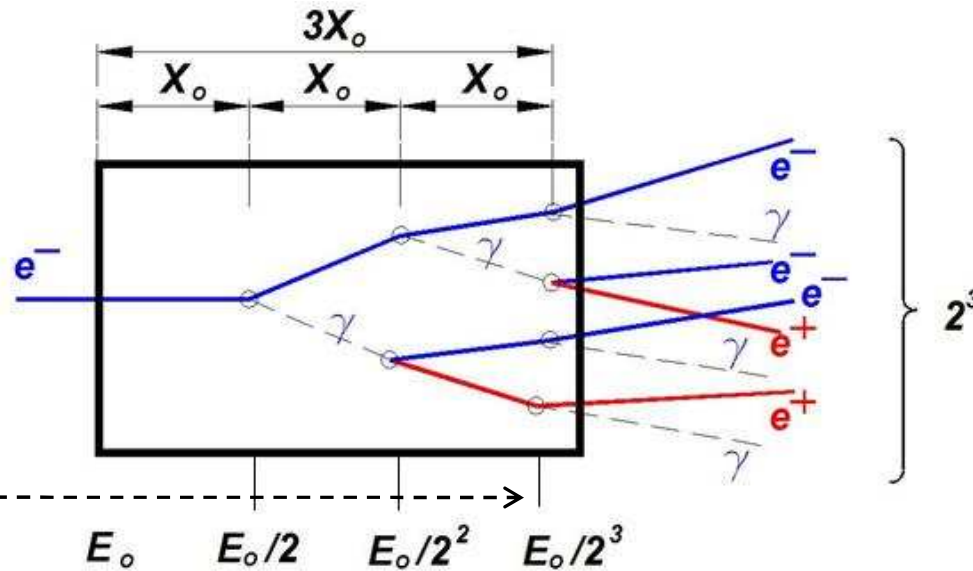
Conventional source



Undulator source



CONVENTIONAL POSITRON SOURCE-CASCADE PROCESS



With the source of gammas Process could be started here

t -thickness in X_0 units

$$X_0^{-1} \cong 4r_0^2 \alpha \frac{N_0}{A} Z(Z+1) \ln\left(\frac{183}{Z^{1/3}}\right) [cm^2 / gram] \quad \leftarrow \text{Radiation length}$$

Number of positrons $\sim N_{pos} \cong N_\gamma \cong N_e \cong N_{tot} / 3 = 2^t / 3$

The shower propagates until the energy of particles reaches $E_{crit} \cong 610 / (Z + 1.24)$

So the shower reaches its maximum at the depth $t_{max} \cong \ln(E_0 / E_{crit}) / \ln 2$

with the number of the particles there about $N_{max} \cong E_0 / E_{crit}$

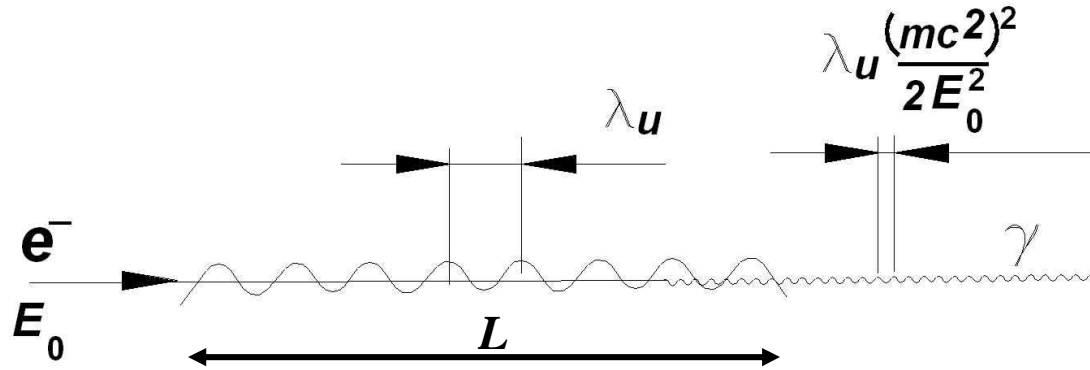
Transverse size of the cascade in maximum is of the order of Molière radius, $R_M \cong X_0 E_s / E_{crit}$

$E_s = \sqrt{4\pi / \alpha} \cdot mc^2 \cong 21.2 MeV$ – is a scale energy.

Effective thickness of target is $l \cong \frac{\langle xx' \rangle}{\langle x'^2 \rangle} \sim 1mm \text{ only}$

GAMMA SOURCE WITH UNDULATOR OR LASER

Undulator corresponds to 90° illumination of energetic electron by laser



$$N_\gamma \cong L \sigma_\gamma n_\gamma \quad \sigma_\gamma \cong (8\pi/3) r_0^2 \quad n_\gamma \cong \frac{H^2}{8\pi \hbar c / \lambda_u} \quad \begin{array}{l} \text{Photon density} \\ H \text{ is magnetic} \\ \text{field value} \end{array}$$

The number of quanta radiated by each electron

$$N_\gamma \cong L r_0^2 \frac{H^2}{\hbar c / \lambda_u} \propto 4\pi\alpha \frac{L}{\lambda_u} K^2 \sim 8.7 \times 10^2 K^2 \sim 150 \quad \text{for } K \sim 0.4$$

$$K = eH\lambda_u / 2\pi mc^2 \cong 0.934 \cdot H[T] \cdot \lambda_u[cm] \quad \text{Deflection parameter}$$

Energy of quanta, n – harmonic number

$$E_{\gamma n} \cong \frac{n \cdot 2.48 \cdot (\gamma / 10^5)^2}{\lambda_u [cm] (1 + K^2 + \gamma^2 \vartheta^2)} [MeV]$$

Angle to observer

That is why undulator installed at ~150 GeV line, where $E_{\gamma max} \sim 20$ MeV

For the reference:

Total energy carried out by these photons~

$$E = N_{\gamma} E_{\gamma} \cong 150 \times 20 \text{ MeV}$$

By all 2×10^{10} particles in a 2800 bunches in 5 Hz ($K=0.4$)

$$E_{tot} = 150 \times 20 \times 10^6 \times 2 \times 10^{10} \times 1.6 \times 10^{-19} \times 5 \times 2800 = 3 \times 2.8 \times 1.6 \times 5 \times 2800 = 135 \text{ kJ/sec}$$

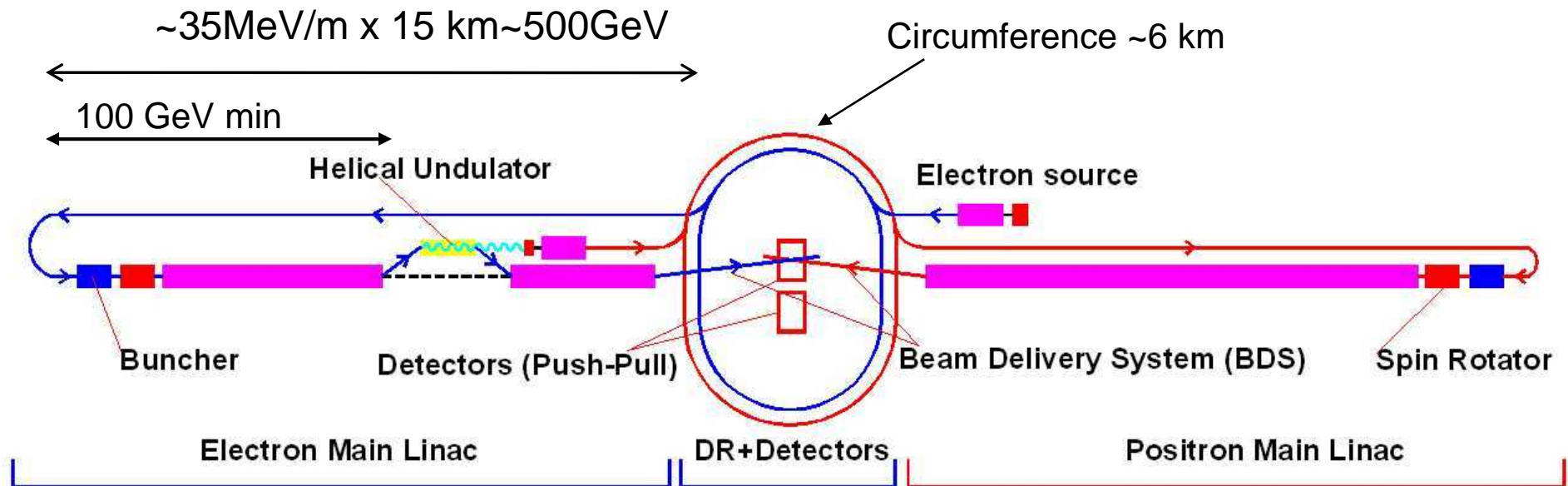
Only ~12% of photons interact with the target.

One can use the second target and combine the positrons in a damping ring.

Rest amount should be dumped.

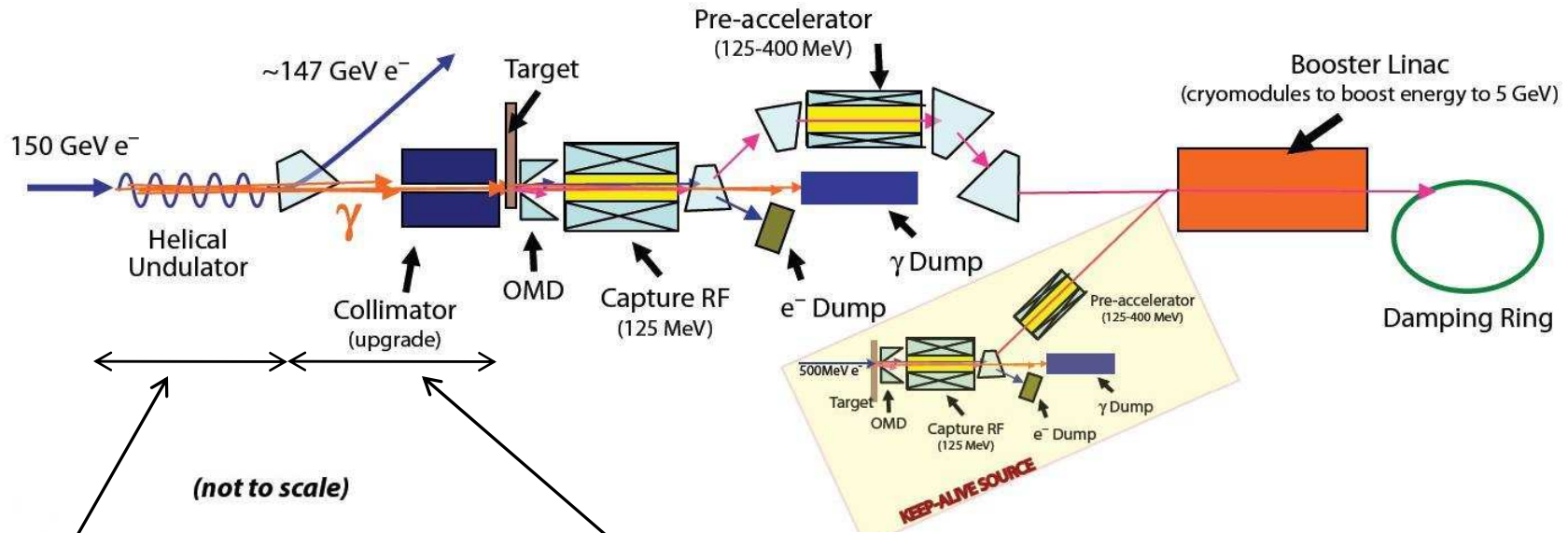
POSITRON SOURCE FOR ILC

The undulator scheme of positron production has been chosen as a baseline for ILC accommodated from TESLA design, originated for VLEPP (Novosibirsk, 1979)



Main advantage of this scheme is that it allows **POLARIZED** (>60%) positron production
In principle, the positrons could be generated by positrons, so the linacs become independent

Conversion system of ILC as it appears in ILC Reference Design Report, ILC-REPORT-2007-001, Vol.3, p.III-41

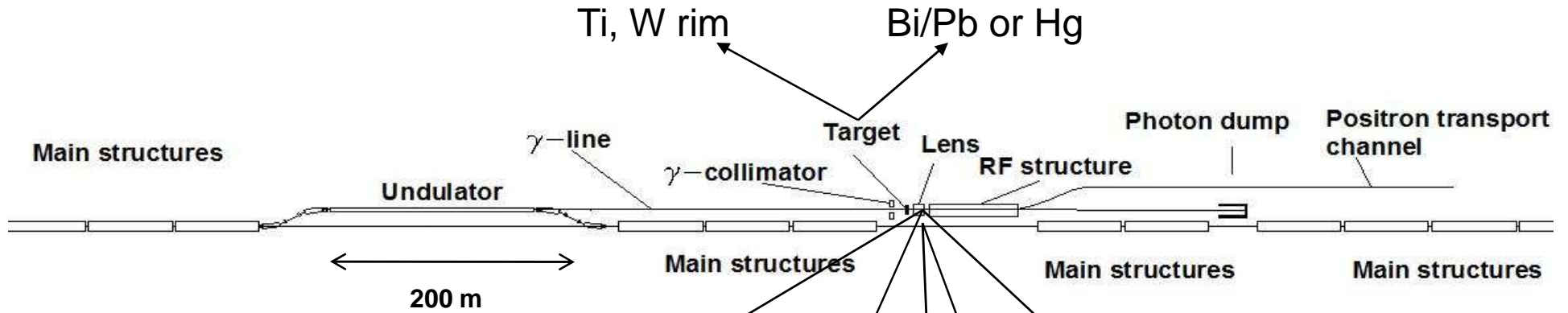


Helical undulator is ~150 m long.

The distance between the end of undulator and the target is ~150-300 m

OMD stands for Optical Matching Device

MORE DETAILED VIEW ON THE UNDULATOR POSITRON SOURCE



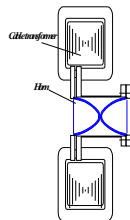
Adiabatic matching device

Original suggestion;
Target immersed in strong field;

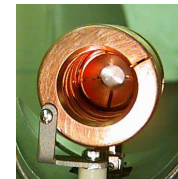
Identified the problems with induced fields in moving Ti metal

Flux concentrator

Under development at
Livermore

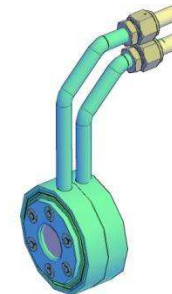


Combined Flux Concentrator and solenoid



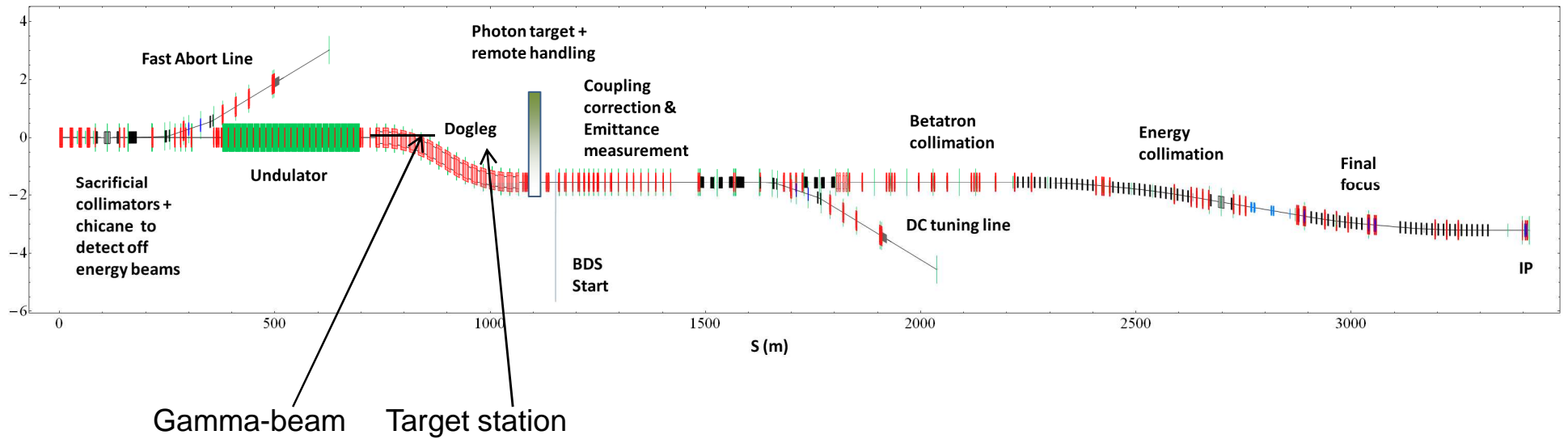
X lens-miniature horn;
 $\text{Ø}=2\text{cm}$, length $\sim 2\text{cm}$

Lithium lens



ONE AMONG LATEST LAYOUTS

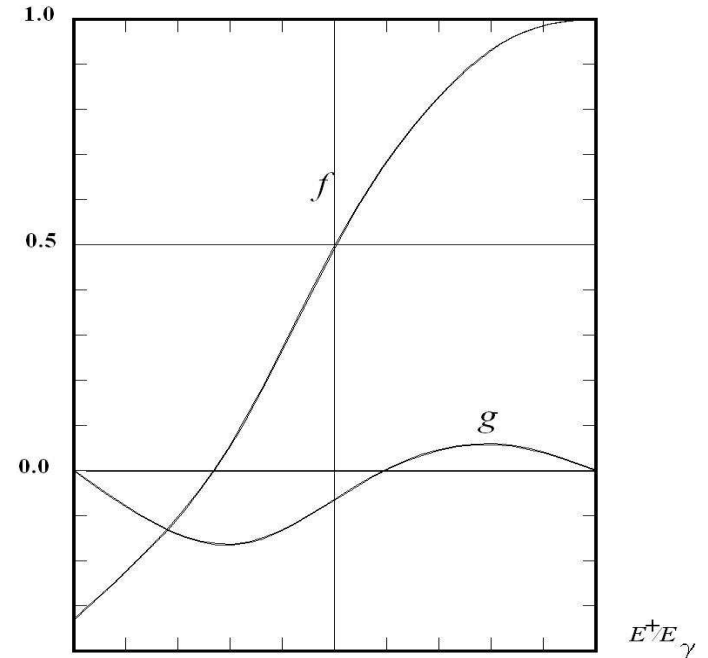
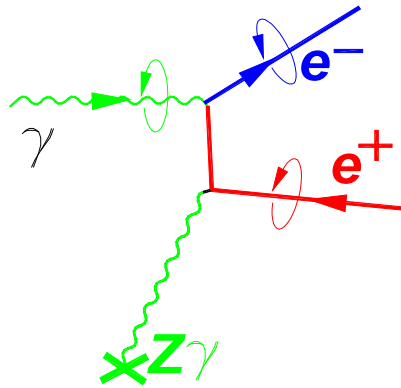
Undulator located at the end of the linac



PRODUCTION OF *POLARIZED* POSITRONS

H.Olsen, L.Maximon, 1959

+cross diagram



f, g as functions of particle's fractional energy $E^+/(E_\gamma - 2mc^2)$

$$\vec{\zeta} = \vec{\xi}_2 \cdot \left[f(E_+, E_-) \cdot \vec{n}_\parallel + g(E_+, E_-) \cdot \vec{n}_\perp \right] = \vec{\zeta}_\parallel + \vec{\zeta}_\perp$$

Photon polarization

Positron polarization

Polarization is a result of selection of positrons by their energy

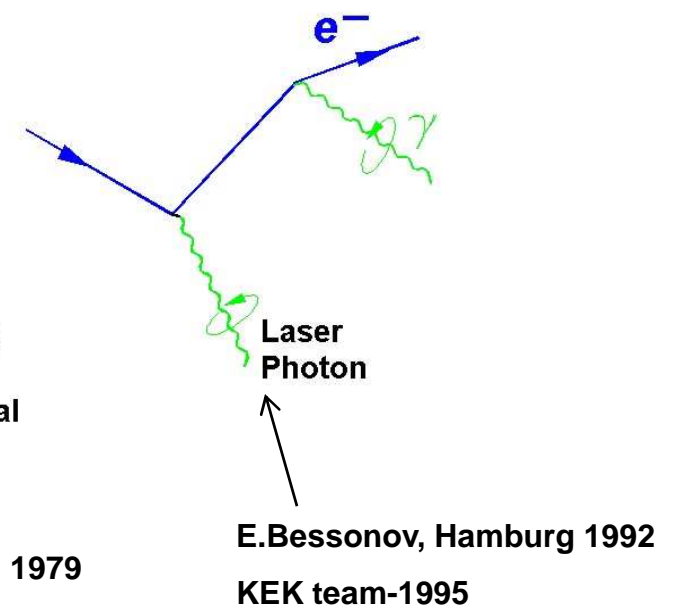
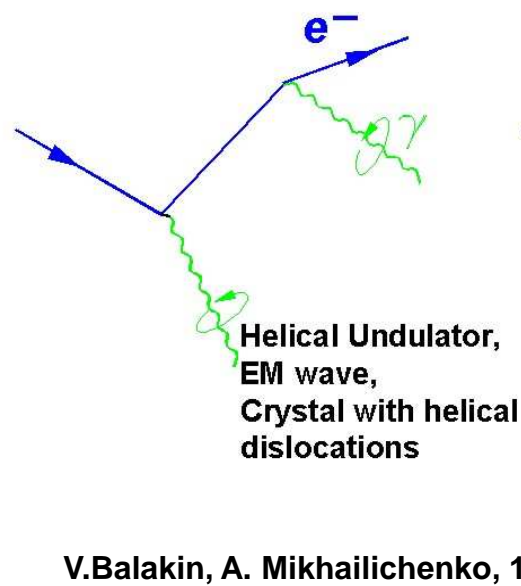
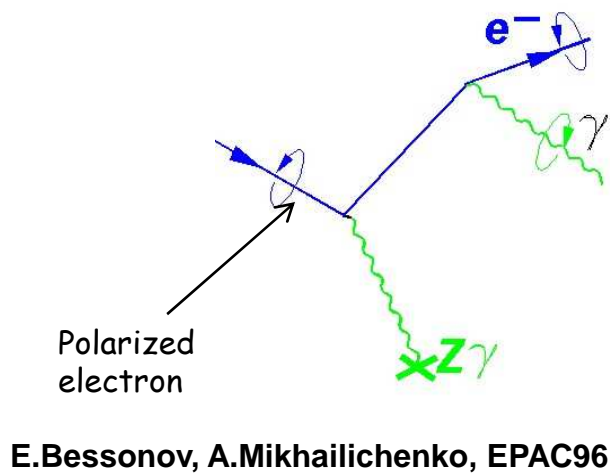
Fragment from publication of Balakin-Mikhailichenko, Budker INP 79-85, Sept. 13, 1979.

Circularly polarized photons are produced in helical fields of minimal period. Much more interesting is to obtain such fields with the help of the usual helical static fields and the electromagnetic waves. It may well be that the method of gamma production in helical crystals can be useful in future.

Scattering on the Laser radiation is the same process as the scattering on the electromagnetic wave.

PRODUCTION OF CIRCULARLY POLARIZED PHOTONS

Well known processes reviewed for practical utilization in a positron source



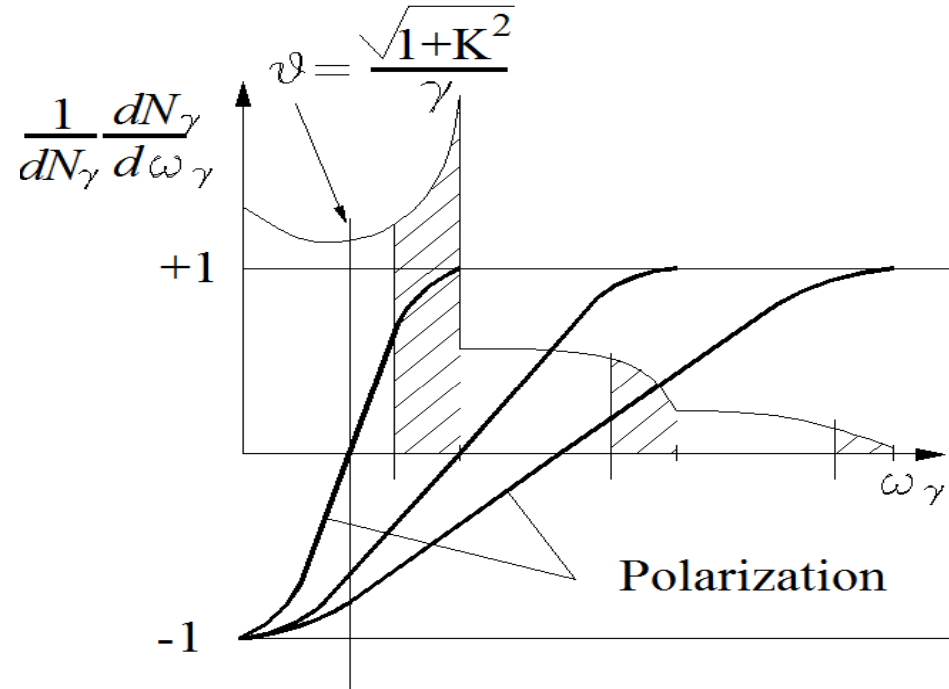
UNDULATOR SHOULD BE HELICAL

Spectral distribution and polarization schematics for Undulator Radiation

All higher harmonics have zero intensity in straight forward direction

Angle of radiation and the energy of the photon are not independent

Polarization curve needs to be convolved with the photon density

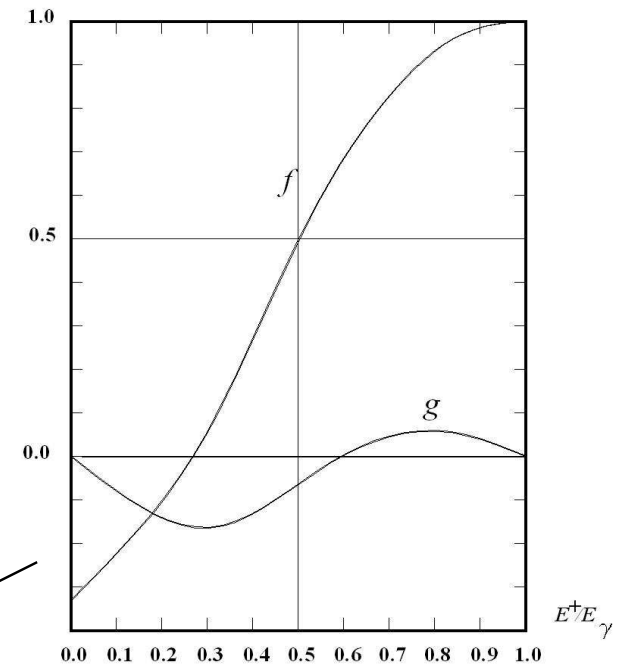
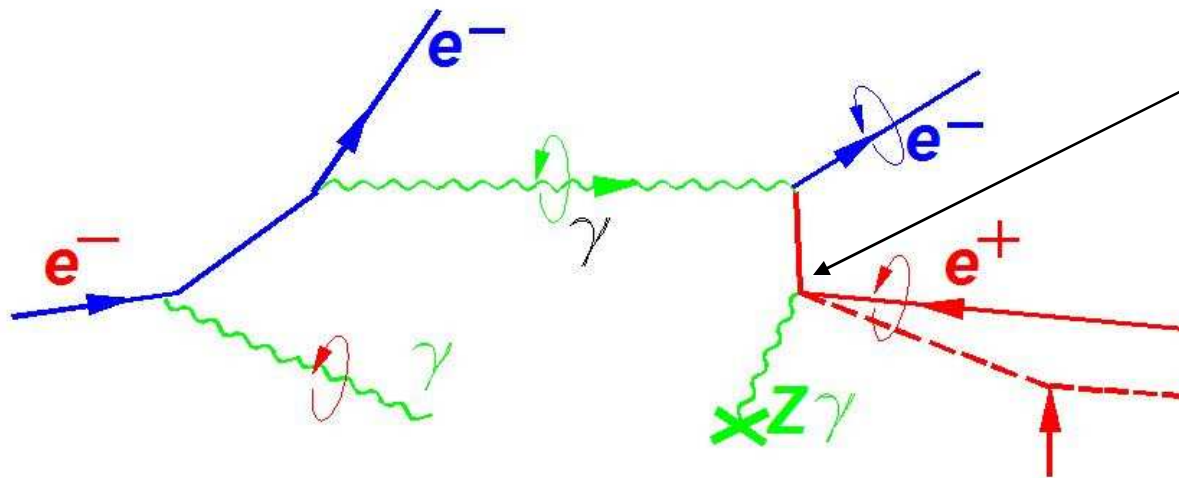


Hatched areas correspond to the passage of radiation through the collimator

Collimator helps to enhance integrated photon polarization

Start to end simulation Code KONN

Initiated in 1986; continued in 2007- 2011



Undulator

Target

Lens

Monte-Carlo

PROGRAM KONN

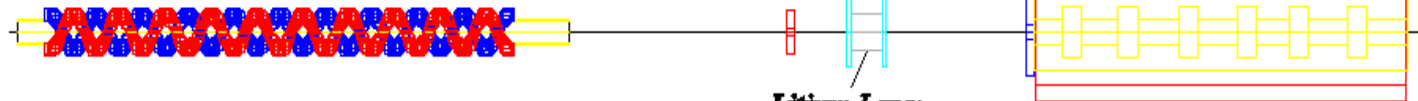
T.A.Vsevolozhskaya, A.A.Mikhailichenko

Monte-Carlo simulation of positron conversion

Energy of the beam;
Length of undulator;
Undulator period $M=L/\lambda_u$;
K-factor;
Emittance;
Beta-function;
Number of harmonics (four);
Number of positrons to be generated;

Target:
Distance to the undulator
Thickness;
Diameter of target;
Material;
Diameter of hole at center;
Step of calculation

Acceleration:
Distance to the lens;
Length of structure;
Gradient;
Diameter of collimator at the entrance;
Diameter of irises;
External solenoidal field;
Further phase volume captured;



CALCULATES at every stage:
Efficiency in given phase volume;
Polarization in given phase volume;
Beam dimensions;
Phase-space distributions;
Beam lengthening;
Energy spread within phase space;

Lithium Lens:
Distance to the target;
Length;
Diameter;
Thickness of flanges;
Material of flanges;
Gradient;
Step of calculations;

Interactive code, now is ~3000 lines

Resulting efficiency and polarization calculated with KONN

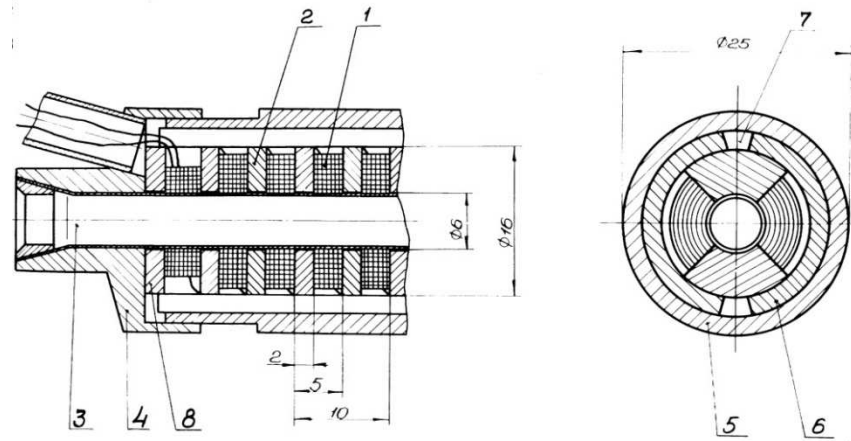
*radius of target is an equivalent of the radius of collimator

Beam energy, GeV	150	250	350	500
Length of undulator, m	170	200	200	200
K factor	0.44	0.44	0.35	0.28
Period of undulator, cm	1.0	1.0	1.0	1.0
Distance to the target, m	150	150	150	>150
Radius of target*, cm	0.049	0.03	0.02	0.02
Emittance, $cm\cdot rad$	1e-9	1e-9	1e-9	1e-9
Bunch length, cm	0.05	0.05	0.05	0.05
Beta-function, m	400	400	400	400
Thickness of target $/X_0$	0.57	0.6	0.65	0.65
Distance to the length, cm	0.5	0.5	0.5	0.5
Radius of the lens, cm	0.7	0.7	0.7	0.7
Length of the lens, cm	0.5	0.5	0.5	0.5
Gradient, MG/cm	0.065	0.065	0.08	0.1
Wavelength of RF, cm	23.06	23.06	23.06	23.06
Phase shift of crest, rad	-0.29	-0.29	-0.29	-0.29
Distance to RF str., cm	2.0	2.0	2.0	2.0
Radius of RF collimator, cm	2.0	2.0	2.0	2.0
Length of RF str., cm	500	500	500	500
Gradient, MeV/cm	0.1	0.1	0.1	0.1
Longitudinal field, MG	0.015	0.015	0.015	0.015
Inner rad. of irises, cm	3.0	3.0	3.0	3.0
Acceptance, $MeV\cdot cm$	5.0	5.0	5.0	5.0
Energy filter, $E > -MeV$	54	74	92	114
Energy filter, $E < -MeV$	110	222	222	222
Efficiency, e^+/e^-	1.5	1.8	1.5	1.5
Polarization, %	70	80	75	70

2. UNDULATOR

Historical remark: First SC undulator with period 10 mm was tested in 1986;

T.A.Vsevolozhskaya et al., " Helical Undulator for the Conversion System of the VLEPP Project", SLAC-TRANS-0225, 13th Int. Conf. on High-Energy Acc., Novosibirsk, 7-11 Aug, 1986.



1-windings, 2-iron yoke, 3-StSteel thin-wall tube, 4-end cup, 5-helium vessel, 6-Iron yoke, 7-groove for Helium.



Length of undulator $\sim 30\text{cm}$, $K_{max} \sim 0.4$ (required $K=0.35$), period 10mm

Undulator designed at Cornell

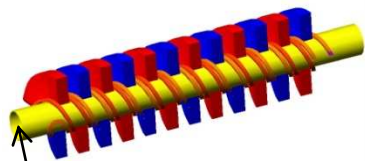


12 –mm period undulator core. Aperture available for the beam is 8 mm clear. Measured $K \sim 0.83$ (Iron yoke removed)

Helical undulator is a device for generation magnetic field of a type

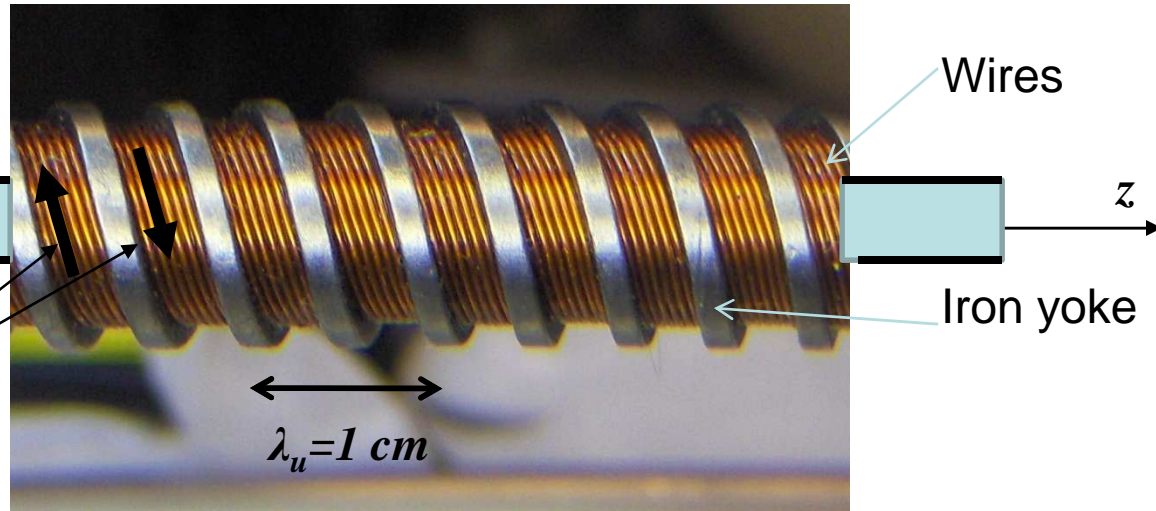
$$\vec{H}_\perp(z) = \vec{e}_x H_{xm} \cos \frac{2\pi z}{\lambda_u} + \vec{e}_y H_{ym} \sin \frac{2\pi z}{\lambda_u}$$

Radius of particle's helix $a \cong eH_\perp \lambda_u^2 / mc^2 \gamma$



Vacuum tube inside

Direction of currents



UNDULATOR DESIGN (CORNELL)

Diameter of cryostat ~10 cm (4")
Length ~4m

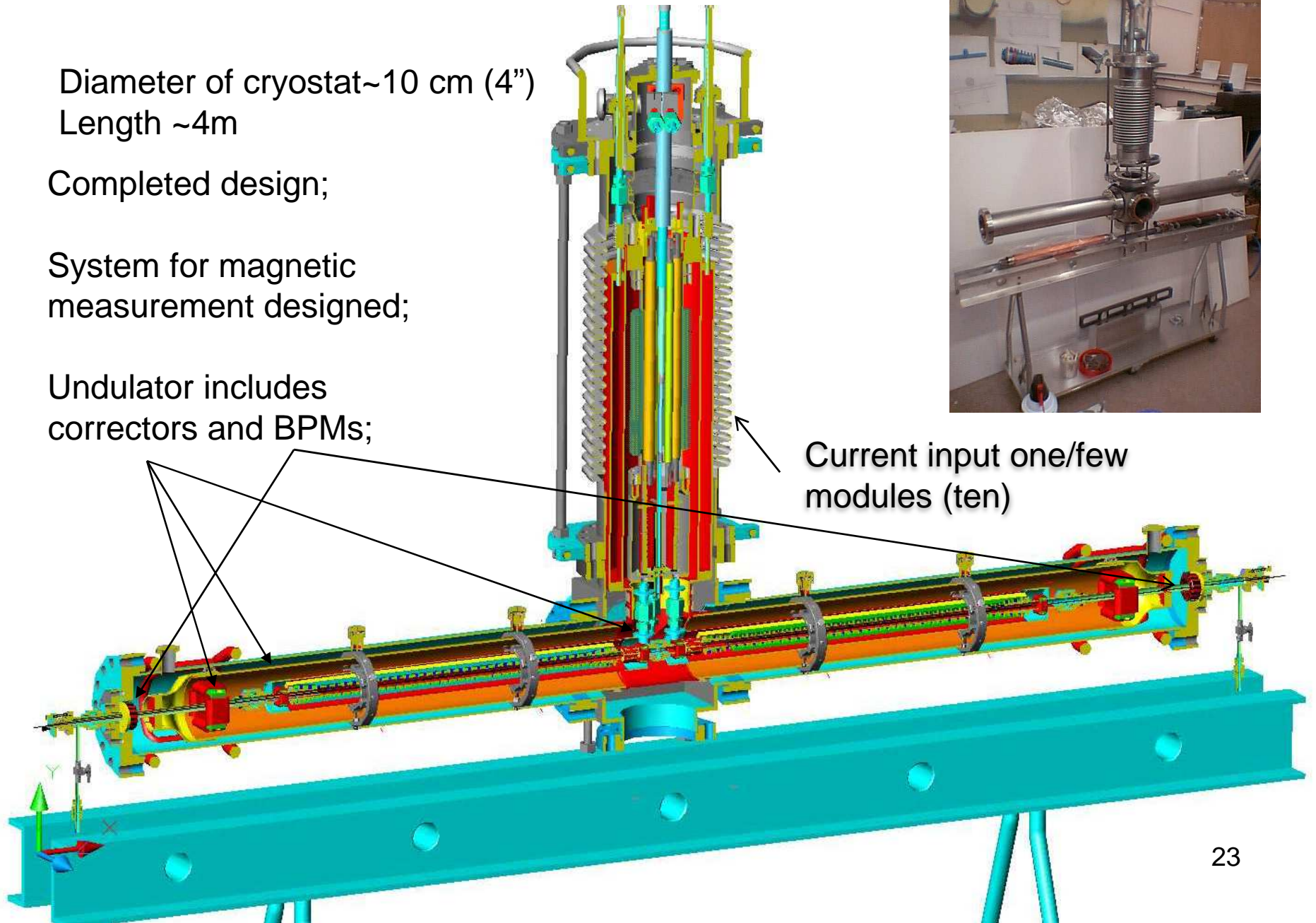
Completed design;

System for magnetic measurement designed;

Undulator includes correctors and BPMs;



Current input one/few modules (ten)



UNDULATOR DESIGN (UK)



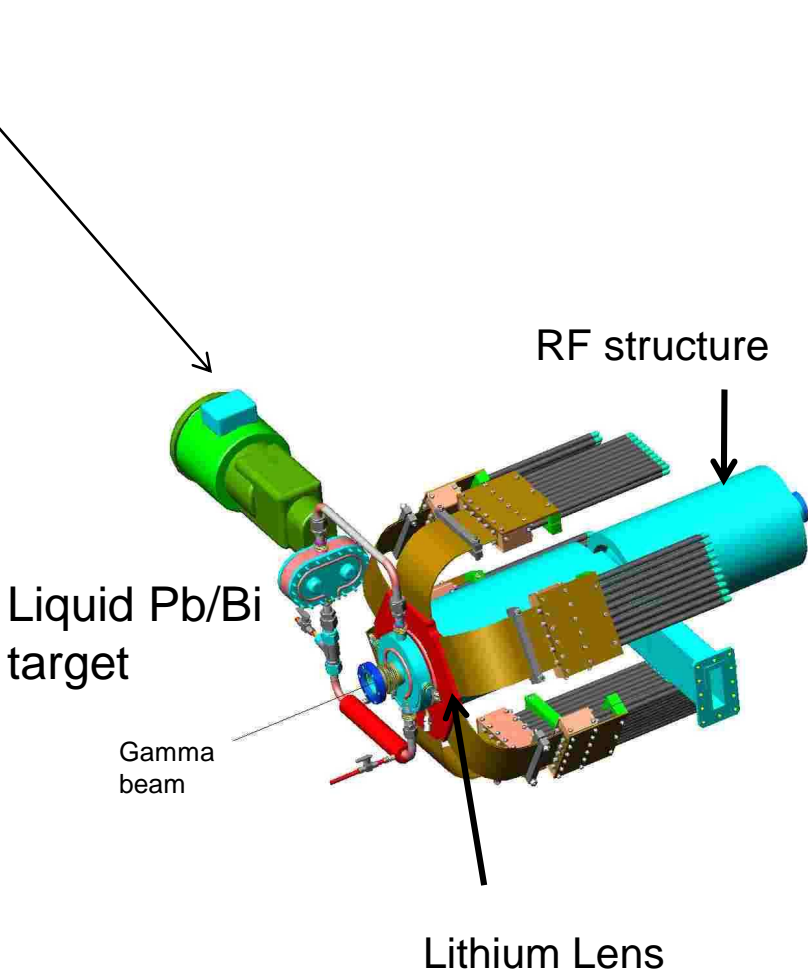
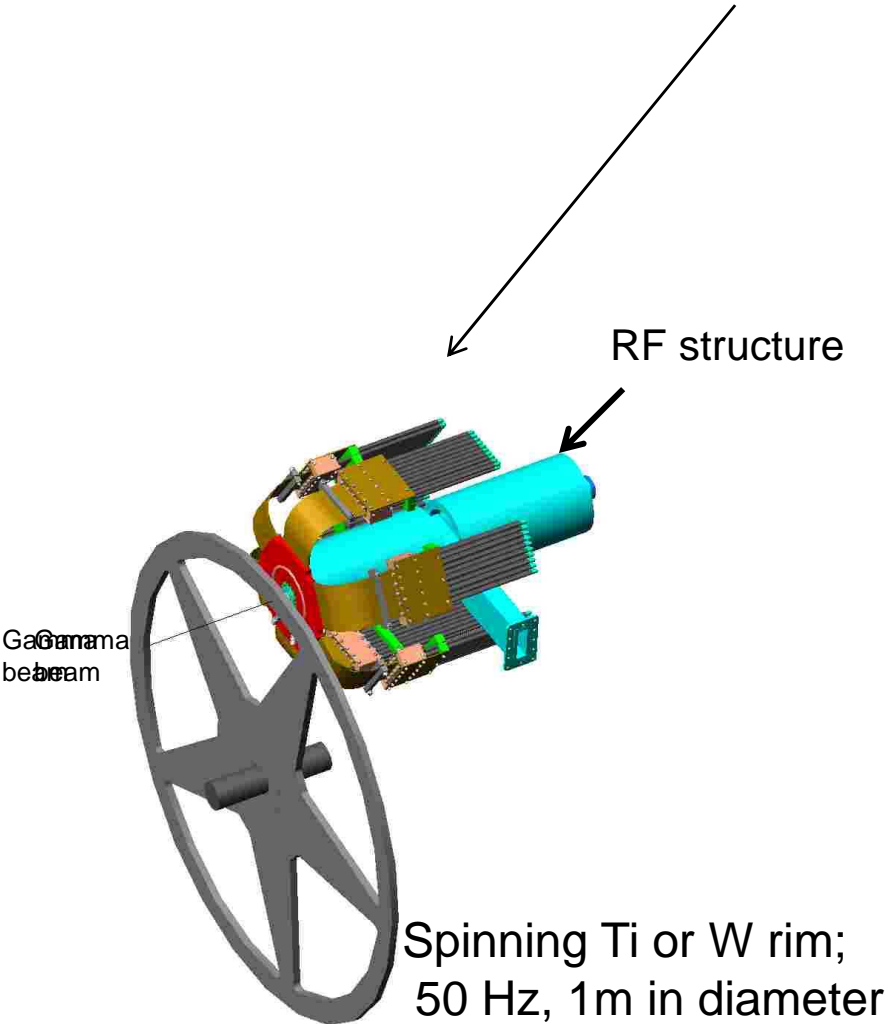
Undulator period	11.5 mm
Field on axis	0.86 T
Peak field homogeneity	<1%
Winding bore	>6 mm
Undulator length	147m; 4 m-long sections
Nominal current	215 A
Winding concentricity	20 μm
Winding tolerances	100 μm
Straightness	100 μm
NbTi wire Cu:SC ratio	0.9
Winding block	9 layers x 7 wire ribbon

Ian Bailey, presentation
at LCWS10 and ILC 10,
Beijing, March 29, 2010

3. TARGET

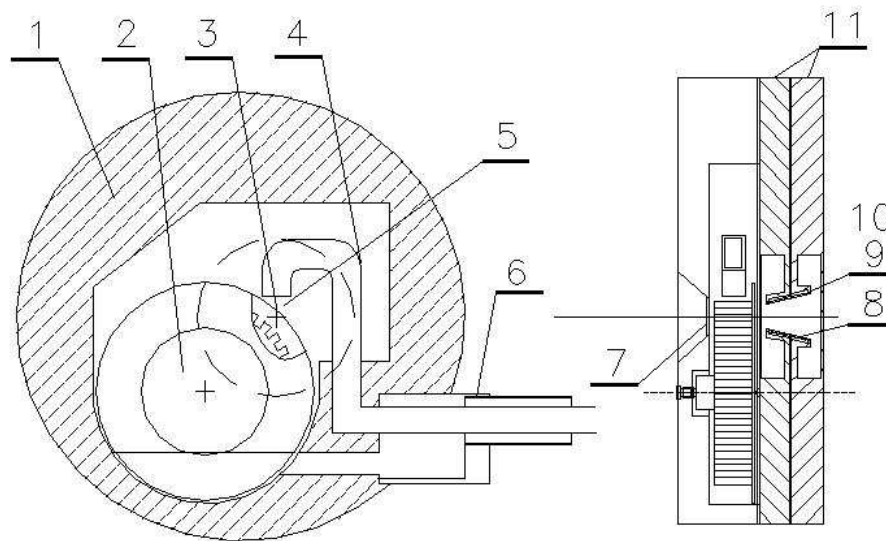
A.Mikhailichenko, “ Liquid Metal Target for ILC”, EPAC06, MOPLS108, Edinburg, Schotland 2006, Proc., pp. 816-818.

Two approaches in the target design

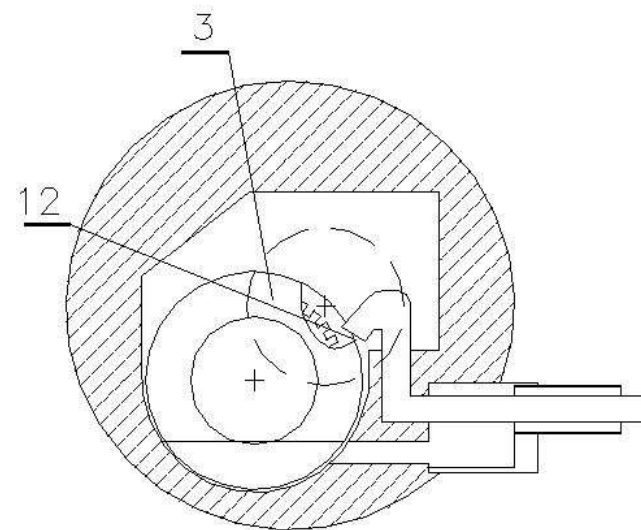


Liquid Mercury target suggested for VLEPP,
1986 A.Mikhailichenko, PHD Thesis

Variant 1



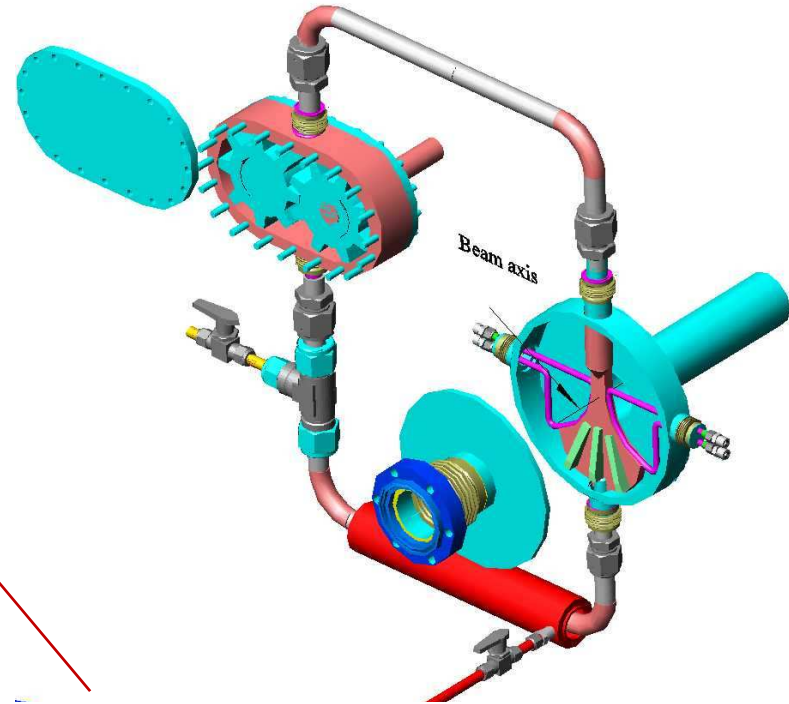
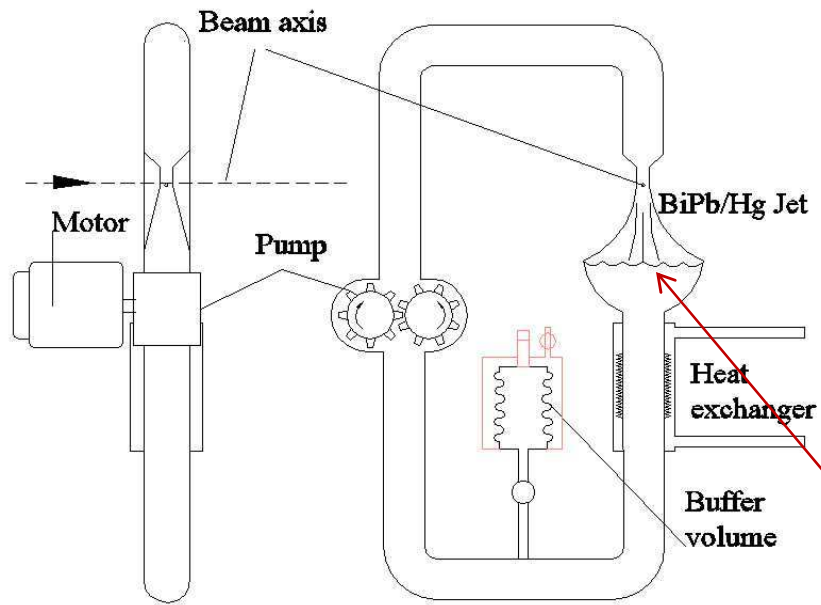
Variant 2



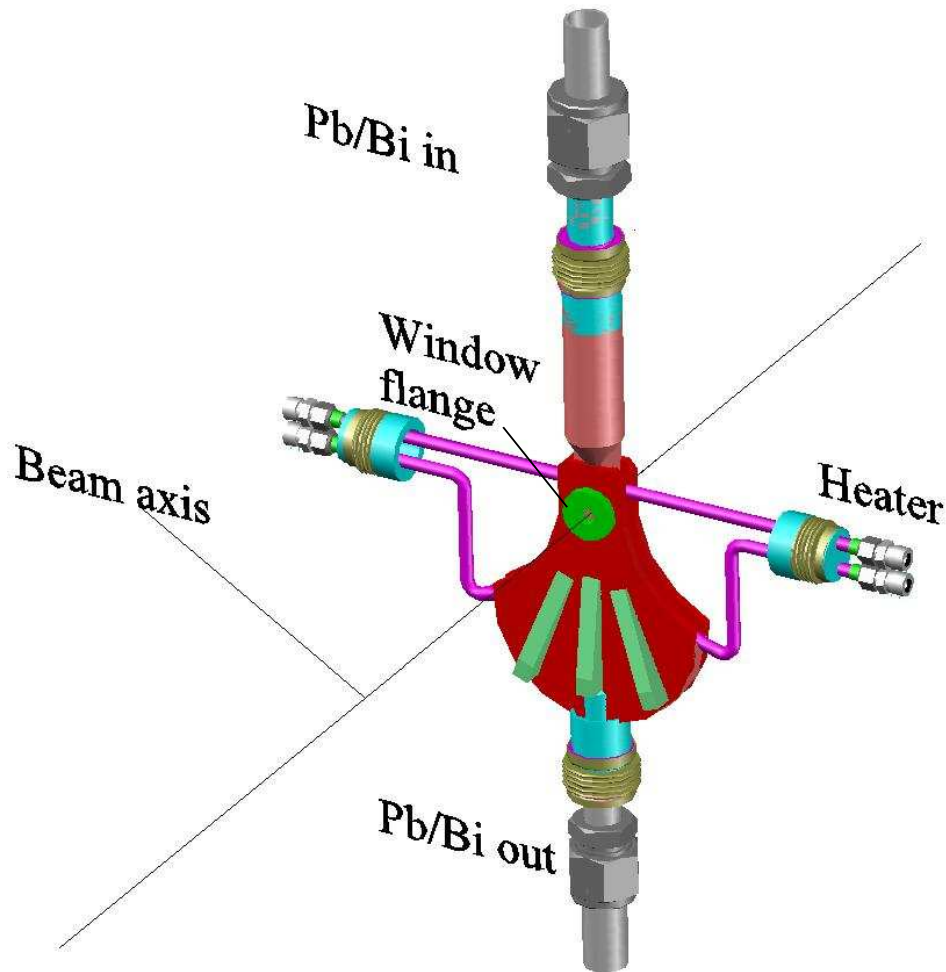
Variant 1. 1-Titanium case, 2 is the teething wheel, 3 is the target focusing point, 4 is the nozzle, 5 is the Mercury jet, 6 is the feeding tubes, 7 is secure Titanium foil, 8 is the conical shaped lens, 9 is the volume with liquid Lithium, 10 is Beryllium made flange, 11 are the current leads made from Titanium.
Variant 2. 3 is the target focusing point, 12 is the nozzle.

Bunch population $N_e=10^{12}$

Liquid metal target concept



Jet hits the liquid metal surface



The jet chamber could be made from Ti (Melt @1668°C) or Niobium (melt @ 2464°C)

Windows cooled by the metal jet itself.

Material for windows: ^4Be ; ^{22}Ti ;

Boron Nitride- BN ($^5\text{B}^7\text{N}$, sublimates @2700°C)

Boron Carbide (B₄C) , melts @2350

Jet cross section is (width x thickness)=
1cmx0.24cm

Jet velocity~10m/s provides for 1 ms the
distance ~1 cm

Hg can be used as well

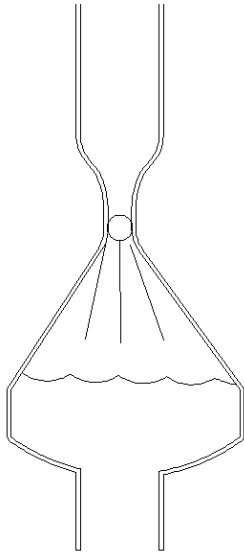
Back window could be omitted; this requires differential pumping and cooled traps.

Careful design required in this case.

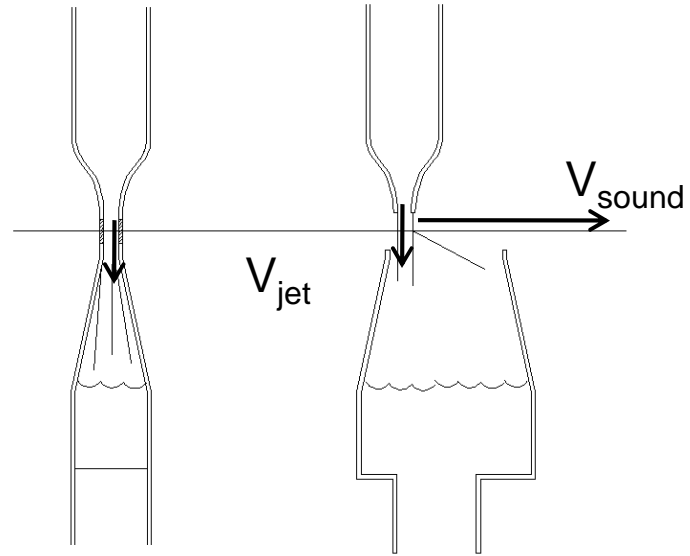
Temperature jump in *out*-window -150°C max after 1 ms train; front window not heated at all.

Windowless jet requires protective shield or distance

Front view



Side view.



Droplets from the target have
a speed of sound

$\rho_p,$

Liquids used for the targeting and cooling

		H₂O	Lithium	Pb-Bi (55wt%/45wt%)	Hg	Ga
ρ	g/cm ³	1.0	0.534	8.94	13.56	5.9
C_v	J/g/°C	4.1813	3.58	0.197	0.1395	0.37
T_{melt}	°C	0	180.54	125.9	-38.83	29.76
T_{boil}	°C	100	1342	1670	357	2204
l_{Xo}	cm	36.08	152.1	0.709	0.48	2.11
Latent heat,	kJ/g	2.26	21.2	0.86(Pb)	0.294	3.6
Nucl.int.length,	cm	83.3	133.6	17.6(Pb)	14.58	23.92
Ionization,	MeV/cm	1.992	0.875	12.7(Pb)	15.31	8.1

Gallium has better performance with Indium.

Gallium metal price is approaching 1000\$/kg, so the system containing 3L of Gallium will have a weight of Ga ~17.7kg and will cost ~18k\$, which is acceptable.

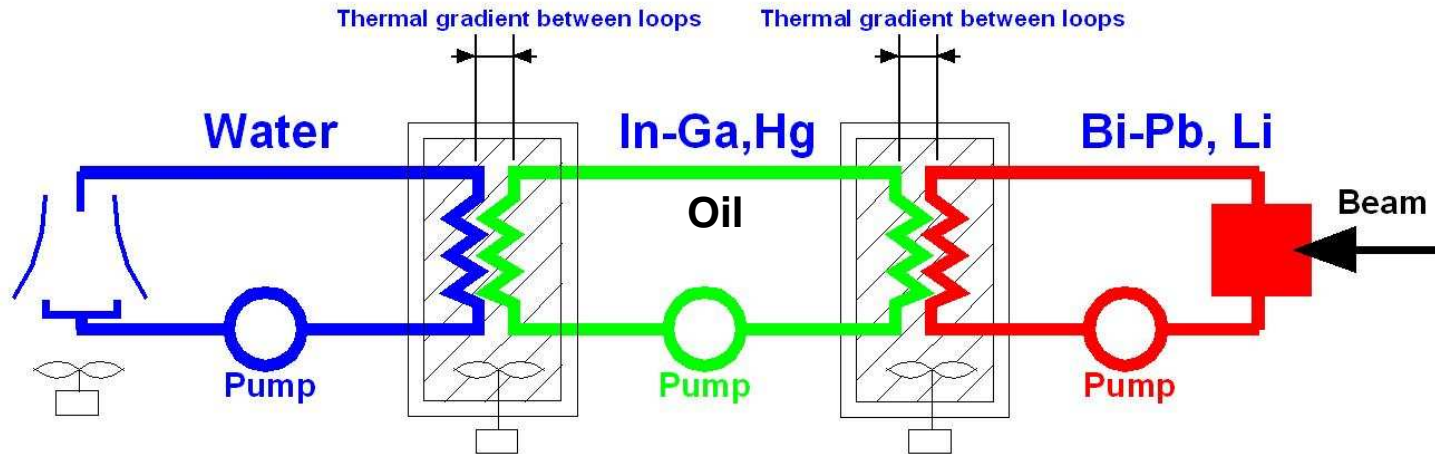
Addition of Indium with its ~750\$/kg will reduce the price, proportionally to percentage of Indium in the alloy. Savings are not drastic, however.

Lithium metal price ~\$64/kg is low at this scale.

Mercury metal trades at 700\$/34.5 kg; 34.5 kg represents so called flask=76 lb.

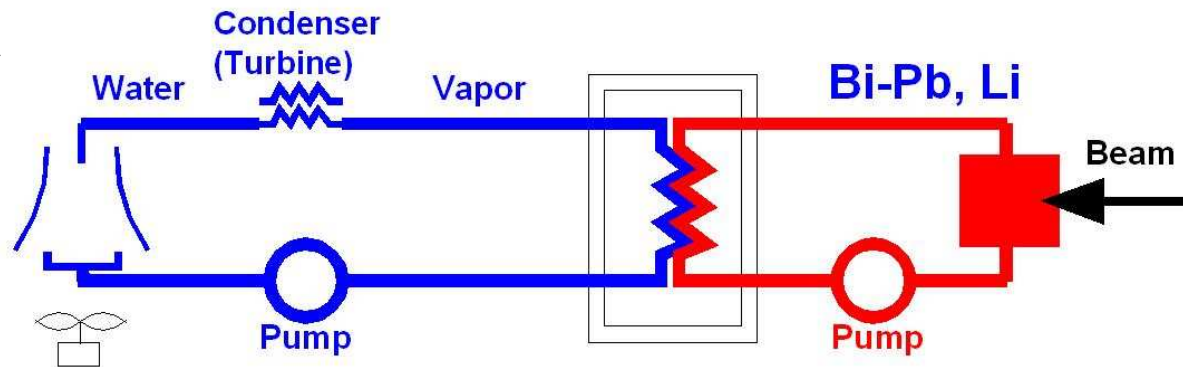
Na-K coolants in use for nuclear reactors, however extreme chemical activity makes usage of this coolant problematic in civil installations.

COOLING SYSTEMS



$$Q = -k \cdot Area \cdot \frac{\Delta T}{l}$$

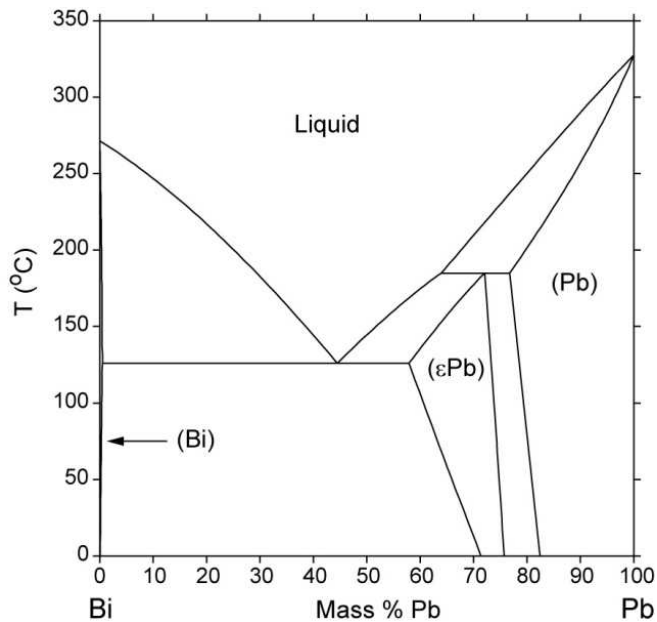
Maximal value of ΔT
defined by the coolant



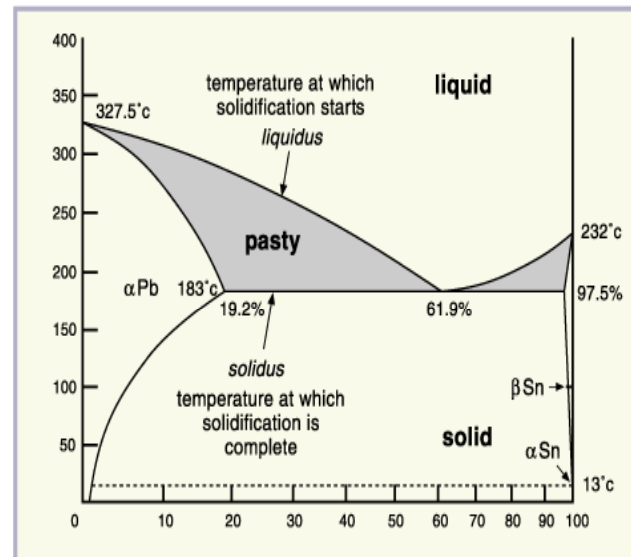
3-contour cooling system, at the top. 2-contour vapor cooling system at the bottom.

Bi-Pb alloy composed with 55.51 Mass% of Bi and 44.49 Mass% of Pb has liquid phase at 125.9°C. Phase diagram of this alloy is rather branchy with different modifications of Pb sub-phases.

Bi Pb diagram



Pb- Sn diagram



Nuclear reactor cooling (Wikipedia)

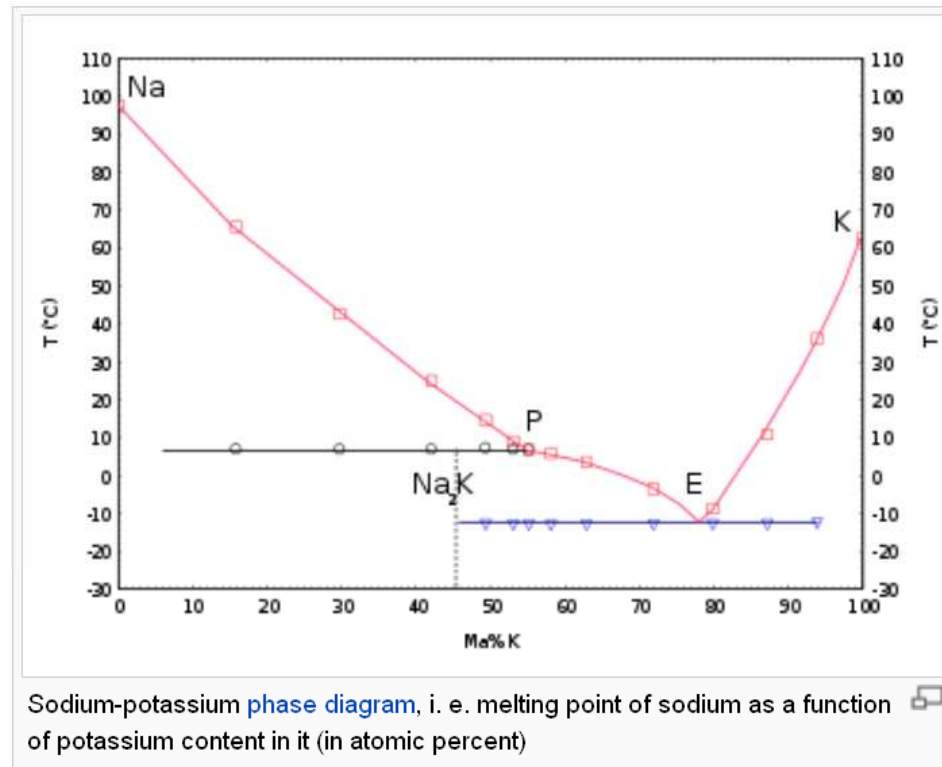
[edit]

Molten sodium is used as a coolant in some types of [fast neutron reactors](#). It has a low neutron absorption [cross section](#), which is required to achieve a high enough neutron flux, and has excellent thermal conductivity. Its high boiling point allows the reactor to operate at ambient pressure. However, using sodium poses certain challenges. The molten metal will readily burn in air and react violently with water, liberating explosive [hydrogen](#). During reactor operation, a small amount of [sodium-24](#) is formed as a result of [neutron activation](#), making the coolant radioactive.

Sodium leaks and fires were a significant operational problem in the first large sodium-cooled fast reactors, causing extended shutdowns at the [Monju Nuclear Power Plant](#) and [Beloyarsk Nuclear Power Plant](#).

Where reactors need to be frequently shut down, as is the case with some research reactors, the alloy of sodium and potassium called [NaK](#) is used. It melts at $-11\text{ }^{\circ}\text{C}$, so cooling pipes will not freeze at room temperature. Extra precautions against coolant leaks need to be taken in case of NaK, because molten potassium will spontaneously catch fire when exposed to air. The [phase diagram](#) with [potassium](#) shows that the mixtures with potassium are liquid at room temperature in a wide concentration range. A compound Na_2K melts at $7\text{ }^{\circ}\text{C}$. The [eutectic mixture](#) with a potassium content of 77 % gives a melting point at $-12.6\text{ }^{\circ}\text{C}$.^[22]

B.F.Gromov et al., “Use of Lead-Bismuth Coolant in Nuclear Reactors and Accelerator-Driven Systems”, Nuclear Engineering and Design 173, (1997) 207-217.



LOSSES FOR DIFFERENT MATERIAL OF TARGET

If energy Q deposited in mass m , then the temperature rise is

$$\Delta T = \frac{Q}{mc_V},$$

where c_V stands for the heat capacity. In its turn, for the 1 cm^2 cross section

$$Q \cong l[\text{cm}] \times 1[\text{cm}^2] \times 2[\text{MeV} / \text{g} / \text{cm}^2] \times \rho[\text{g} / \text{cm}^3].$$

For the gamma target, the length l is a fraction of radiation length, $l \cong \frac{1}{2} X_0 / \rho$,

$$Q \cong X_0 \times 1[\text{MeV}]$$

From the other hand $m = \rho \times 1[\text{cm}^2] \times \frac{X_0}{2\rho} = \frac{1}{2} X_0 \times 1[\text{g}]$,

so the temperature gain goes to be

$$\Delta T \cong \frac{2}{c_V[\text{J} / \text{g} / ^\circ\text{K}]} [^\circ\text{K}] \left(\cong \frac{2A}{25[\text{Mol} / \text{g} / ^\circ\text{K}]} \cong \text{const} : (D - P \text{ law}) \right)$$

For Ti $c_V=0.5 \text{ J/g} / ^\circ\text{K}$; for W $c_V=0.134 \text{ J/g} / ^\circ\text{K}$; for Pb $c_V=0.13 \text{ J/g} / ^\circ\text{K}$,

So ratio of temperatures comes to

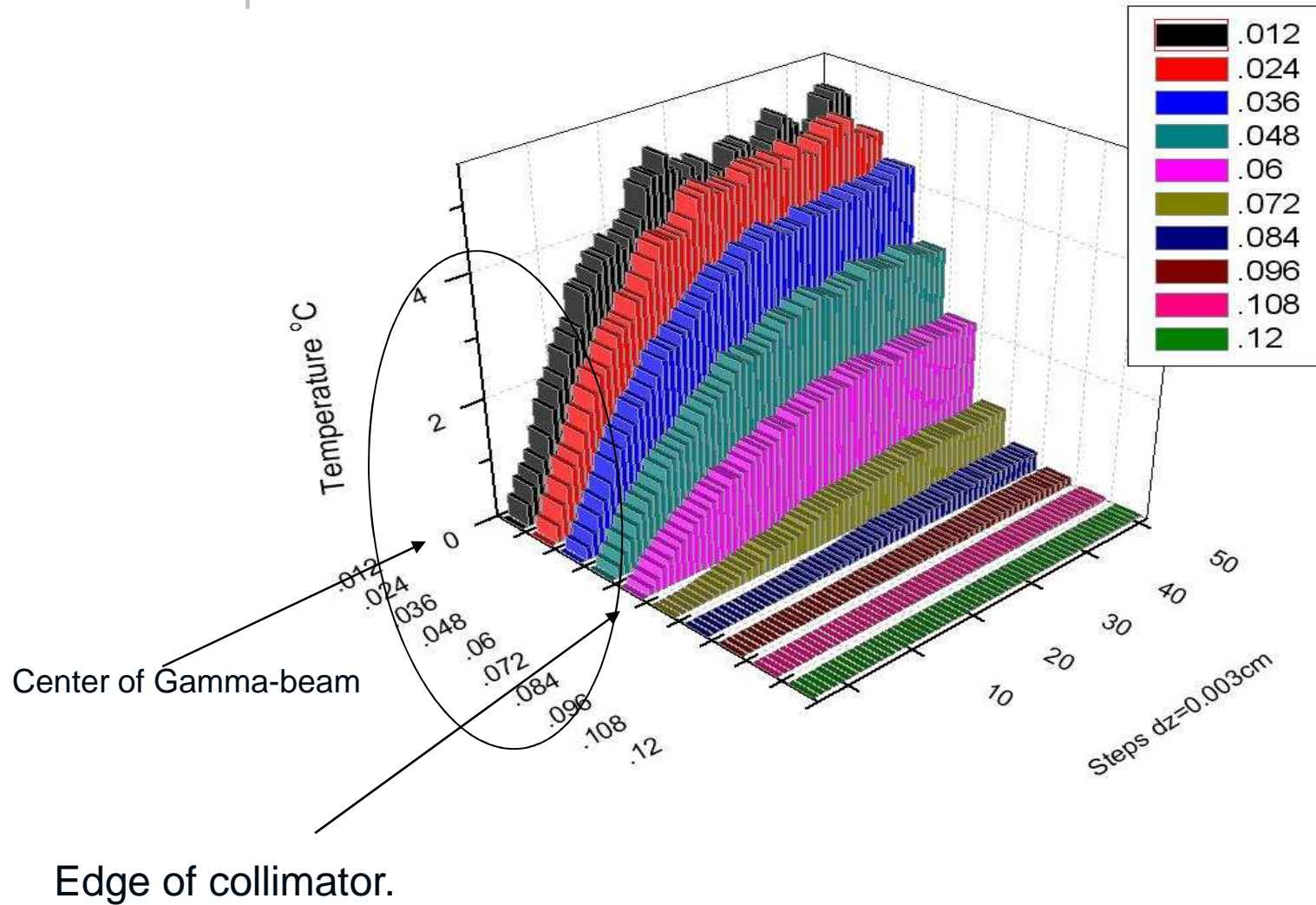
$$\Delta T_{Ti} : \Delta T_W : \Delta T_{Pb} \cong 1 : 3.7 : 3.8; \quad (A_{Ti} : A_W : A_{Pb} \cong 47 : 183 : 207)$$

The ratio difference in temperature gain is not so drastic; however it is important if the temperature approaching the melting threshold.

Usage of heavier targets desirable from the point of lowering of focal depth (~10 times) needed to be serviced by capturing optics, however. Also, the positron production efficiency is higher for heavier materials. All together this gives ~50% higher yield for W compared with Ti.

THE TEMPERATURE ALONG THE W TARGET FOR DIFFERENT RADIUSES

per 10^{13} initial electrons; spinning target; KONN



Each particle radiates 2.76 GeV in undulator

Rim W target;

R=50 cm

f=50 Hz

K=0.92

Eff=1.6

Effp=32%

Lund=35m

$\lambda_u=1.15$ cm

Dis=300 m

G=45kG/cm

I=110kA

Rcoll=0.5cm

DISTRIBUTION OF TEMPERATURE IN TARGET T<R,Z> DEG PER 10¹³ INITIAL ELECTRONS

DELTA R = .100 cm, DELTA Z = .003 cm

Collimator

R→										
.008	.005	.002	.001	.000	.000	.000	.000	.000	.000	.000
.300	.113	.030	.004	.000	.000	.000	.000	.000	.000	.000
.581	.219	.051	.008	.000	.000	.000	.000	.000	.000	.000
.840	.317	.068	.011	.001	.000	.000	.000	.000	.000	.000
1.106	.416	.083	.010	.001	.000	.000	.000	.000	.000	.000
1.408	.504	.097	.011	.001	.000	.000	.000	.000	.000	.000
1.654	.579	.113	.013	.001	.000	.000	.000	.000	.000	.000
1.858	.662	.122	.013	.001	.000	.000	.000	.000	.000	.000
2.060	.749	.135	.014	.001	.000	.000	.000	.000	.000	.000
2.276	.816	.143	.013	.002	.000	.000	.000	.000	.000	.000
2.432	.886	.156	.014	.002	.000	.000	.000	.000	.000	.000
2.616	.946	.158	.015	.002	.000	.000	.000	.000	.000	.000
2.797	.997	.165	.015	.001	.000	.000	.000	.000	.000	.000
2.874	1.051	.175	.016	.001	.000	.000	.000	.000	.000	.000
3.001	1.118	.181	.016	.001	.000	.000	.000	.000	.000	.000
3.053	1.167	.188	.018	.001	.000	.000	.000	.000	.000	.000
3.240	1.220	.203	.019	.001	.000	.000	.000	.000	.000	.000
3.322	1.276	.202	.018	.002	.000	.000	.000	.000	.000	.000
3.428	1.303	.213	.019	.001	.000	.000	.000	.000	.000	.000
3.532	1.385	.221	.018	.002	.000	.000	.000	.000	.000	.000
3.581	1.416	.225	.018	.001	.000	.000	.000	.000	.000	.000
3.649	1.431	.227	.019	.001	.000	.000	.000	.000	.000	.000
3.732	1.483	.232	.018	.002	.000	.000	.000	.000	.000	.000
3.807	1.479	.239	.019	.001	.000	.000	.000	.000	.000	.000
3.788	1.511	.249	.022	.002	.000	.000	.000	.000	.000	.000
3.845	1.534	.246	.021	.002	.000	.000	.000	.000	.000	.000
3.901	1.562	.248	.020	.002	.000	.000	.000	.000	.000	.000
3.984	1.590	.253	.021	.001	.000	.000	.000	.000	.000	.000
3.966	1.643	.254	.020	.001	.000	.000	.000	.000	.000	.000
4.029	1.636	.257	.019	.002	.000	.000	.000	.000	.000	.000
4.089	1.699	.260	.019	.001	.000	.000	.000	.000	.000	.000
4.131	1.712	.266	.021	.001	.000	.000	.000	.000	.000	.000
4.220	1.738	.257	.021	.001	.000	.000	.000	.000	.000	.000
4.261	1.731	.268	.021	.001	.000	.000	.000	.000	.000	.000
4.267	1.743	.268	.021	.001	.000	.000	.000	.000	.000	.000
4.219	1.748	.270	.020	.001	.000	.000	.000	.000	.000	.000
4.278	1.750	.270	.024	.001	.000	.000	.000	.000	.000	.000
4.308	1.769	.274	.022	.001	.000	.000	.000	.000	.000	.000
4.334	1.773	.279	.021	.001	.000	.000	.000	.000	.000	.000
4.315	1.808	.274	.024	.001	.000	.000	.000	.000	.000	.000
4.342	1.824	.275	.025	.001	.000	.000	.000	.000	.000	.000
4.307	1.830	.282	.024	.001	.000	.000	.000	.000	.000	.000
4.440	1.850	.277	.025	.001	.000	.000	.000	.000	.000	.000
4.406	1.847	.281	.024	.001	.000	.000	.000	.000	.000	.000
4.435	1.864	.275	.024	.001	.000	.000	.000	.000	.000	.000
4.421	1.865	.270	.024	.001	.000	.000	.000	.000	.000	.000
4.424	1.893	.277	.023	.001	.000	.000	.000	.000	.000	.000
4.394	1.912	.284	.022	.001	.000	.000	.000	.000	.000	.000
4.452	1.929	.276	.023	.001	.000	.000	.000	.000	.000	.000

Now the target is not spinning

DISTRIBUTION OF TEMPERATURE IN TARGET T(R,Z) DEG PER 10¹³ INITIAL ELECTRONS

DELTA R = .100 cm, DELTA Z = .003 cm

Collimator

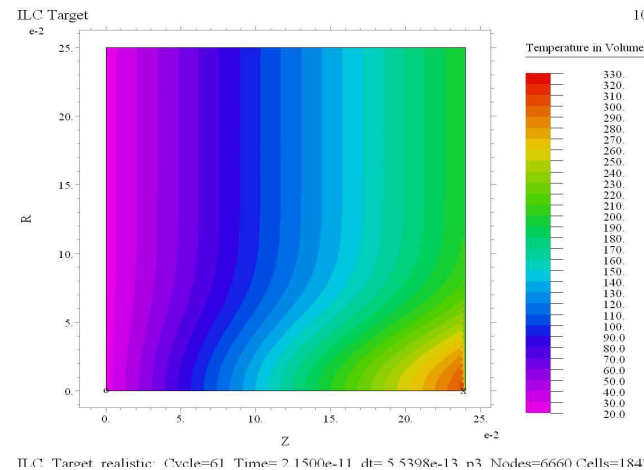
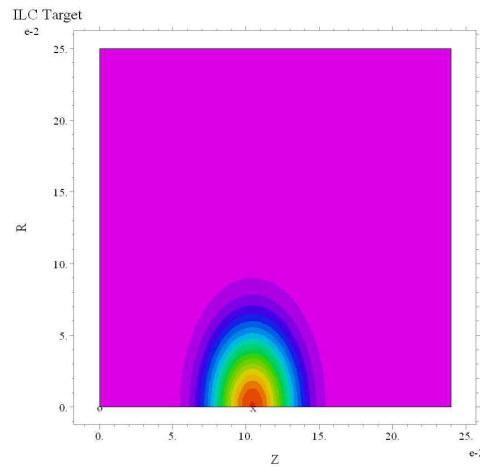
R→										
.178	.111	.052	.012	.001	.001	.000	.000	.000	.000	.000
6.306	2.380	.628	.076	.004	.001	.000	.000	.000	.000	.000
12.211	4.606	1.062	.160	.009	.002	.000	.000	.000	.000	.000
17.650	6.666	1.420	.233	.020	.001	.002	.000	.000	.000	.000
23.229	8.744	1.735	.215	.022	.001	.001	.000	.000	.000	.000
29.563	10.592	2.031	.237	.023	.000	.000	.000	.000	.000	.000
34.737	12.165	2.363	.272	.025	.001	.000	.000	.000	.000	.000
39.023	13.906	2.565	.268	.026	.001	.000	.000	.000	.000	.000
43.268	15.722	2.833	.297	.025	.000	.000	.000	.000	.000	.000
47.793	17.145	3.002	.270	.032	.000	.000	.000	.000	.000	.000
51.077	18.602	3.274	.302	.033	.000	.000	.000	.000	.000	.000
54.937	19.866	3.320	.311	.042	.000	.000	.000	.000	.000	.000
58.733	20.944	3.455	.312	.028	.000	.000	.000	.000	.000	.000
60.357	22.063	3.681	.329	.025	.000	.000	.000	.000	.000	.000
63.027	23.468	3.808	.333	.029	.000	.000	.000	.000	.000	.000
64.106	24.499	3.939	.378	.030	.000	.000	.000	.000	.000	.000
68.045	25.610	4.259	.396	.025	.001	.000	.000	.000	.000	.000
69.764	26.800	4.235	.379	.032	.000	.000	.000	.000	.000	.000
71.979	27.366	4.476	.399	.026	.000	.000	.000	.000	.000	.000
74.173	29.083	4.638	.378	.038	.000	.000	.000	.000	.000	.000
75.208	29.744	4.727	.378	.022	.001	.000	.000	.000	.000	.000
76.633	30.043	4.762	.397	.030	.000	.000	.000	.000	.000	.000
78.364	31.152	4.869	.378	.032	.000	.000	.000	.000	.000	.000
79.947	31.063	5.025	.399	.031	.000	.000	.000	.000	.000	.000
79.545	31.740	5.219	.456	.038	.000	.000	.000	.000	.000	.000
80.736	32.216	5.176	.448	.032	.000	.000	.000	.000	.000	.000
81.911	32.812	5.205	.423	.033	.001	.000	.000	.001	.000	.000
83.666	33.400	5.312	.440	.029	.000	.000	.000	.000	.000	.000
83.296	34.506	5.341	.428	.030	.001	.000	.000	.000	.000	.000
84.613	34.365	5.394	.392	.041	.000	.000	.000	.000	.000	.000
85.876	35.674	5.450	.400	.030	.001	.000	.000	.000	.000	.000
86.751	35.954	5.579	.432	.027	.000	.000	.000	.000	.000	.000
88.622	36.495	5.402	.434	.025	.000	.000	.000	.000	.000	.000
89.485	36.344	5.629	.440	.026	.001	.000	.000	.000	.000	.000
89.609	36.608	5.621	.433	.022	.000	.000	.000	.000	.000	.000
88.595	36.706	5.672	.429	.030	.001	.000	.000	.000	.000	.000
89.832	36.755	5.675	.494	.026	.000	.000	.000	.000	.000	.000
90.468	37.159	5.757	.472	.029	.001	.000	.000	.000	.000	.000
91.011	37.239	5.867	.449	.026	.000	.000	.000	.000	.000	.000
90.623	37.963	5.753	.507	.022	.000	.000	.000	.000	.000	.000
91.176	38.300	5.777	.515	.026	.001	.000	.000	.000	.000	.000
90.441	38.423	5.921	.494	.026	.000	.000	.000	.000	.000	.000
93.246	38.856	5.822	.534	.028	.000	.000	.000	.000	.000	.000
92.526	38.793	5.903	.513	.026	.000	.000	.000	.000	.000	.000
93.128	39.141	5.767	.496	.018	.001	.000	.000	.000	.000	.000
92.849	39.155	5.677	.498	.025	.000	.000	.000	.000	.000	.000
92.913	39.756	5.822	.493	.018	.000	.000	.000	.000	.000	.000
92.267	40.144	5.969	.467	.017	.001	.000	.000	.000	.000	.000
93.494	40.505	5.786	.490	.020	.000	.000	.001	.000	.000	.000

We used FlePDE code also for calculation of temperature and pressure with equations;

Temperature $\nabla(k\nabla T) + \dot{Q} = \rho c_V \dot{T}$ Pressure $\ddot{P} - \nabla(c_0^2 \nabla P) = \frac{\Gamma}{V_0} \dot{Q}$

$$\dot{Q} = \sum_i \frac{2cQ_{bunch}}{\pi\sqrt{\pi}\sigma_z\sigma_{\perp\gamma}^2 l_T} \frac{z}{l_T} \exp\left(-\frac{(z+z_0-c(t-i\cdot t_0))^2}{\sigma_z^2}\right) \cdot \exp\left(-\frac{r^2}{\sigma_{\perp\gamma}^2}\right)$$

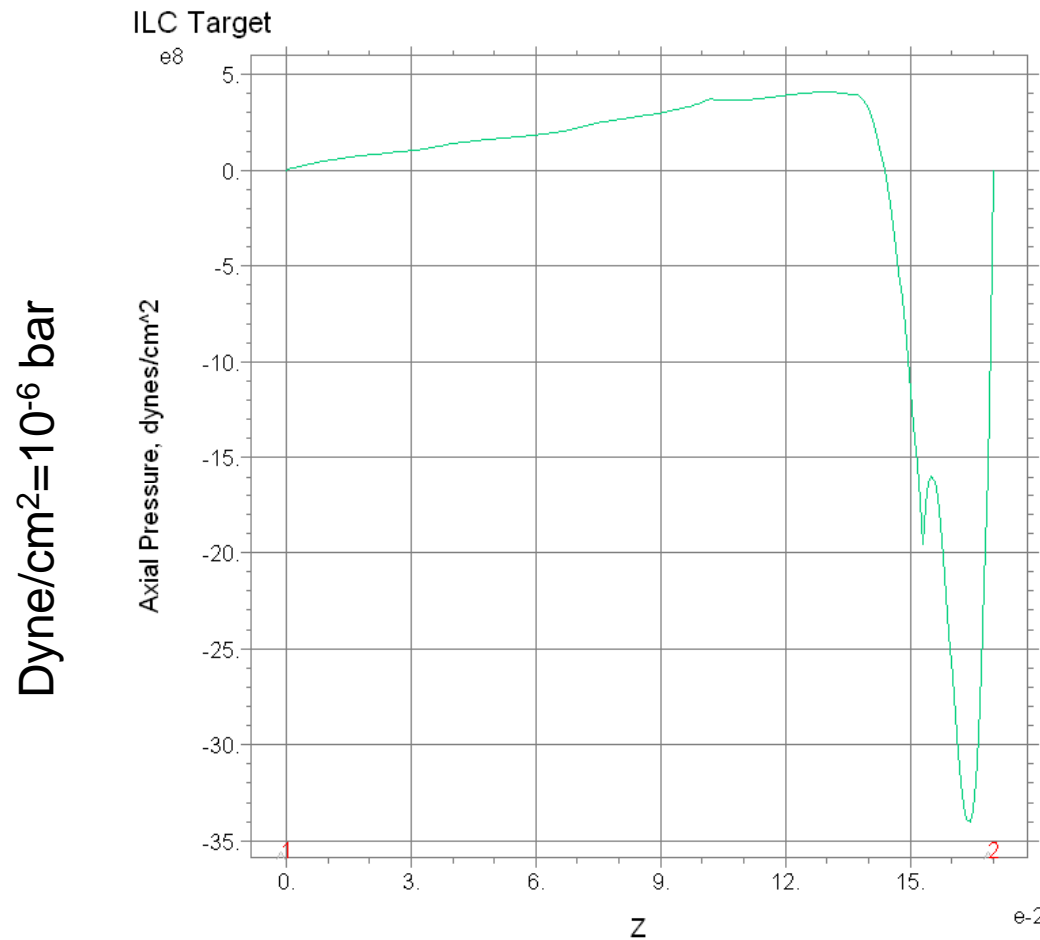
$\Gamma(V) = V / c_V (\partial P / \partial T_V)$ characterizing the ratio of the thermal pressure to the specific thermal energy called Grüneisen coefficient.



Instant position of the bunch moving in the target, at the left. Isotherms right after the bunch passage, at the right.

The negative pressure phenomenon confirmed here: after the bunch passed at the exit side the substantial negative pressure developed.

This effect is a general one and might be important for the targets made from **Carbon**.



10:53:28 1/18/11
FlexPDE 6.15

Axial Pressure, dynes/cm²
from (0.,0.)
to (long,0.)

1: pres

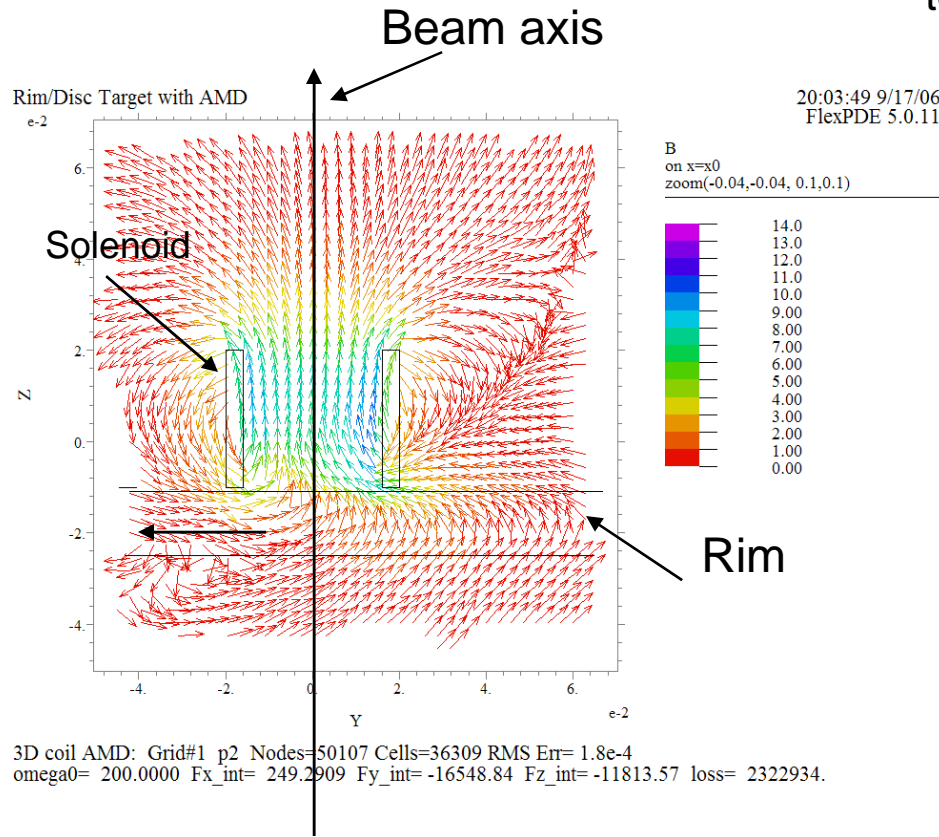
Energy leaved in the
target by a single
bunch is ~0.1 Joule



ILC_Target_with_pressure: Cycle=10264 Time= 1.0000e-10 dt= 8.6496e-15 P3 Nodes=1500 Cells=394 RMS Err= !
sigmar= 0.250000 sigmaz= 0.050000 Surf_Integral= -9.271943

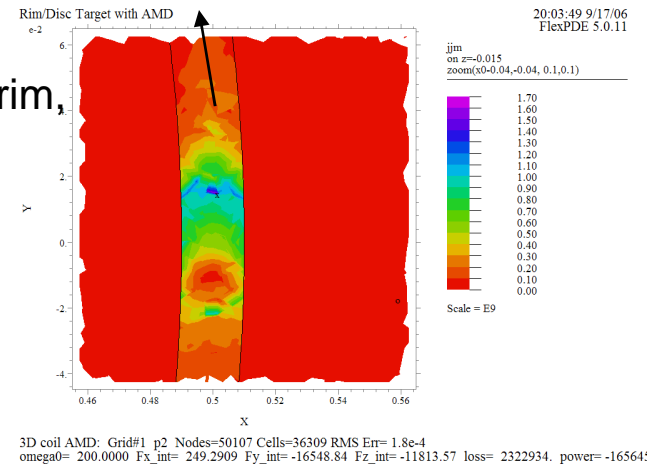
Pressure along the target; beam passed from the left to the right 0.1 ns ago

IT WAS FOUND, THAT MOVING METAL PERTURBS MAGNETIC FIELD OF OMD

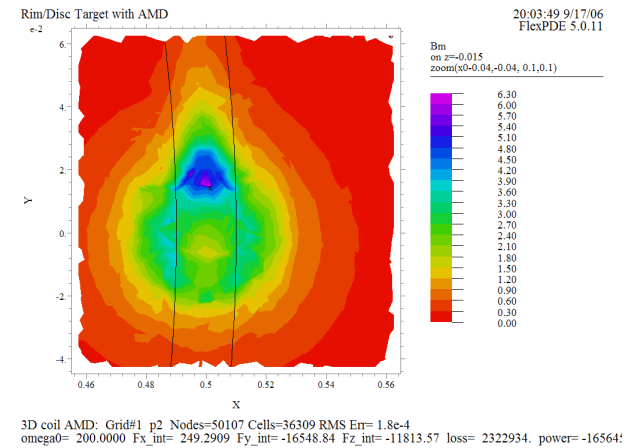


Spinning rim, side view

Spinning rim,
top view



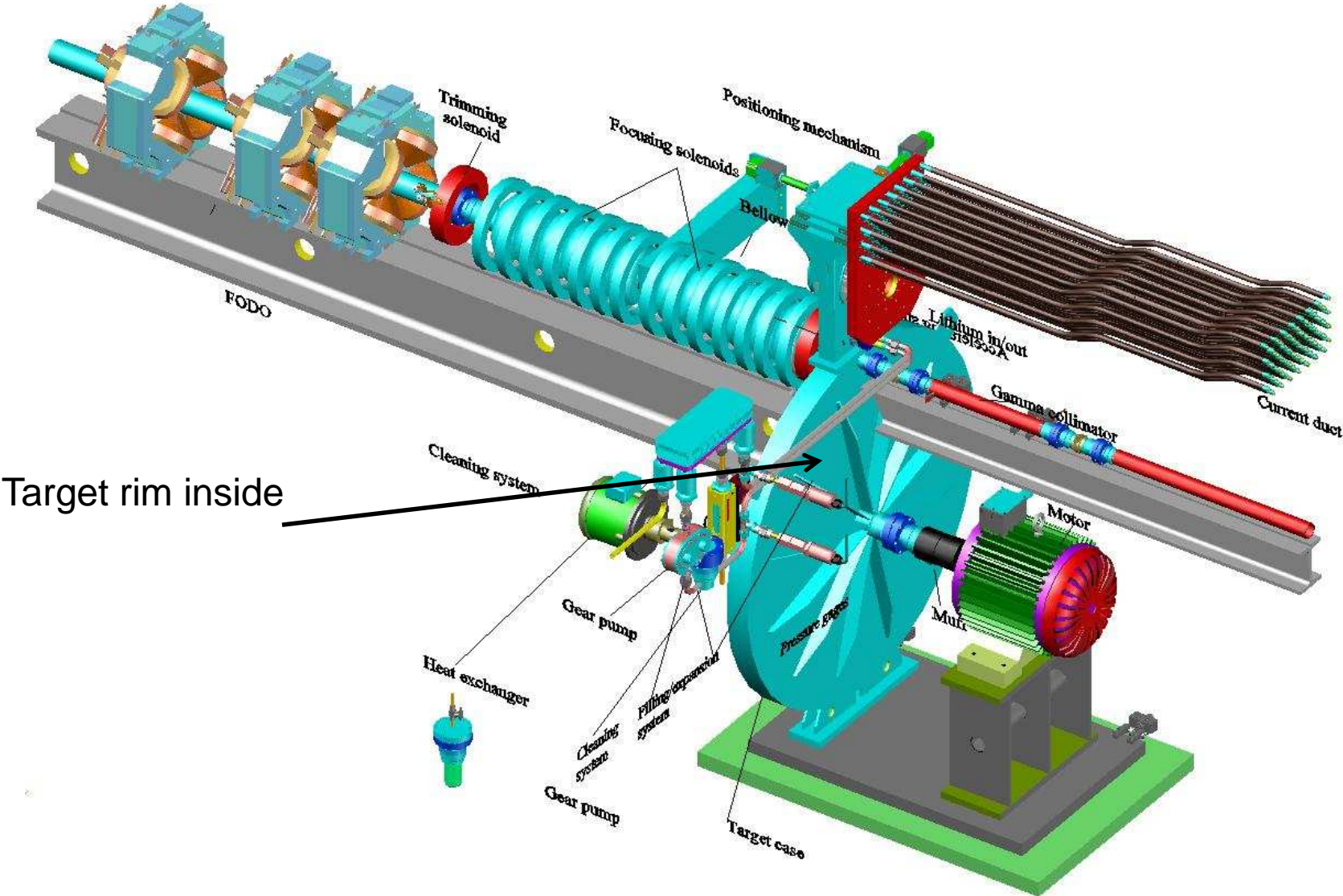
Modulus of field in a rim



Modulus of field between the coil and the rim

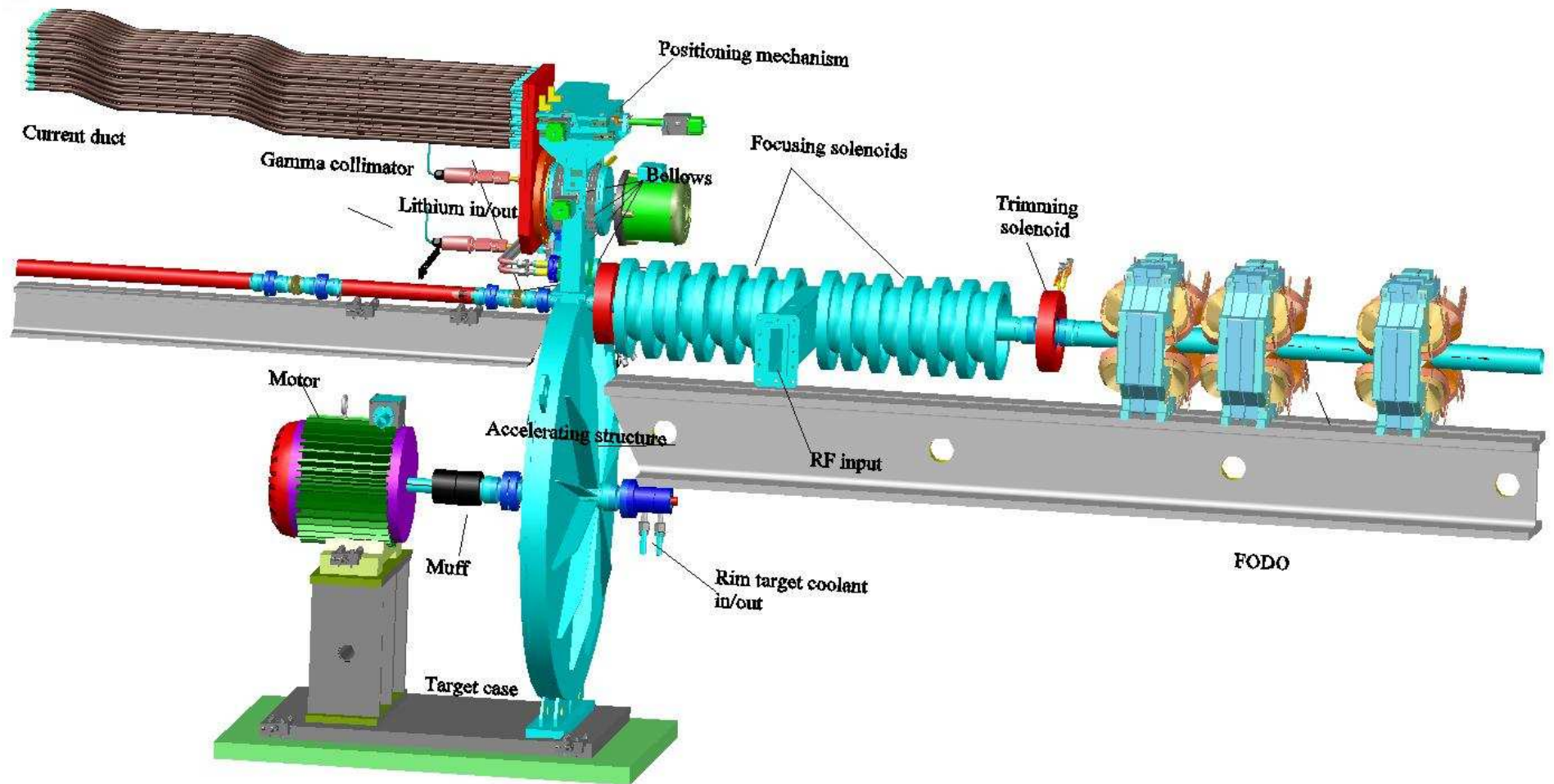
Lithium lens has no stray fields

Target station. Spinning rim, Lithium lens.



Target rim inside

View from the other side



4. LITHIUM LENS

A.Mikhailichenko," Lithium Lens (I)", CBN -09-4, Aug 2009, 17pp.

<http://www.lepp.cornell.edu/public/CBN/2009/CBN09-4/CBN%2009-04.pdf>

A.Mikhailichenko," Lithium Lens (II)", CBN -10-3, Aug 2010, 37pp

<http://www.lepp.cornell.edu/public/CBN/2010/CBN10-3/CBN%2010-03.pdf>

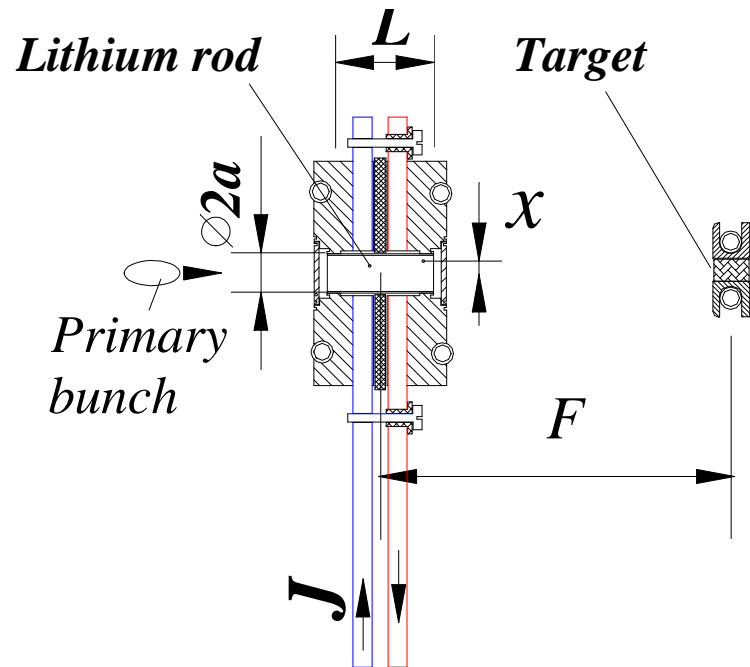
LITHIUM LENS BASICS

If steady current I runs through the round conductor having radius a , its azimuthal magnetic field inside the rod could be described as

$$H_{\vartheta}(r) = \frac{0.4\pi I r}{2\pi a^2}$$

where magnetic field is measured in Gs, a –in cm , I –in Amperes. Current density comes to $j_s = I / \pi a^2$. A particle, passed through the rod, will get the transverse kick

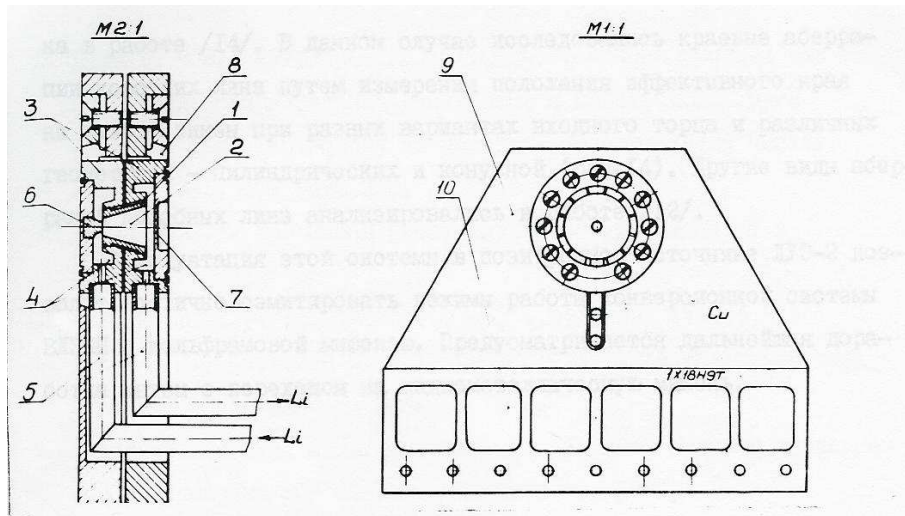
$$\alpha \cong \frac{H(x) \cdot L}{(HR)} \cong \frac{0.2ILx}{a^2 \cdot (HR)}$$



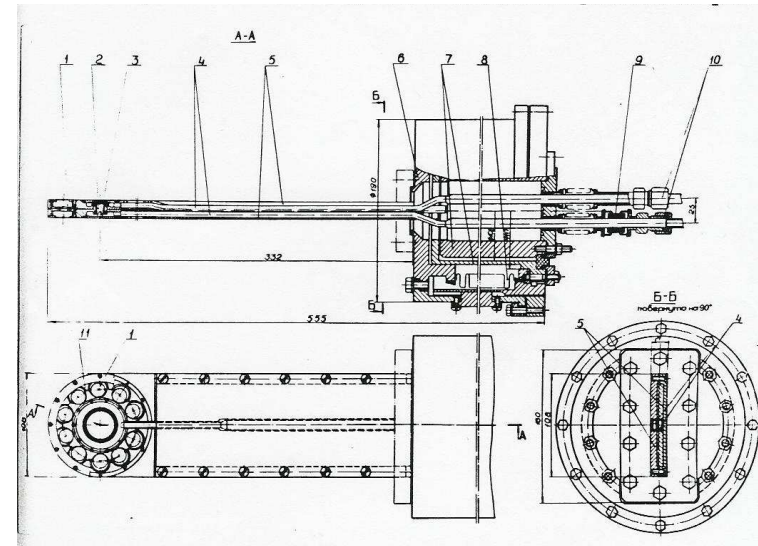
This picture drawn for the focusing of electron beam to the target

So the focal distance could be defined as the following $F \cong \frac{a^2 \cdot (HR)}{0.2IL} \sim 1cm$

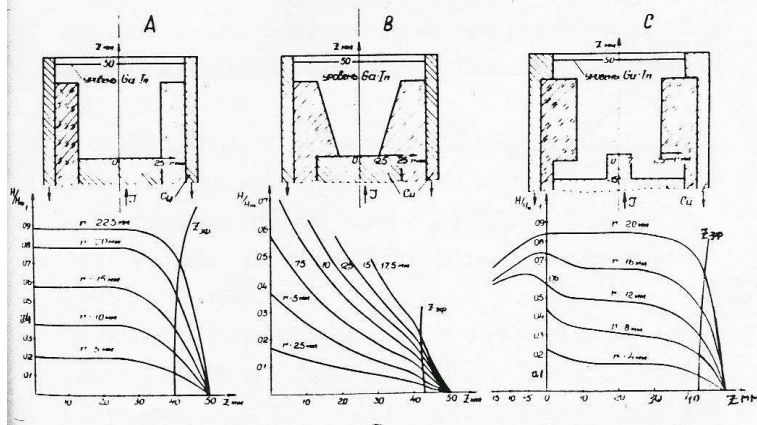
T.A.Vsevoljskaja, A.A.Mikhailichenko, **G.I.Silvestrov**, A.D.Cherniakin,
 "To the Conversion System for Generation of Polarized Beams in VLEPP", BINP Internal Report,
 1986



1-conic lens body; 2- working volume; 3- lens case; 4- buffer volumes; 5- feeding tubes for liquid Li; 6- target; 7- exit flange; 8- conic contacts; 9- flat current leads; 10- slots for heat flow reduction.



1-ex-centric contact pushers; 2-conic lens body; 3-W target; 4-Ti tubing for LI supply; 5-flat current leads; 6-vacuum chamber; 7-coaxial fraction of current leads; 8-bellows; 9-ceramic insulators; 10-conical gasket; 11-set of ex-centric pushers.



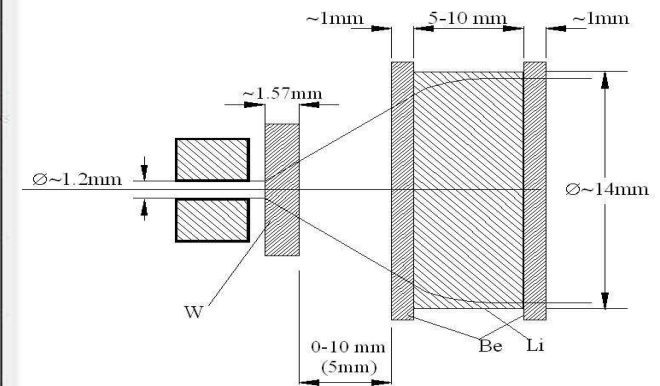
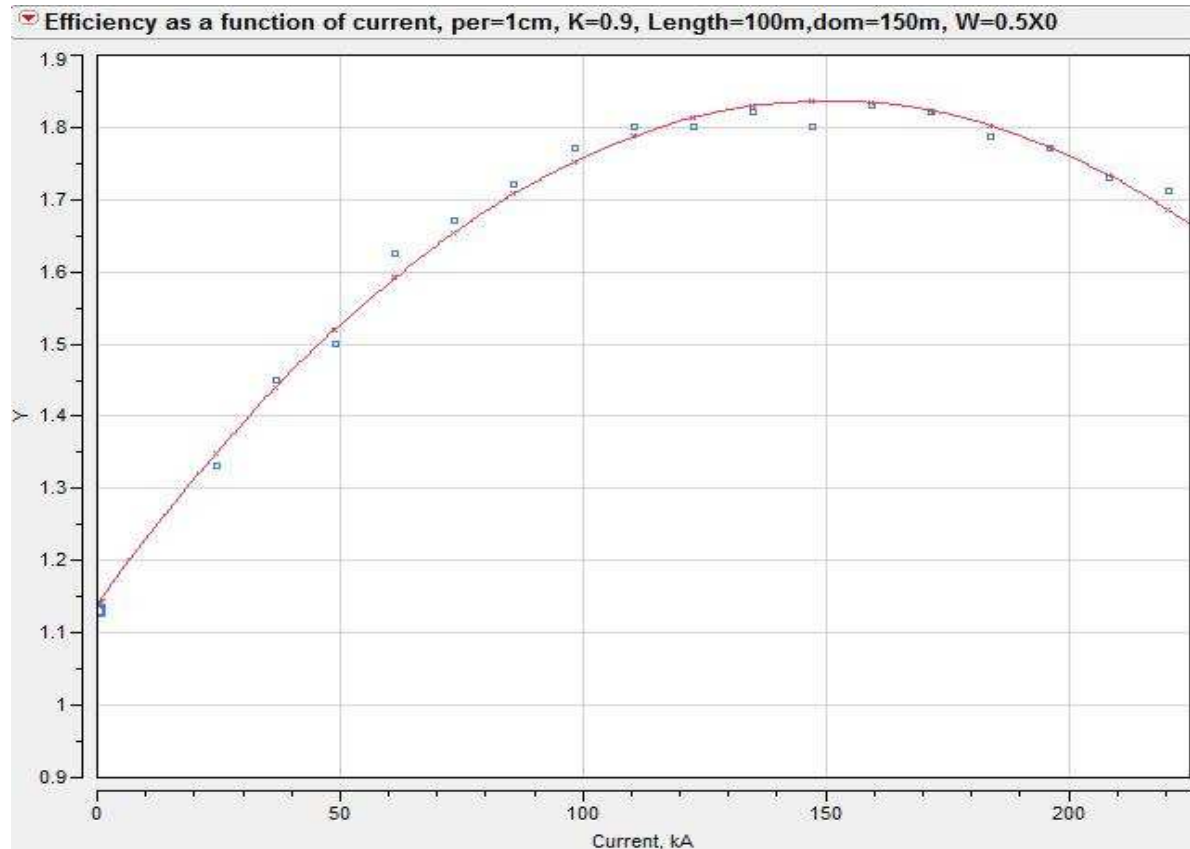
Field measured in liquid Gallium model.

A-cylindrical lens with homogenous current leads supply at the end

B- conical lens with the same current feed

C -lens with cylindrical target at the entrance flange

First of all, how important is the lens for the collection business?

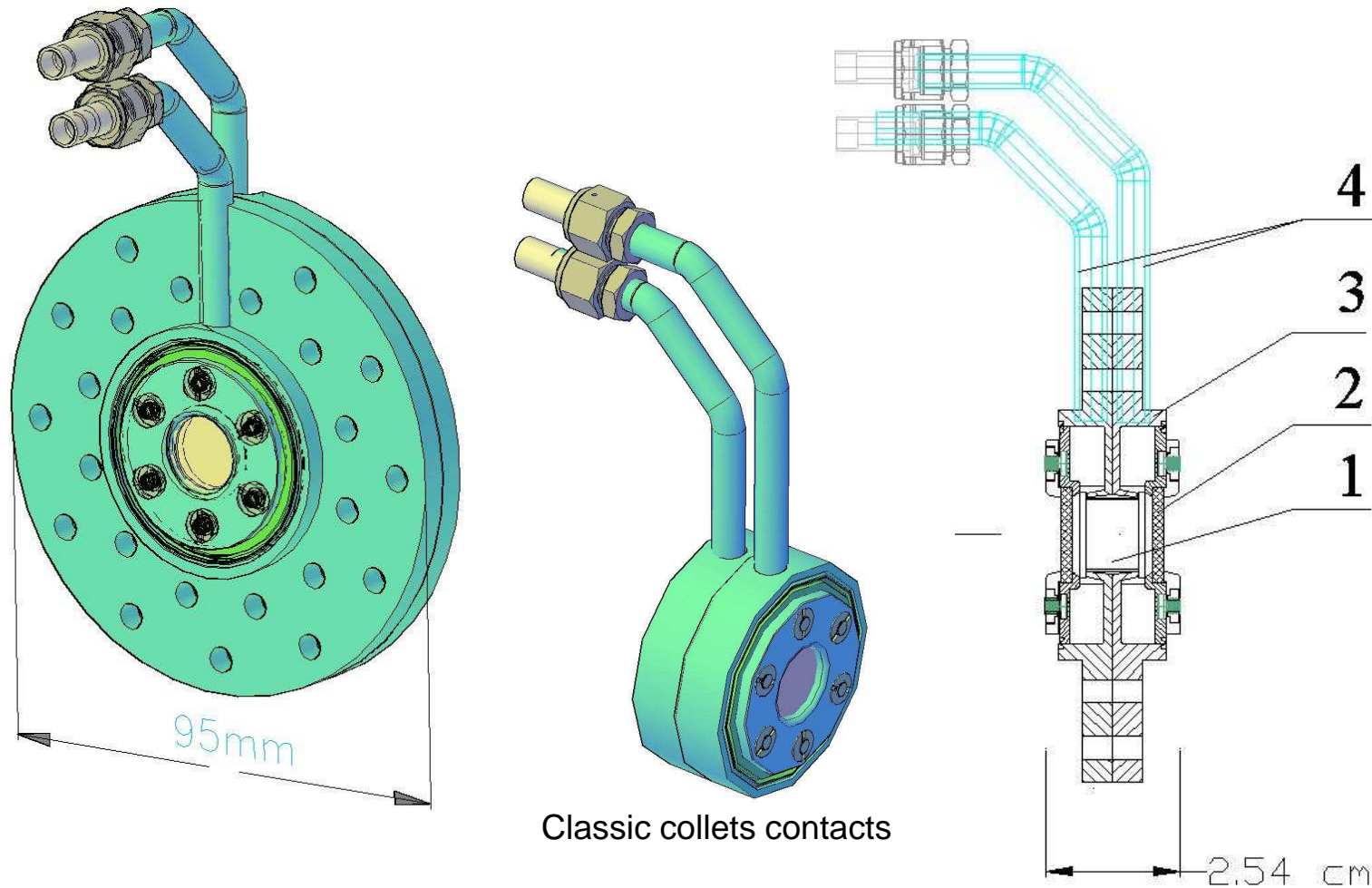


Typical dimensions

Efficiency of positron production normalized to the primary electron as function of feeding current in a lens. $K=0.9$, 100m long undulator, lens is 0.5 cm-long, $\epsilon \approx 6\text{MeV}\cdot\text{cm}$.

One can see that LL potentially adds ~70% of positrons. But even without lens the efficiency is more than one already.

Lens with liquid Lithium for ILC design



Lithium Lens for ILC positron source; extended flanges serve for electrical contact. 1—volume with Lithium, 2—window (Be/BC/BN), 3—electrical contacts with caverns for Li, 4—tubing for Lithium in/out. At the center- the latest design.

Windows attachment technique

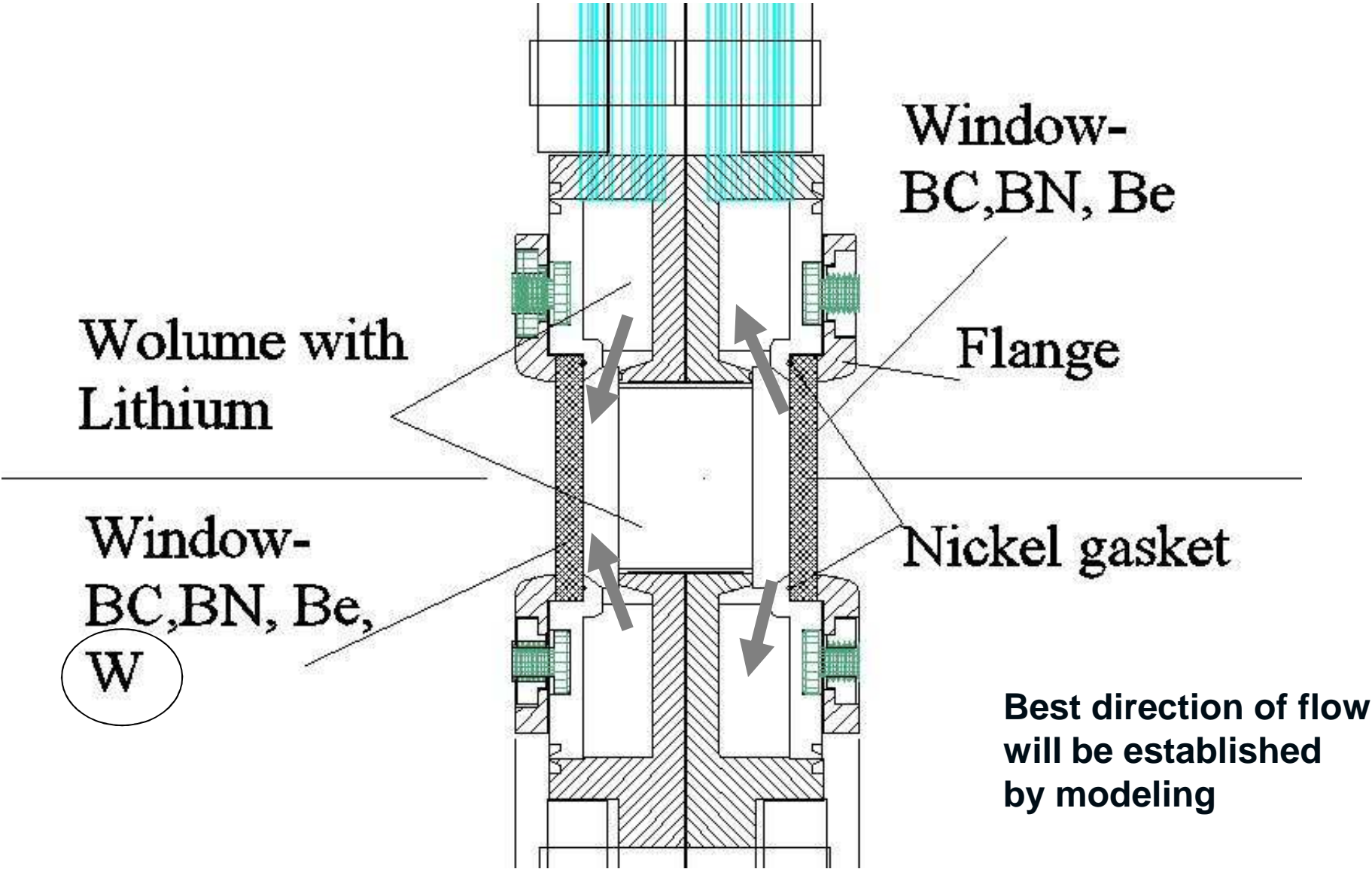
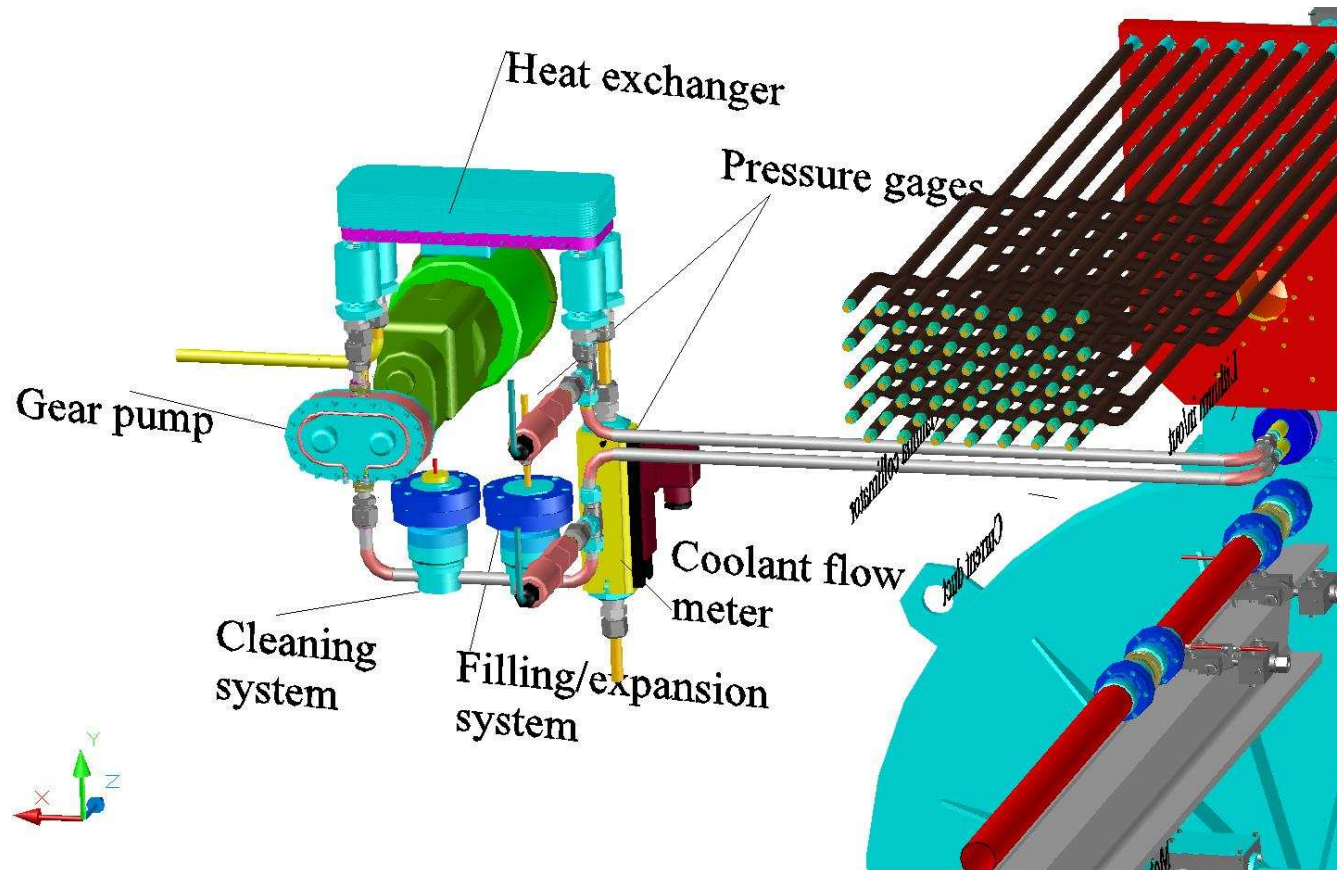


Table 1: properties of Li¹, Be, BC, BN, W

	Units	Li	Be	BN	B ₄ C	W
Atomic number, Z	-	3	4	5/7	5/6	74
Yong modulus	GPa	4.9	287	350-400	450	400
Density, ρ	$[g/cm^3]$	0.533	1.846	3.487	2.52	19.254
Specific resistance	$Ohm-cm$	1.44×10^{-5}	1.9×10^{-5}	$>10^{14}$	7.14×10^{-3}	5.5×10^{-6}
Length of X_o , lX_o	cm	152.1	34.739	27.026	19.88	0.35
Boil temperature	$^{\circ}C$	1347	2469	Sublim. at melt	3500	5660
Melt temperature	$^{\circ}C$	180.54	1287	2973	2350	3410
Compressibility	cm^2/kg	8.7×10^{-6}	9.27×10^{-7}			2.93×10^{-7}
Grüneisen coeff.	-					2.4
Speed of sound (long)	m/sec	6000	12890	16400	14920	5460
Specific heat	$J/g^{\circ}K$	3.6	1.82	1.47	0.95	0.134
Heat conductivity	$W/cm^{\circ}C$	0.848	2	7.4	0.3-0.4	1.67
Thermal expansion	$1/^{\circ}C$	4.6×10^{-6}	11×10^{-6}	2.7×10^{-6}	5×10^{-6}	4.3×10^{-6}

¹ Total mass of Lithium in ~70kg human body is ~7mg.

Lithium loop



Gear pump with Zirconium ceramic gears and case is desirable for elimination of back current flow along the cooling loop

Temperature in lens

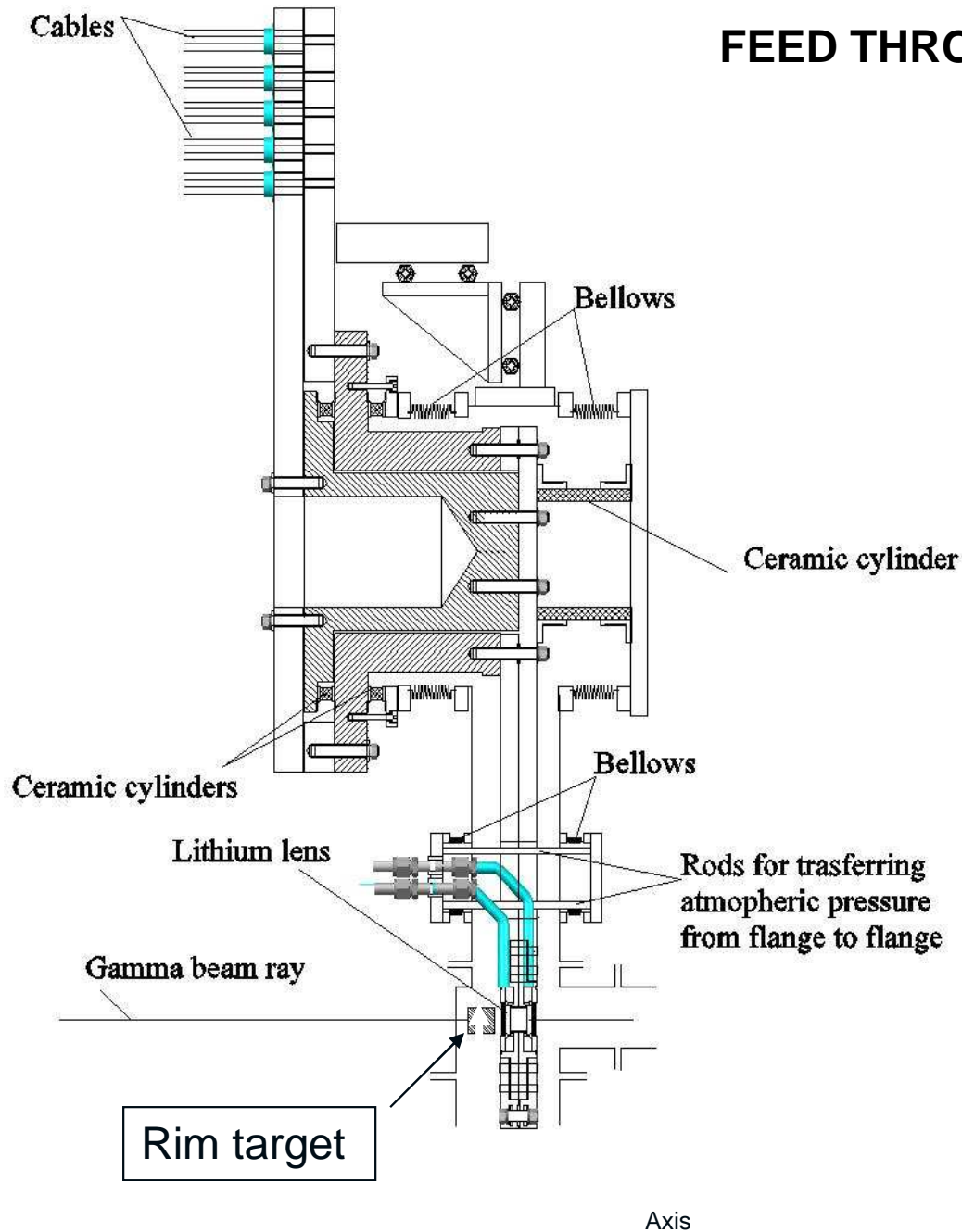
K=0.92; $\lambda=1.15$; Eff=1.6; Effp=32%; Undulator length=35m; Distance to target=300m

DISTRIBUTION OF TEMPERATURE IN LENS T(R,Z) DEG PER 10^{13} INITIAL ELECTRONS

DELTA R = .070 cm, DELTA Z = .050 cm, PHOTONS GENERATED = 76991

Be entr.	↑	39.396	23.757	16.011	11.015	6.154	3.953	2.325	1.351	.861	.275
	↓	38.128	22.818	15.563	10.848	6.569	4.287	2.792	1.669	1.254	.433
Li	↑	15.000	9.208	6.263	4.499	2.633	1.745	1.173	.689	.425	.162
		14.017	8.512	6.076	4.383	2.648	1.802	1.217	.795	.492	.197
		13.356	7.904	5.805	4.219	2.664	1.849	1.276	.875	.568	.198
		12.685	7.414	5.488	4.143	2.651	1.842	1.333	.948	.609	.205
		12.128	6.922	5.273	4.042	2.591	1.882	1.314	.968	.652	.221
		11.566	6.518	5.049	3.814	2.604	1.856	1.315	.959	.663	.221
		11.103	6.203	4.873	3.616	2.603	1.802	1.297	.904	.709	.213
		10.406	6.081	4.592	3.504	2.588	1.751	1.305	.913	.663	.226
		9.889	5.853	4.370	3.399	2.467	1.774	1.240	.915	.659	.224
		9.733	5.852	4.353	3.523	2.629	1.944	1.376	1.030	.738	.238
Be exit	↑	19.89	12.03	9.07	6.89	4.98	3.58	2.46	1.72	1.25	.40
	↓	20.17	12.17	9.15	6.93	5.04	3.76	2.65	1.84	1.42	.48

FEED THROUGH IN DETAIL



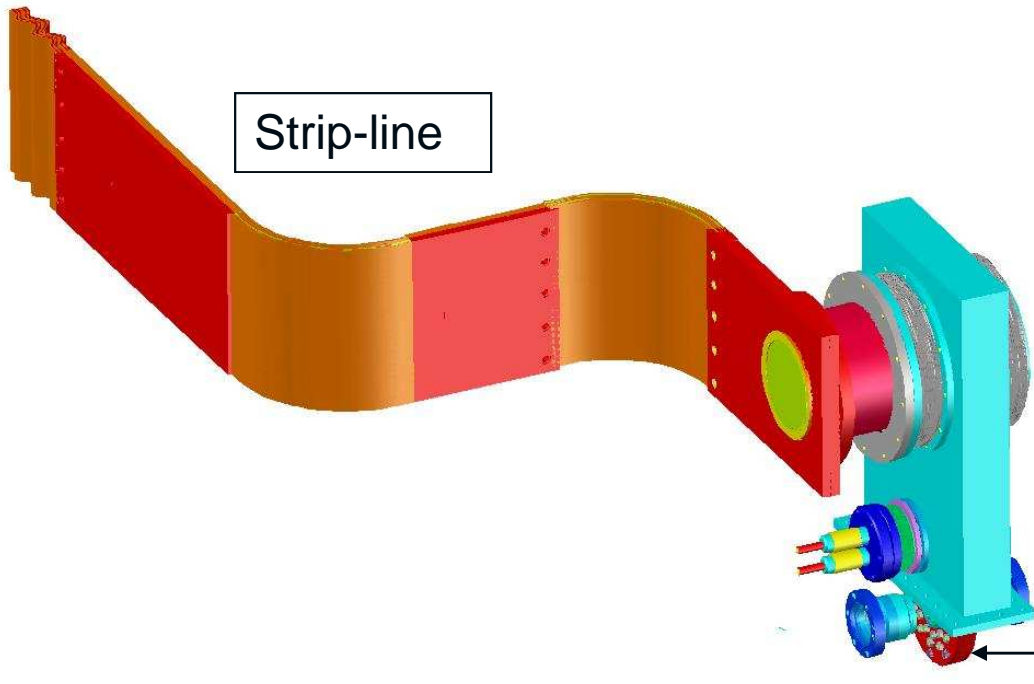
System with two bellows excludes net force from atmospheric pressure;

Positioning system serves for adjustment the distance between target and lens –what is required by optimization of yield/heating for the entrance window

Variants of current duct



Cables with non organic insulation



Strip-line

Li Lens

Current duct must be able to transfer ~ 150 kA in ~4 ms pulse with repetition rate up to 10 Hz

Li lens

EQUATIONS FOR MODELING WITH FlexPDE

Electromagnetics

$$\vec{E} = -\frac{\partial \vec{A}}{\partial t} - \text{grad}(U) \quad \vec{B} = \text{rot}(\vec{A}) \quad \vec{j} = \sigma \cdot (\vec{E} + \vec{v} \times \vec{B}) \quad \text{div}(\vec{j}) = 0$$

$$\text{div}(\text{grad}(A_x)) + \mu \cdot j_x = 0 \quad \text{div}(\text{grad}(A_y)) + \mu \cdot j_y = 0 \quad \text{div}(\text{grad}(A_z)) + \mu \cdot j_z = 0 \quad \Delta Q_{\text{tot}} = \int_0^{\Delta T} dt \int_V (\vec{j} \cdot \vec{E}) dV = \int_0^{\Delta T} dt \int_V \frac{j^2}{\sigma} dV$$

Hydrodynamics

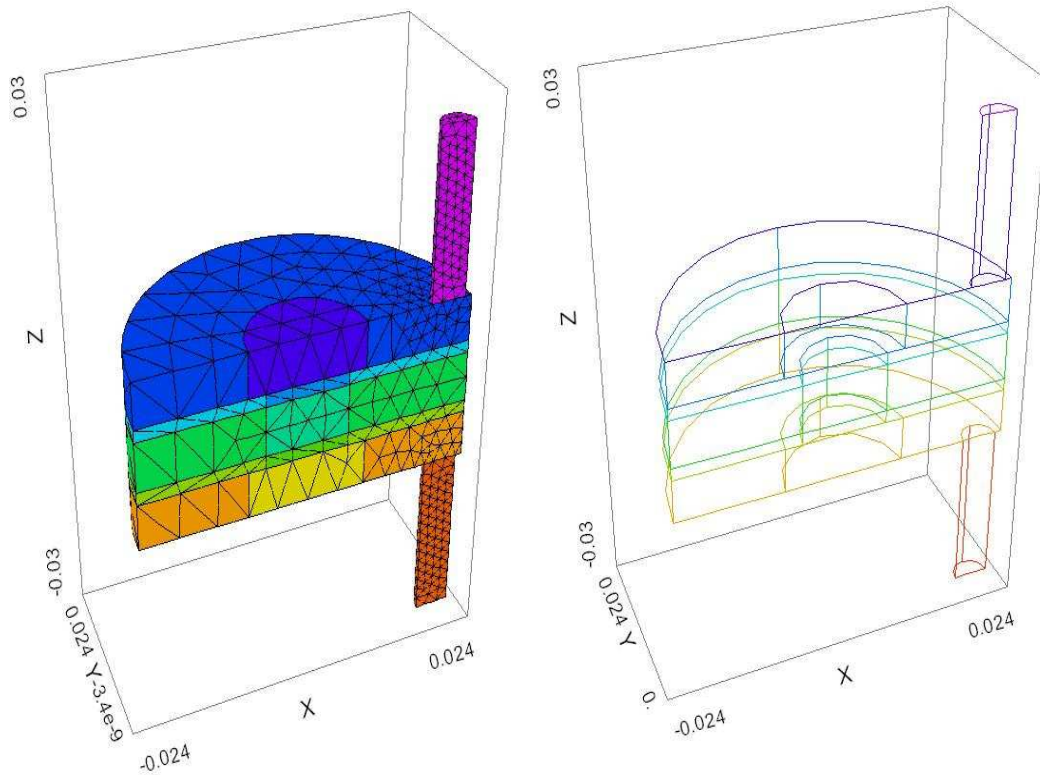
$$\frac{\partial}{\partial t} \rho v_i = -\frac{\partial \Pi_{ik}}{\partial x_k} \quad \text{momentum flux density tensor} \quad \Pi_{ik} = P \cdot \delta_{ik} + \rho \cdot v_i v_j - \sigma'_{ik} - \mu_0 (H_i H_k - \frac{1}{2} H^2 \delta_{ik}) \quad \text{Deviatoric stress tensor} \quad \sigma'_{ij} = \eta \left(\frac{\partial v_i}{\partial x_j} + \frac{\partial v_j}{\partial x_i} - \frac{2}{3} \delta_{ij} \frac{\partial v_k}{\partial x_k} \right) + \zeta \cdot \delta_{ij} \frac{\partial v_k}{\partial x_k}$$

$$\text{In vector form} \quad \rho \cdot \left(\frac{\partial \vec{v}}{\partial t} + (\vec{v} \cdot \vec{\nabla}) \vec{v} + \text{grad}(P) - \eta \cdot \nabla^2 \vec{v} \right) = (\vec{j} \times \vec{B})$$

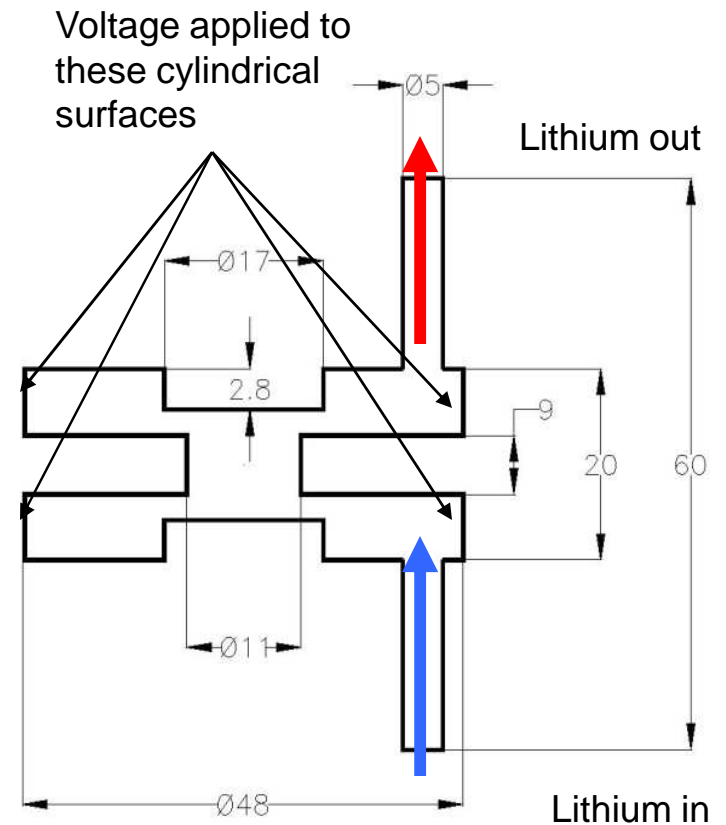
$$\text{For pressure} \quad \text{div}(\text{grad}(P)) \left\{ -\frac{1}{c_B^2} \frac{\partial^2 P}{\partial t^2} \right\} = \text{div}(\vec{j} \times \vec{B}) - \rho \cdot \text{div} \left(\frac{\partial \vec{v}}{\partial t} + (\vec{v} \cdot \vec{\nabla}) \vec{v} \right) + C \eta \cdot \text{div}(\vec{v}) \left\{ -\Gamma \cdot \ddot{Q}(\vec{r}, t) \right\}$$

Temperature

$$\rho \cdot C_p \left(\frac{\partial T}{\partial t} + \vec{v} \cdot \text{grad}(T) \right) - \text{div}(k \cdot \text{grad}(T)) + P \cdot \text{div}(\vec{v}) = (\vec{j} \cdot \vec{E}) + \sigma'_{ik} \frac{\partial v_i}{\partial x_k} + \dot{Q}(\vec{r}, t)$$



Model as it appears in FlexPDE

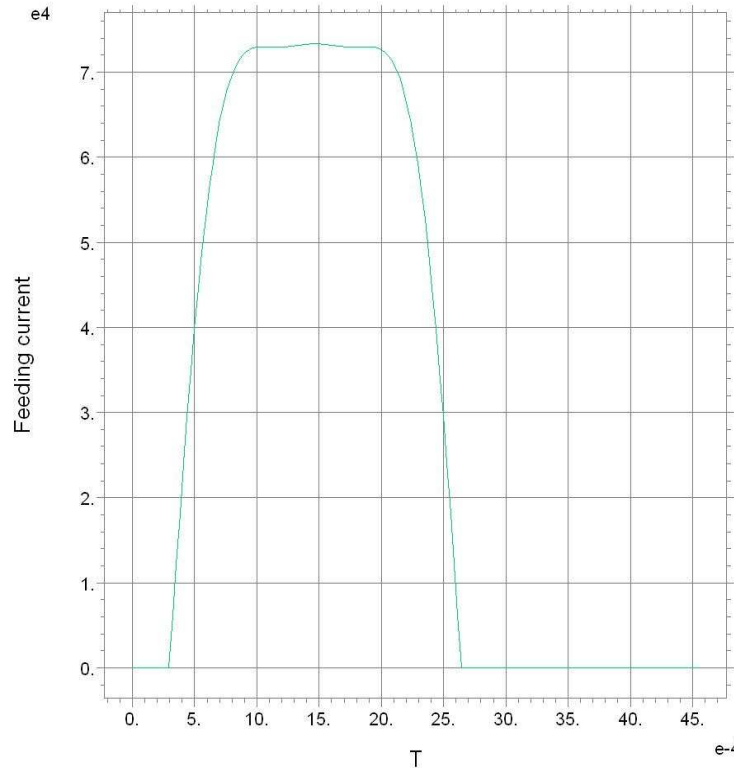


Dimensions, *mm*

Feeding voltage composed with three odd harmonics 1,3,5

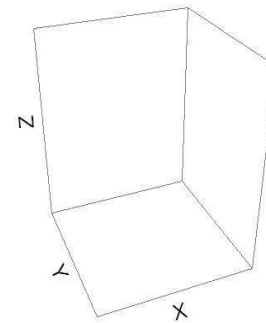
Lithium Lens with Viscous Flow-3

12:11:14 1/5/10
FlexPDE 6.11



HISTORY

1: Current_tot

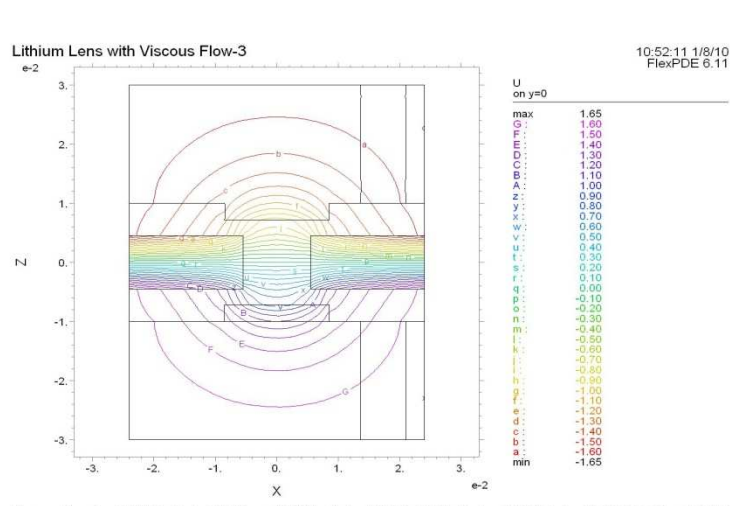


Viscose flow Jan 4 2010: Cvcle=160 Time= 4.5531e-3 dt= 2.6118e-5 P2 Nodes=17741 Cells=12198 RMS Err= 0.0615

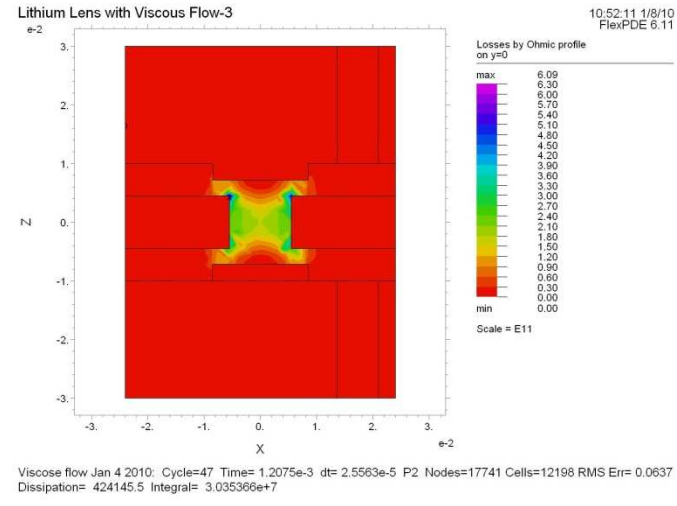
Voltage applied

$$U(t) = U_0 \cdot \left[-4.5 \cdot \sin\left(\frac{\pi \cdot (t - \tau/10)}{\tau}\right) - 0.9 \cdot \sin\left(\frac{3\pi \cdot (t - \tau/10)}{\tau}\right) - 0.17 \cdot \sin\left(\frac{5\pi \cdot (t - \tau/10)}{\tau}\right) \right]$$

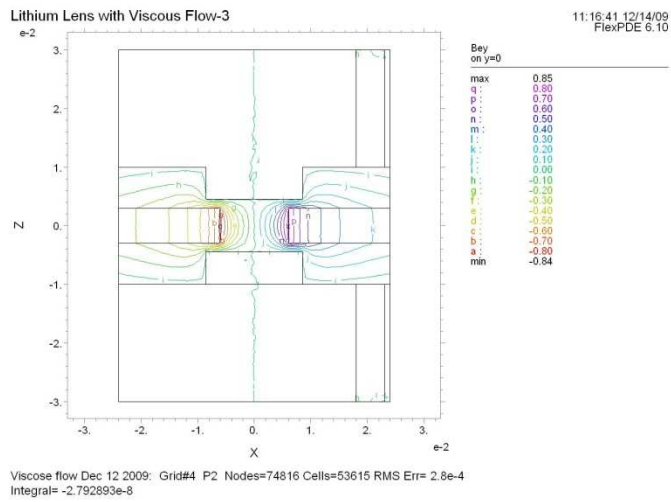
Calculation done with FlexPDE[®] code (frames from the cinema)



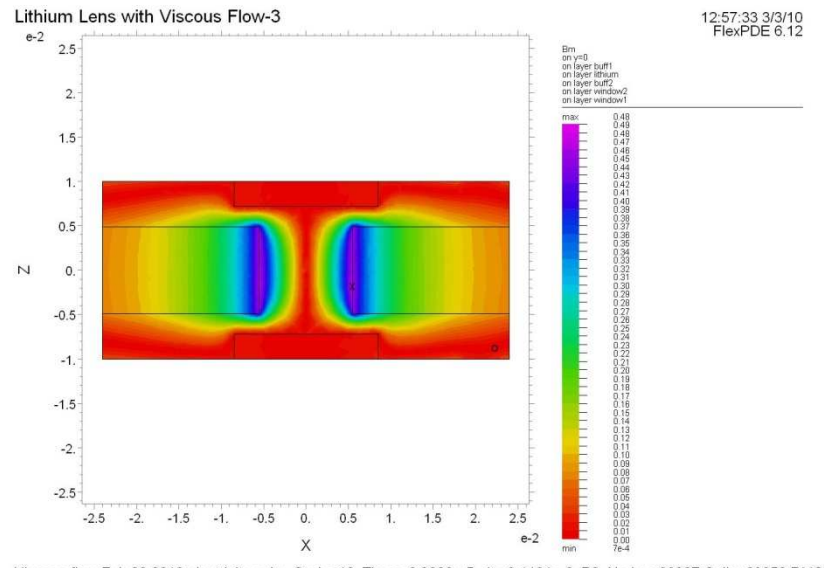
Potential



Ohmic losses

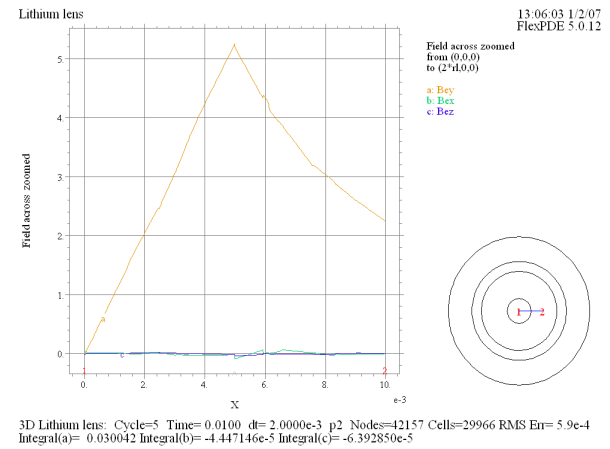
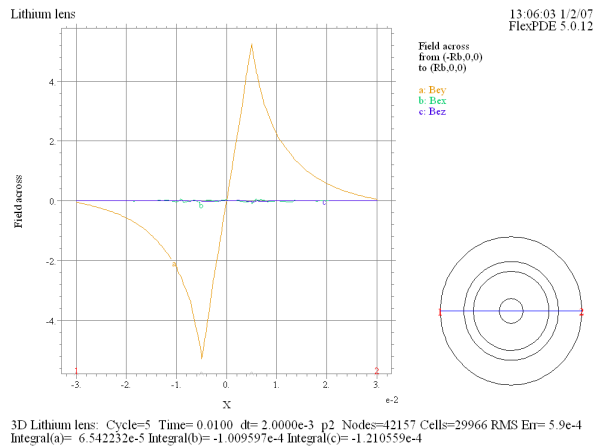
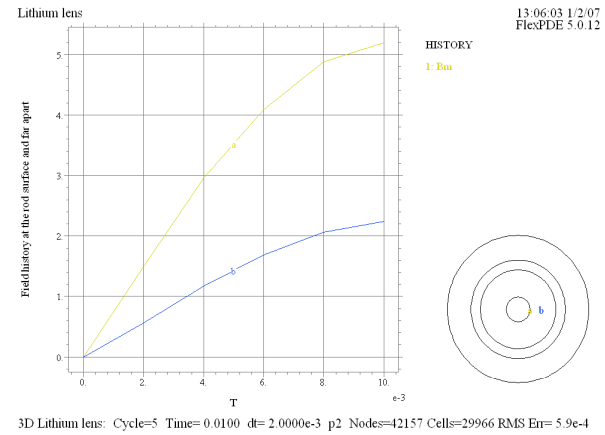
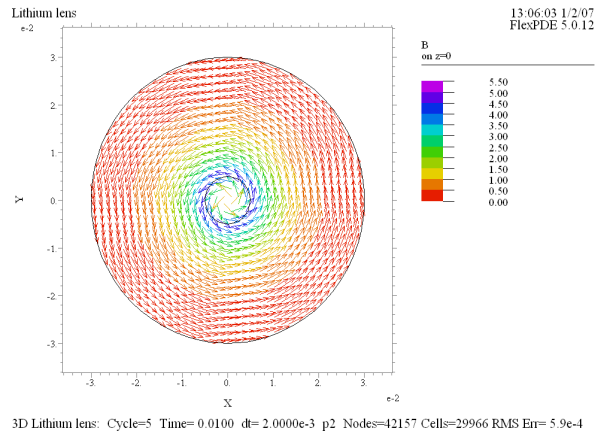


Magnetic field; I=0.5cm



Magnetic field I=1cm

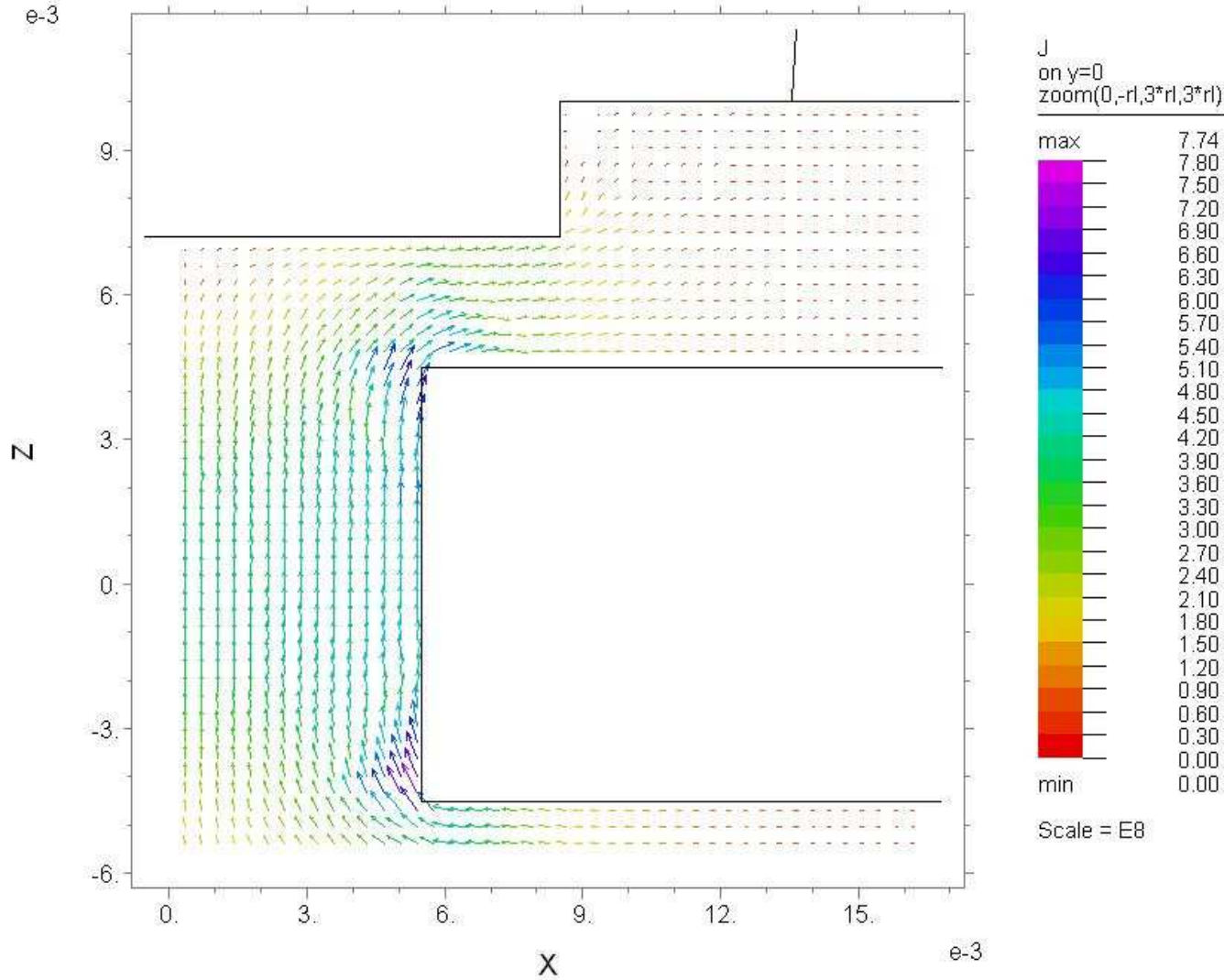
Spatial field distribution over time



Current flow

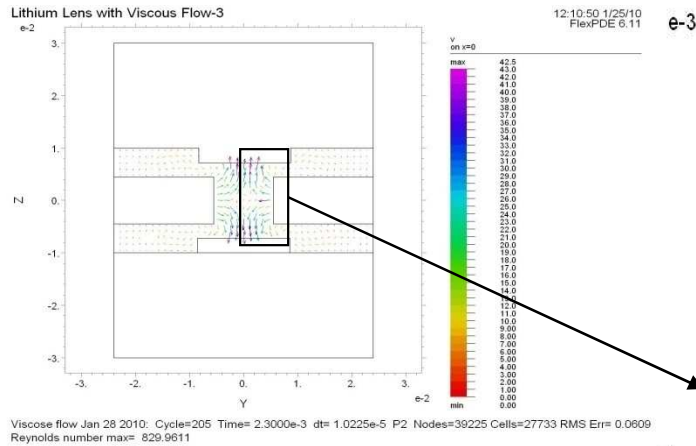
Lithium Lens with Viscous Flow-3

20:38:19 1/4/10
FlexPDE 6.11



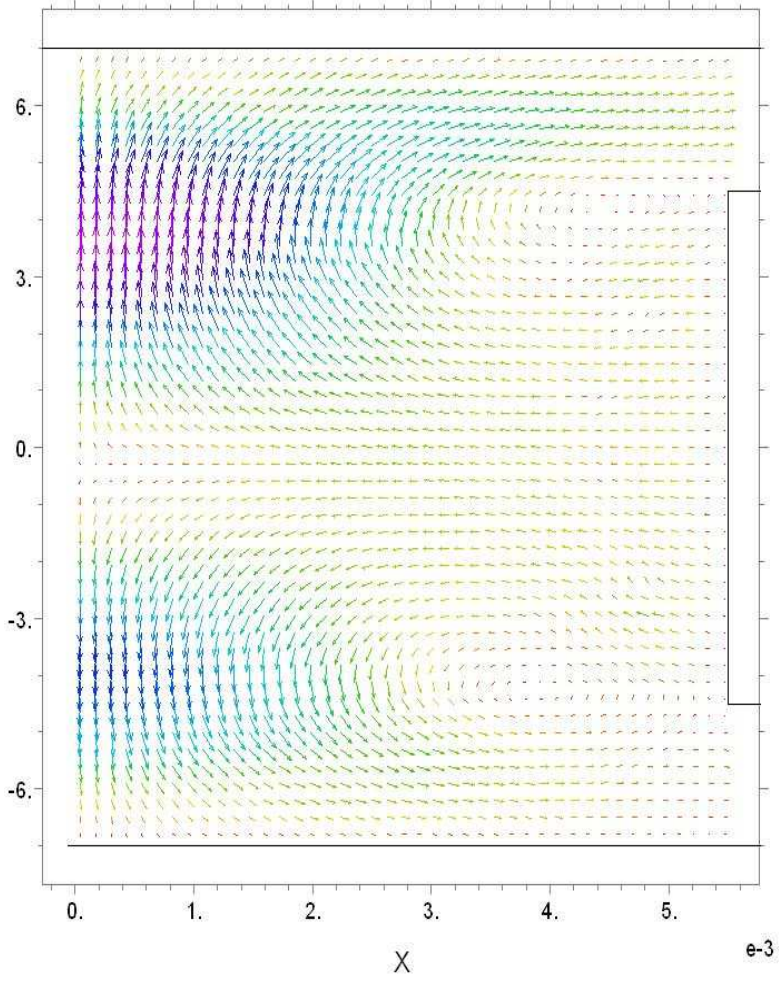
Viscose flow Jan 4 2010: Cycle=88 Time= 2.4381e-3 dt= 2.6118e-5 P2 Nodes=17741 Cells=12198 RMS Err= 0.0609
Power of dissipation, Watts= 126634.3

Identified vortex lithium flow



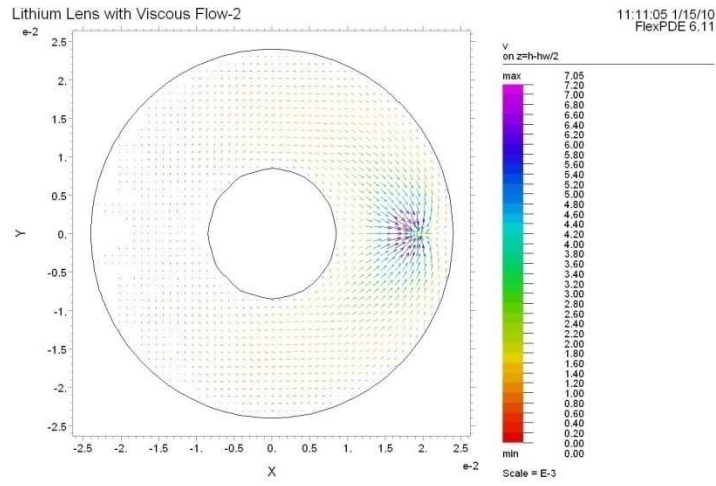
Lithium Lens with Viscous Flow-3

10:15:45 12/22/09
 FlexPDE 6.11

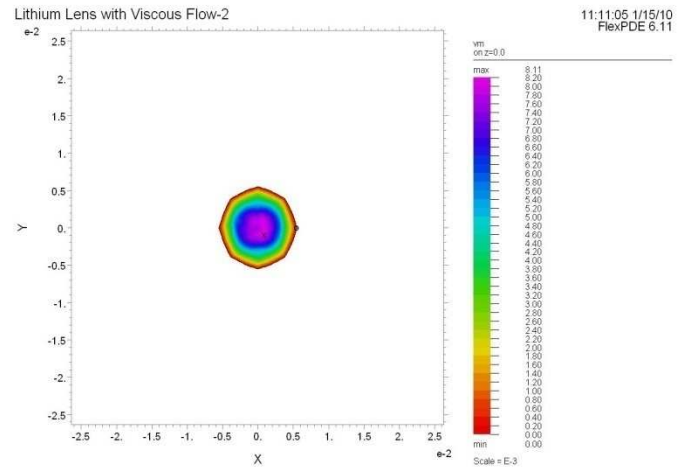


$$\text{grad}(P) \cong (\vec{j} \times \vec{B})$$

Viscose flow Dec 21 2009: Grid#1 P2 Nodes=51508 Cells=36675 RMS Err= 0.0248
 Stage 2 Reynolds number max= 0.034599

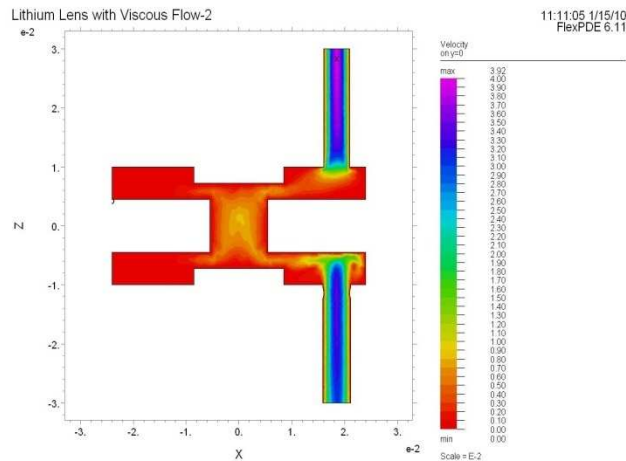


just Viscose flow 2: Cycle=30 Time= 1.1500e-3 dt= 4.0900e-5 P2 Nodes=8745 Cells=4959 RMS Err= 5.8e-4 Re= 2353.704



just Viscose flow 2: Cycle=30 Time= 1.1500e-3 dt= 4.0900e-5 P2 Nodes=8745 Cells=4959 RMS Err= 5.8e-4 Re= 2353.704 Integral= 3.737796e-7

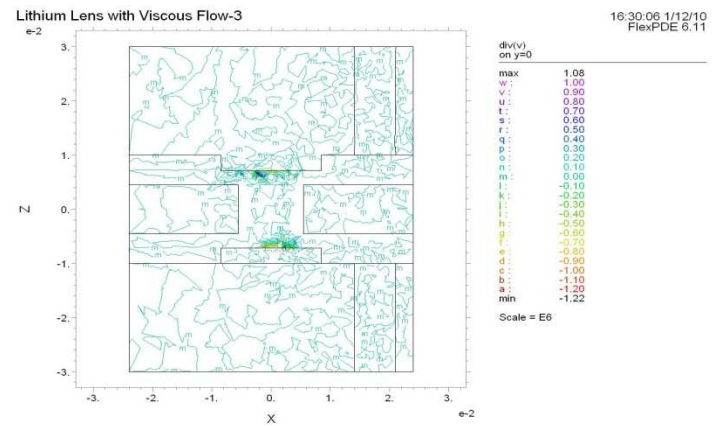
Velocity profile just below outlet tube.



just Viscose flow 2: Cycle=12 Time= 3.2200e-4 dt= 4.0900e-5 P2 Nodes=8745 Cells=4959 RMS Err= 5.7e-4 Re= 2354.940 Integral= 6.752512e-6

Laminar flow of Lithium

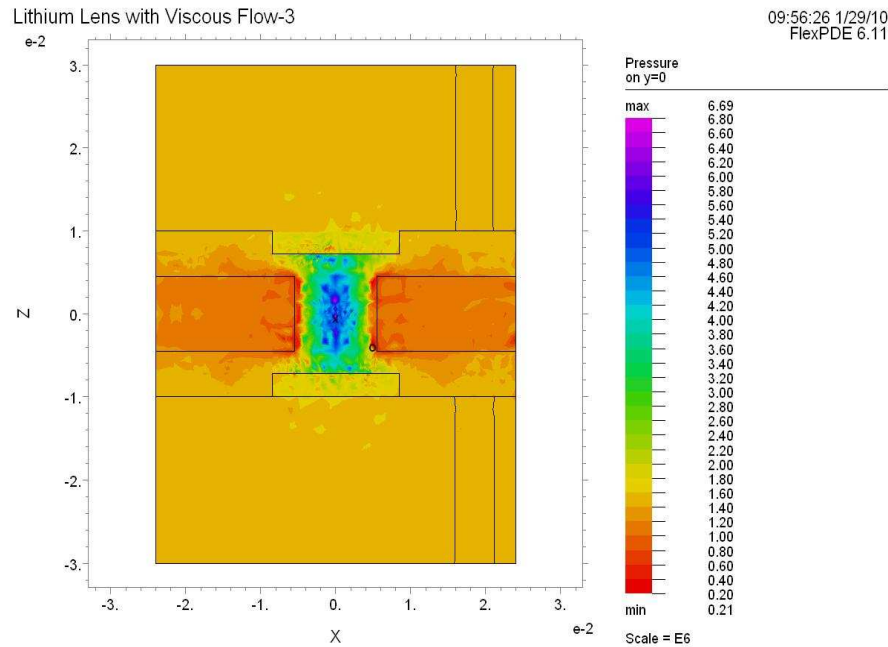
Velocity profile in the middle of model (across the plane with central point $\{x=0, y=0, z=0\}$).



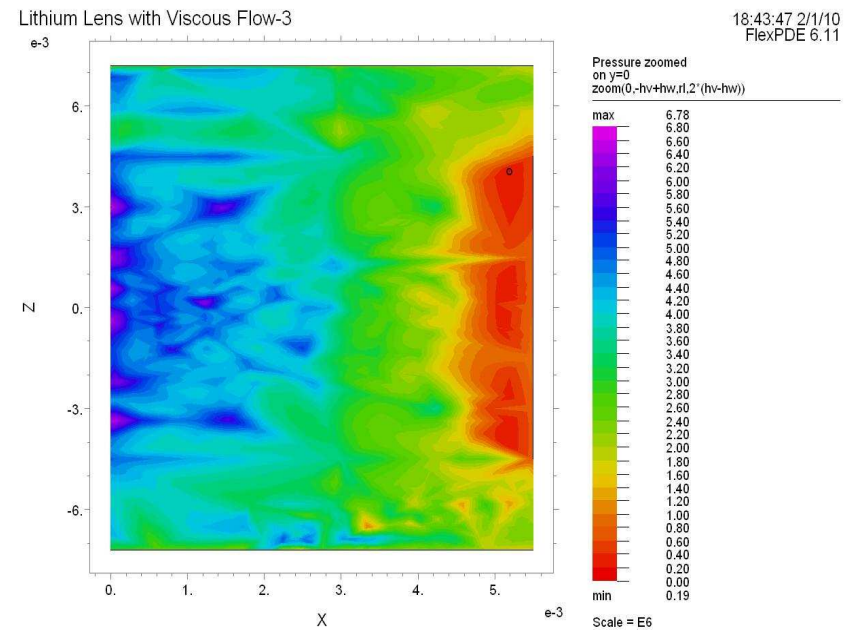
Viscose flow Jan 12 2010: Cycle=25 Time= 5.7500e-4 dt= 2.2024e-5 P2 Nodes=25907 Cells=18151 RMS Err= 5.7222 Reynolds number max= 1.369384e+7 Integral= -1.496218

Contour plot of $div(\mathbf{v})$; it is zero practically everywhere with numeric accuracy.

PRESSURE DYNAMICS



Viscose flow Jan 28 2010: Cycle=135 Time= 1.4950e-3 dt= 1.0225e-5 P2 Nodes=55609 Cells=39554 RMS Err= 0.0559
Integral= 4451.796



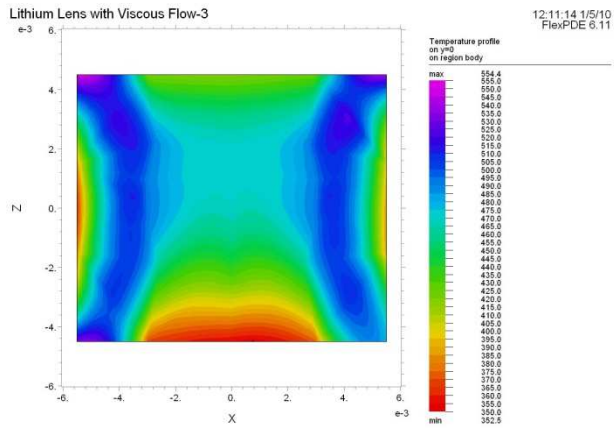
Viscose flow Feb 2 2010: Cycle=165 Time= 1.8400e-3 dt= 1.0780e-5 P2 Nodes=73398 Cells=52442 RMS Err= 0.0304
Reynolds number max= 1635.005 Integral= 278.4650

Pressure in a volume while current is running

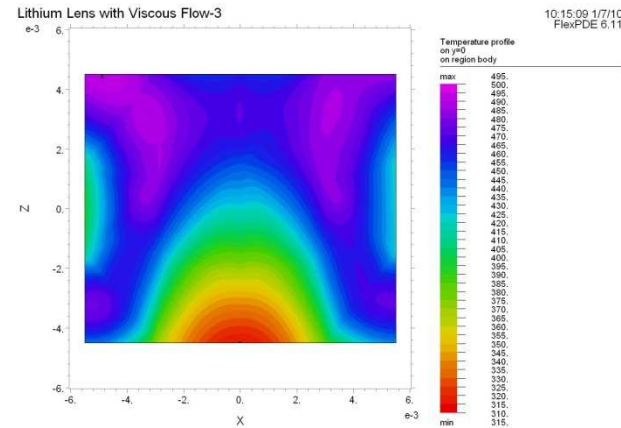
Pressure from previous Figure zoomed at central region, term $\mathbf{J} \times \mathbf{B}$ in on.

Time is ~1.84 msec from beginning of process

Temperature dynamics



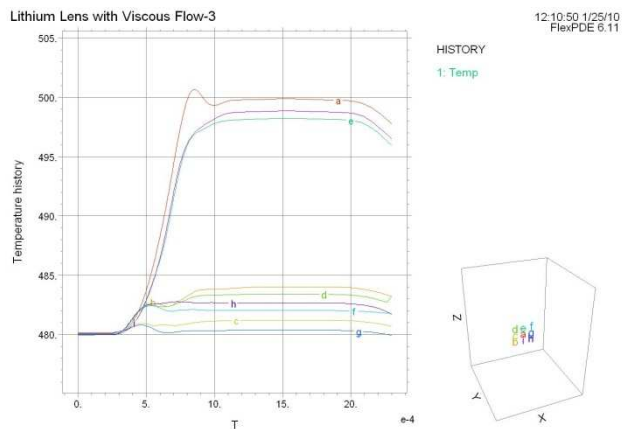
Viscose flow Jan 4 2010: Cycle=100 Time= 4.5531e-3 dt= 2.6118e-5 P2 Nodes=17741 Cells=12198 RMS Err= 0.0615
Dissipation= 2.069478e-303 Integral= 0.045868



Viscose flow Jan 4 2010: Cycle=405 Time= 0.0115 dt= 2.5563e-5 P2 Nodes=17741 Cells=12198 RMS Err= 0.0615
Dissipation= 1.009784e-19 Integral= 0.043638

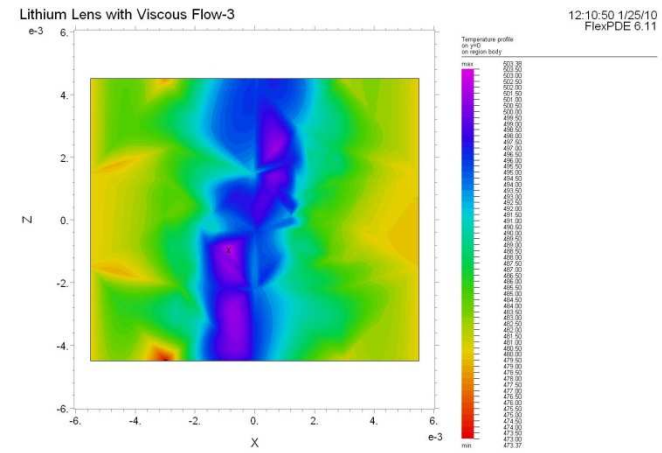
Temperature profile painted, 4.5 msec passed since start

Temperature profile painted, 11.5 msec passed since start; just in/out temperature fixed



Viscose flow Jan 28 2010: Cycle=205 Time= 2.3000e-3 dt= 1.0225e-5 P2 Nodes=39225 Cells=27733 RMS Err= 0.0609

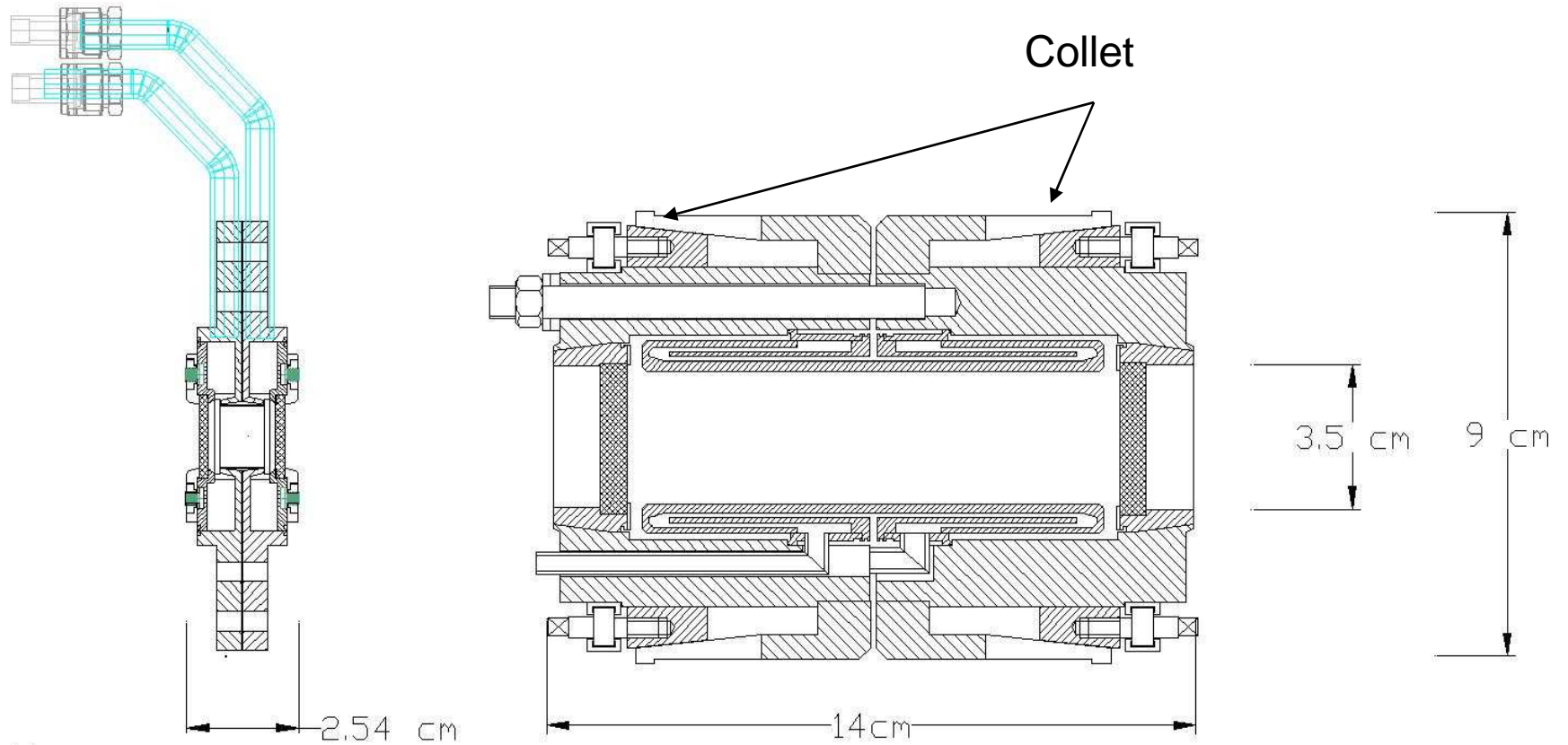
Temperature history at the same points, when the walls temperature kept constant at 480°K



Viscose flow Jan 28 2010: Cycle=205 Time= 2.3000e-3 dt= 1.0225e-5 P2 Nodes=39225 Cells=27733 RMS Err= 0.0609
Dissipation= 149575.4 Integral= 0.048271

Temperature profile painted, 2.3 msec passed since start; just in/out temperature fixed

Li lens for ILC and Li lens for collection of antiprotons

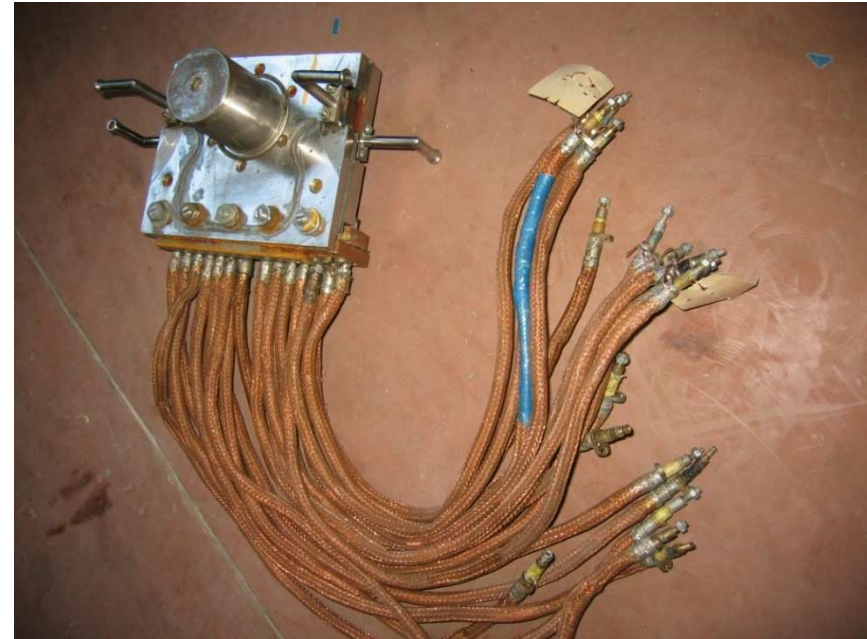
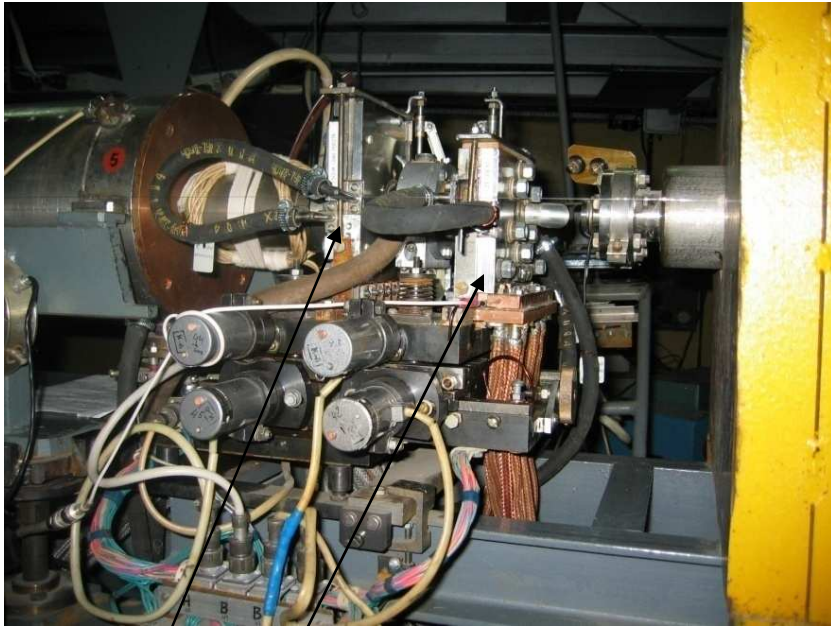


Lithium lenses represented with the same scale factor.

	Positrons	Antiprotons	Neutrino factory
Diameter, <i>cm</i>	1.4	2-3.6	1.8- 6
Length, <i>cm</i>	1	10	15
Current, <i>kA</i>	<75	~850	500
Pulse duty, <i>msec</i>	~4	0.1	~1
Repetition rate, <i>Hz</i>	5	0.7	0.7
Resistance $\mu\Omega$	32	50	27
Gradient, <i>kG/cm</i>	<65	55	45
Surface field, <i>kG</i>	43	100	80-40
Pulsed Power, <i>kW</i>	~360	36000	6750
Average Power, <i>kW</i>	~7.5	3.6	4.7
Temperature gain/pulse, $^{\circ}K$	85	80	80
Pressure at axis, <i>atm</i>	~19	400	256-64

Doublet of Solid Lithium lenses in Novosibirsk BINP

Photo- courtesy of Yu Shatunov



First lens is used for focusing of primary 250 MeV electron beam onto the W target,

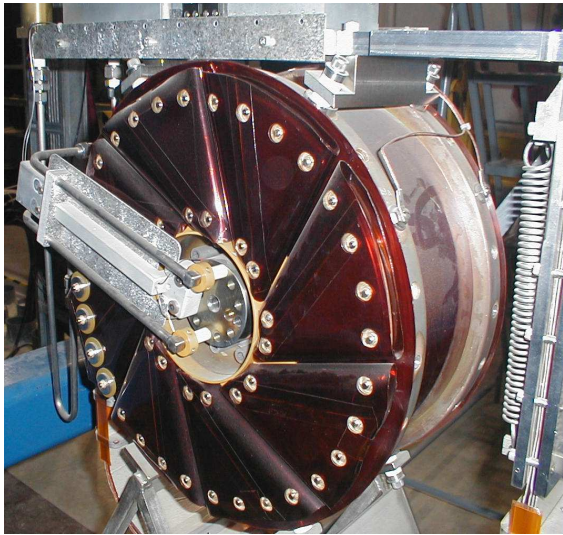
Second lens installed after the target and collects positrons at ~150MeV

Number of primary electrons per pulse $\sim 2 \cdot 10^{11}$; ~ 0.7 Hz operation (defined by the beam cooling rate in a Damping Ring)

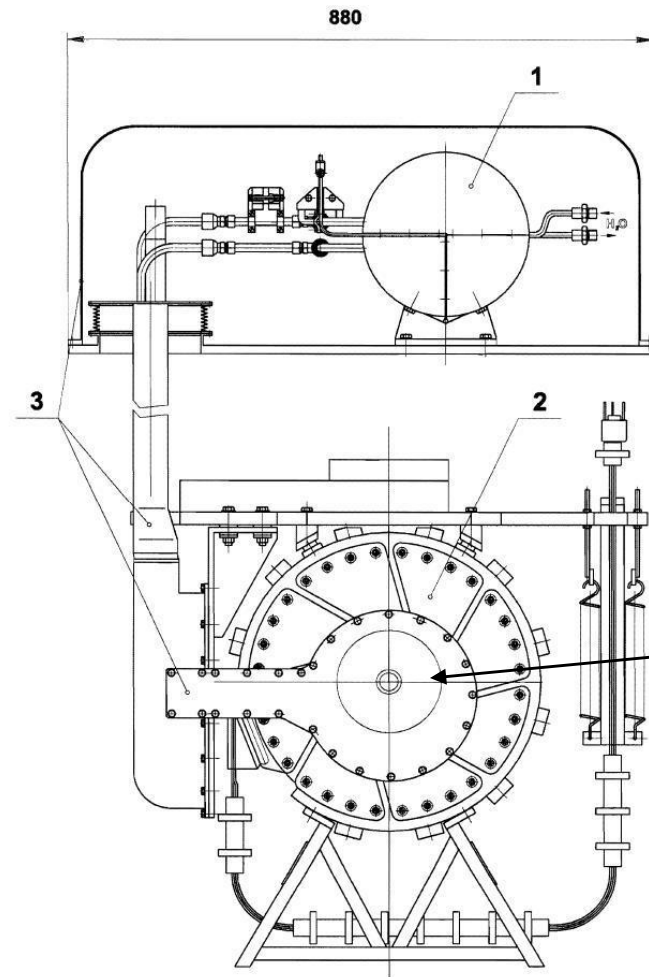
Lenses shown served ~ 30 Years without serious problem (!)

Lenses designed at BINP Novosibirsk for FERMILAB

Lens with liquid Lithium



Lens with solid LI



1-liquid lithium pump; 2-toroidal transformer; 3-lithium circuit protection.

B.Bayanov et al., "Liquid Lithium Lens for FermiLab Antiproton Source", Novosibirsk BINP, 98-23, 1998.

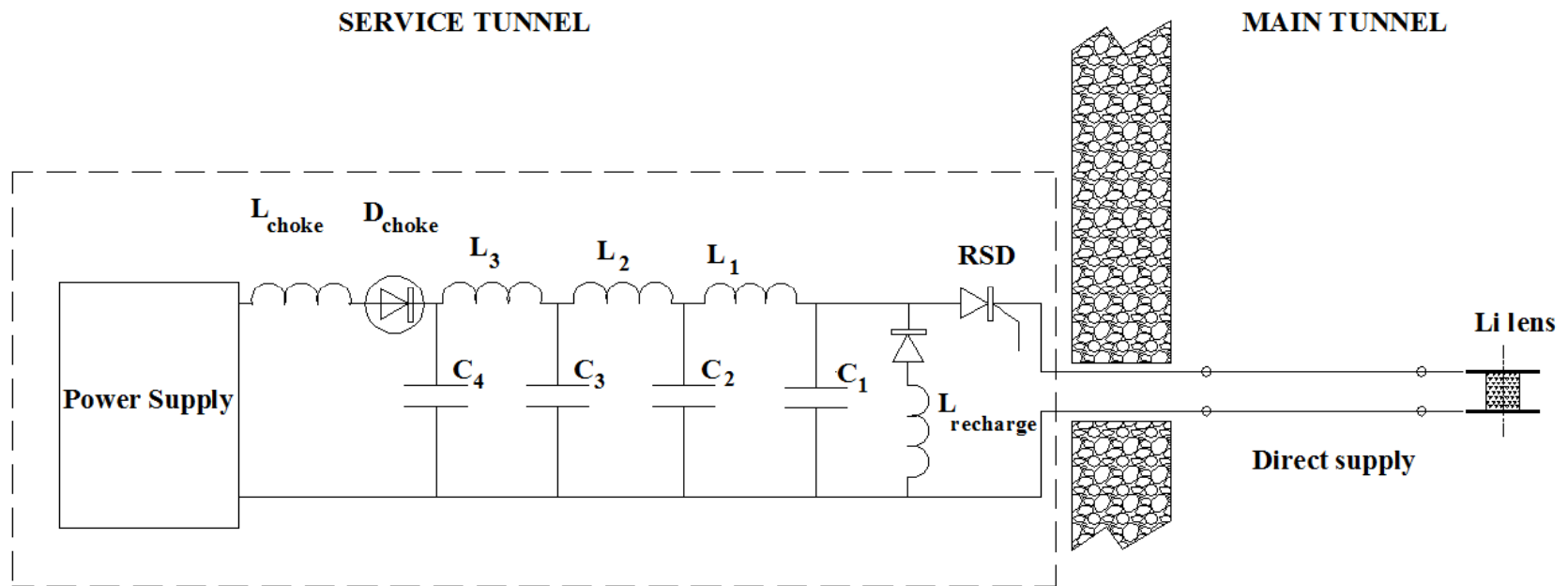
NEW TYPE OF COMMUTATORS FOR HIGH CURRENT



Fig.2. Reverse – switched diodes for peak current from 200 kA to 500 kA and blocking voltage of 2400 V, encapsulated in hermetic metal – ceramic housing and without housing (RSD sizes of 64, 76, and 100 mm)

S.A. Belyaev, V.G.Bezuglov, V.V.Chibirikin, G.D.Chumakov, I.V.Galakhov, S.G.Garanin, S.V.Grigorovich, M.I.Kinzibaev, A.A.Khapugin, E.A.Kopelovich, F.A.Flar, O.V.Frolov, S.L.Logutenko, V.A.Martynenko, V.M.Murugov, V.A.Osin, I.N.Pegoev, V.I.Zolotovskii, "New Generation of High-Power Semiconductor Closing Switches for Pulsed Power Applications", 28 ICPIG, July 15-20, 2007, Prague, Czech Republic, Topic#17, pp.1525-1528.

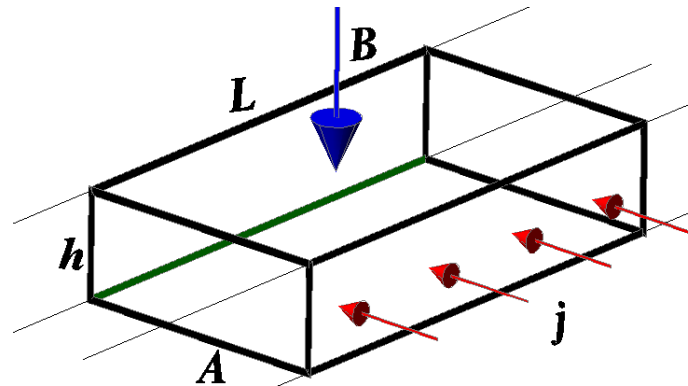
POWER SUPPLY SCHEMATICS



WITH RDS, THE POWER SUPPLY IS PRETTY GUARANTEED

PUMPS

MGD pump



$$\vec{\nabla}P = \vec{j} \times \vec{B} \cong |\vec{j}| \cdot B$$

$$\Delta P = |\vec{j}| B \cdot L$$

$$\Delta P = \frac{I \cdot B \cdot L}{L \cdot h} = \frac{I \cdot B}{h}$$

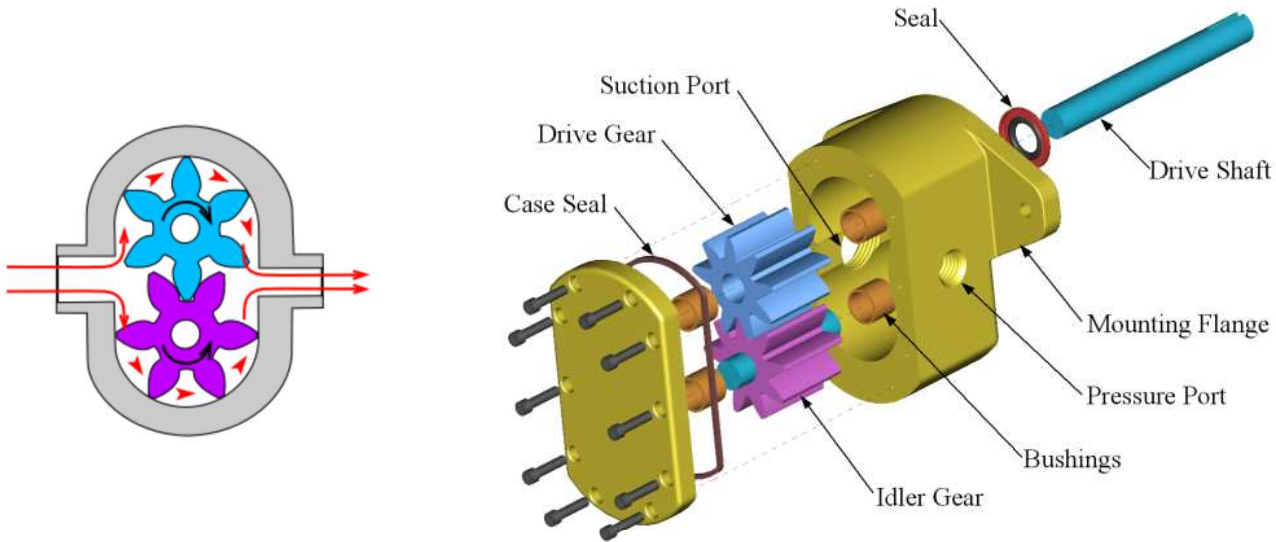
For example, if $I=400$ A, $h=4$ mm, $B=1$ T, then $\Delta P=10^5$ Pa ~ 1 atm

The flow meter works with the same components as the pump. $\vec{E} = \vec{v} \times \vec{B}$

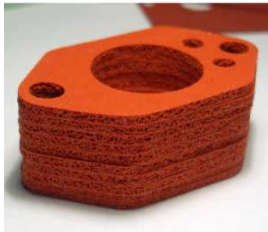
So the E.M.F. will be $v \times B \times A$.

For example, if $v=1$ m/s, $B=1$ T, $A=10$ cm = 0.1 m, then $E.M.F.=0.1$ V, i.e. the macroscopic value, which could be measured pretty accurately.

Gear pump (From Wikipedia)



Made from 316 StSteel, Ti, Ceramics, etc.



HT gaskets.

Auburn Co. (at the left) and McNeil Co. (at the right).

Materials: Aluflex (-54°C--+500°C),
Blue-Gard (+370°C)
Fiberfrax(+700°C--+1260°C) Viton
(+220°C)

One example

SCHERZINGER
PUMP TECHNOLOGY

Scherzinger

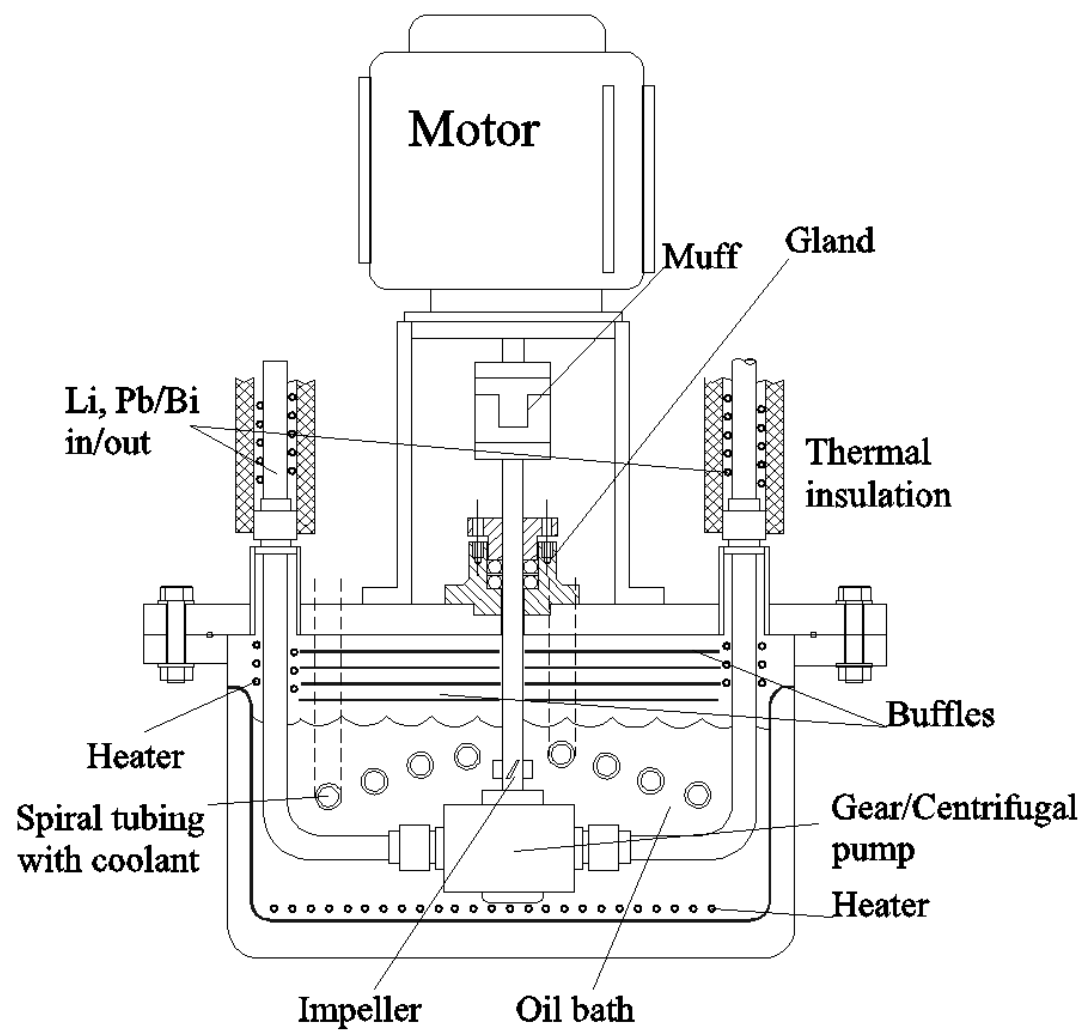


Transfer pumps for high temperature applications

Extreme temperatures and low viscosities, particularly with thermal oils, are no problem for these transfer pumps.

Fluid transfer remains reliable even at temperatures up to 300°C and low viscosities.

- Flow rates: 1 m³/h or 2.5 m³/h
- Differential pressure: Max. 10 bars



Pump setup. This pump is working for Bi/Pb, Li, Ga, Hg

Piston-type pump

B.Bayanov et al., "Liquid Lithium Lens for FermiLab Antiproton Source", Novosibirsk BINP, 98-23, 1998.

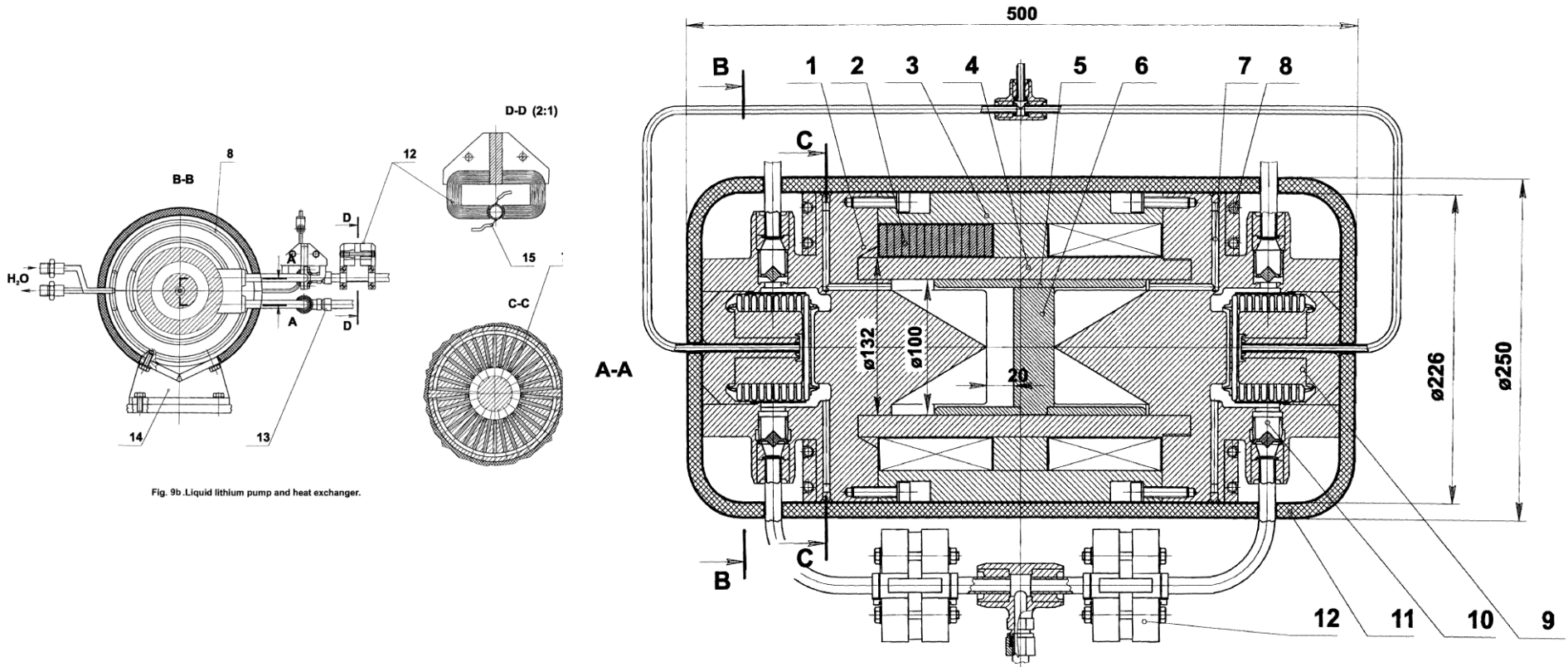


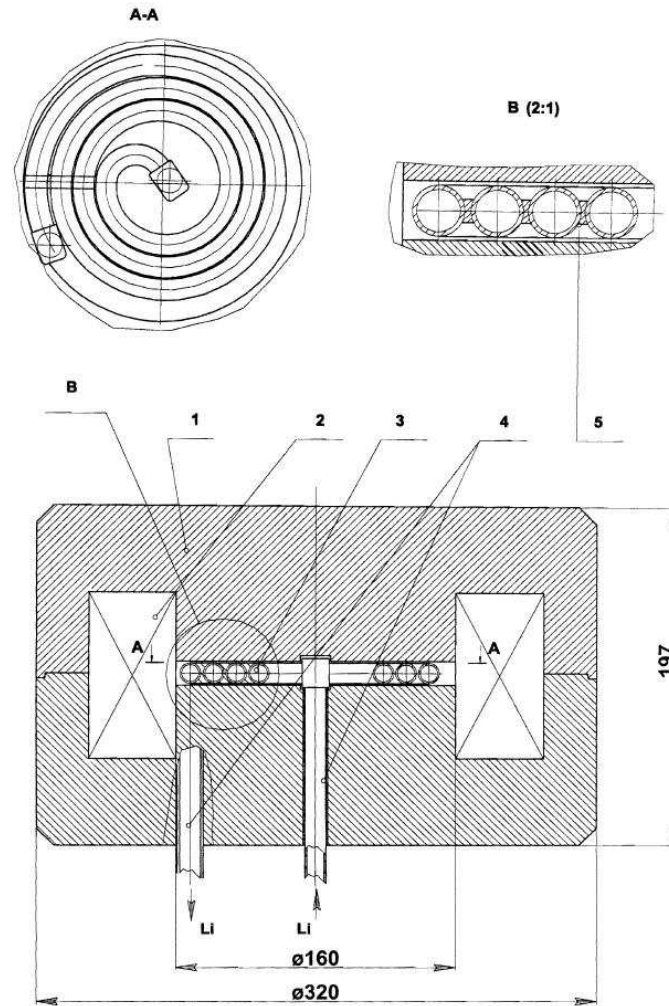
Fig. 9b. Liquid lithium pump and heat exchanger.

Fig.9a. Liquid lithium pump and heat exchanger.

- 1-face disks; 2-exciting coil; 3-return yoke; 4-inside ferromagnetic wall of cylinder; 5-plunger;
- 6-ferromagnetic insert of plunger; 7-cooling channels of heat exchanger; 8-cooling water;
- 9-system to apply and control of liquid lithium static pressure; 10- switching valves;
- 11 - thermo-insulation; 12-system to measure liquid flow rate; 13-jont of liquid lithium pipes;
- 14-pump support; 15 -contacts for potential measurements.

Spiral type

B.Bayanov et al., "Liquid Lithium Lens for FermiLab Antiproton Source", Novosibirsk BINP, 98-23, 1998.



- 1-DC magnet yoke;
- 2-exciting coils;
- 3-spiral type;
- 4-liquid Lithium inputs;
- 5-soldered shortened inserts.

Liquid lithium pump of spiral type.

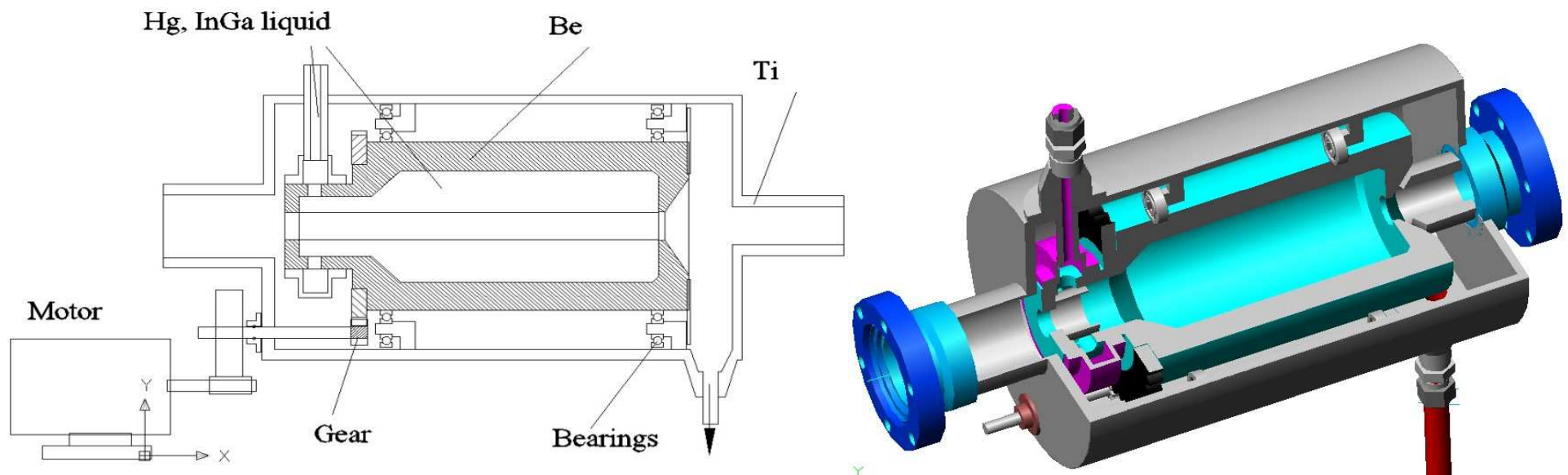
5. COLLIMATORS AND THE PHOTON DUMP

A.Mikhailichenko," Physical Foundations for Design of High Energy Beam Absorbers",
CBN09-9, Oct. 23, 2008, Cornell, LEPP,
<http://www.lns.cornell.edu/public/CBN/2008/CBN08-8/CBN08-8.pdf>

High Power Collimator for the Main Beam

Installed in front of the undulator

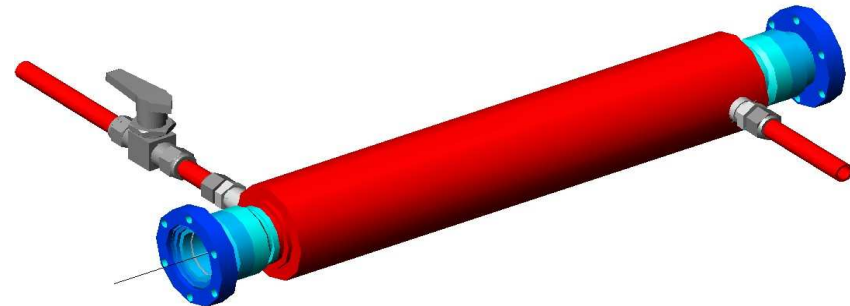
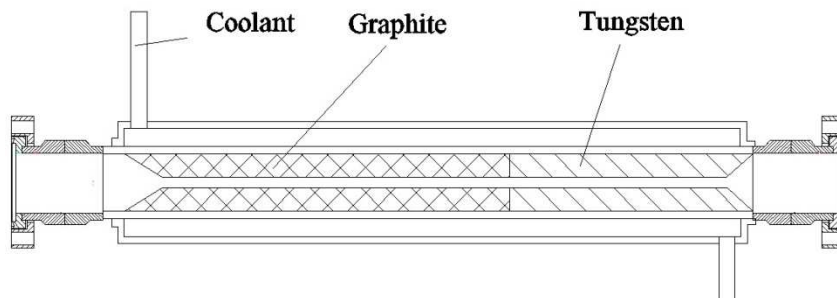
Spinning Liquid metal formed a cylinder as result of centrifugal force



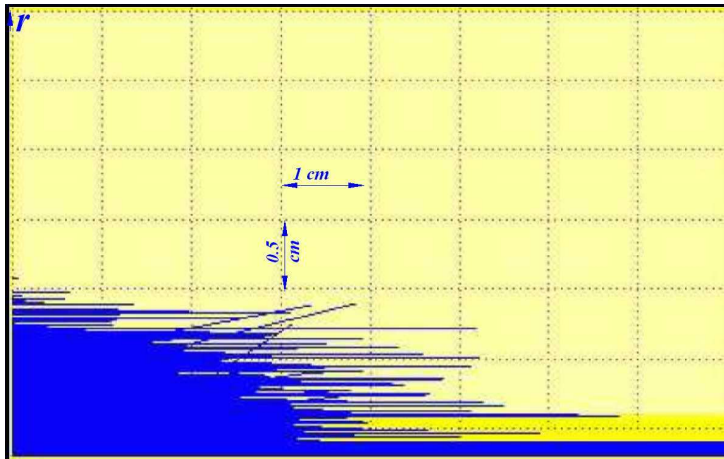
High average power collimator. Beam is coming from the right.

Collimator for gammas

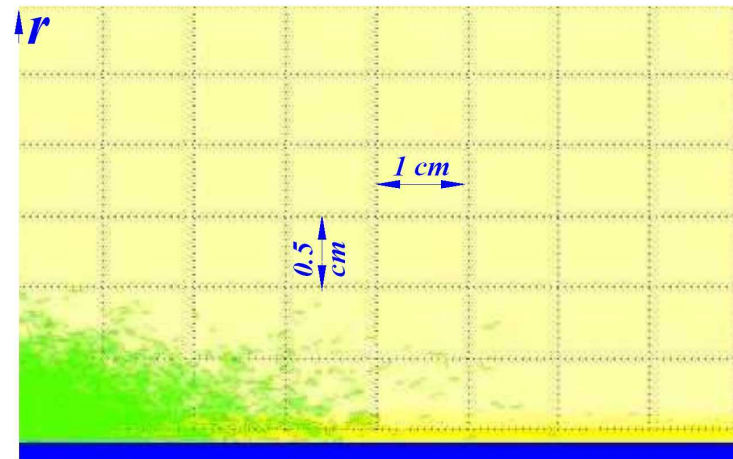
Pyrolytic Graphite (PG) is used here. The purpose of it is to increase the beam diameter, before entering to the W part. Vacuum outgassing is negligible for this material. Heat conductivity $\sim 300 \text{ W/m}\cdot\text{K}$ is comparable with metals. *Beryllium* is also possible here, depending on task.



Transverse dimensions defined by Moliere radius

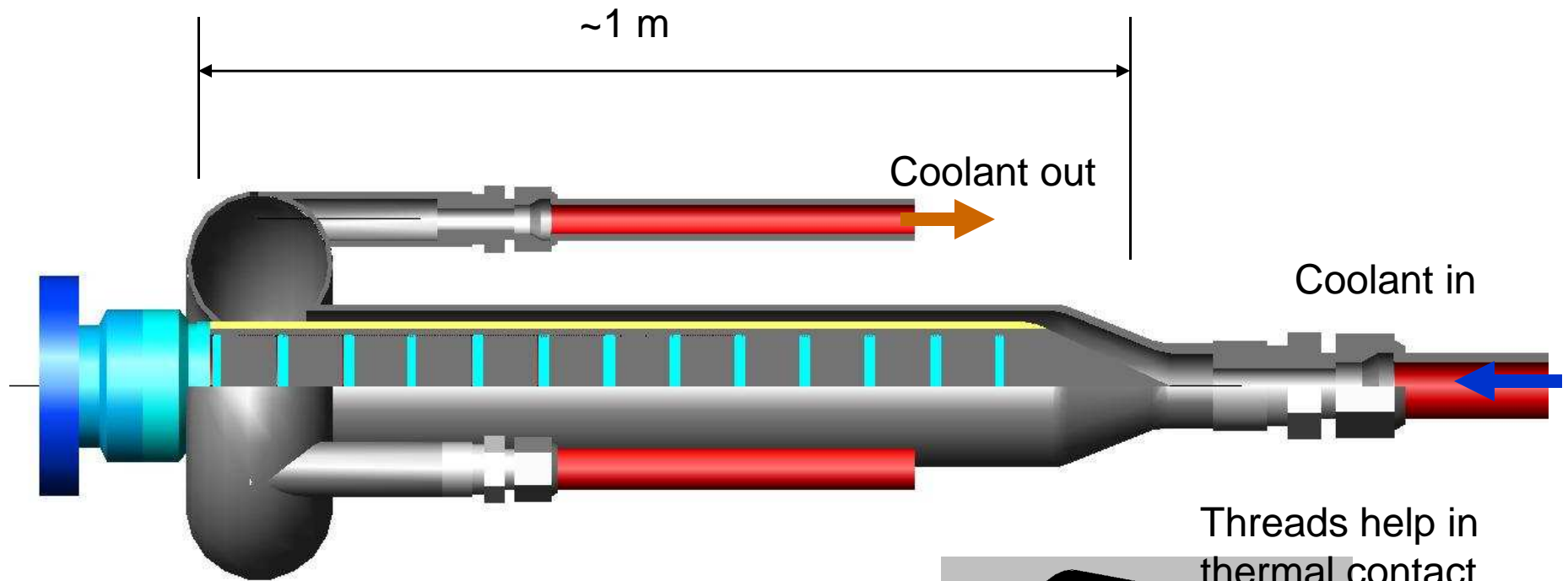


Gamma-beam. $\sigma_\gamma = 0.5 \text{ cm}$, diameter of the hole (blue strip at the bottom) $d = 2 \text{ mm}$. Energy of gamma-beam coming from the left is 20 MeV .



Positron component of cascade

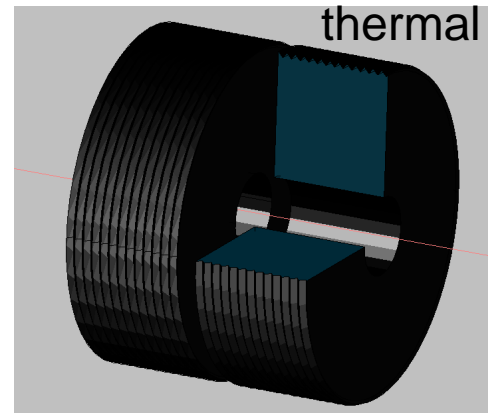
Gamma dump with PG and Ti baffles



Power 200kW requires coolant flow rate for temperature jump 20°C

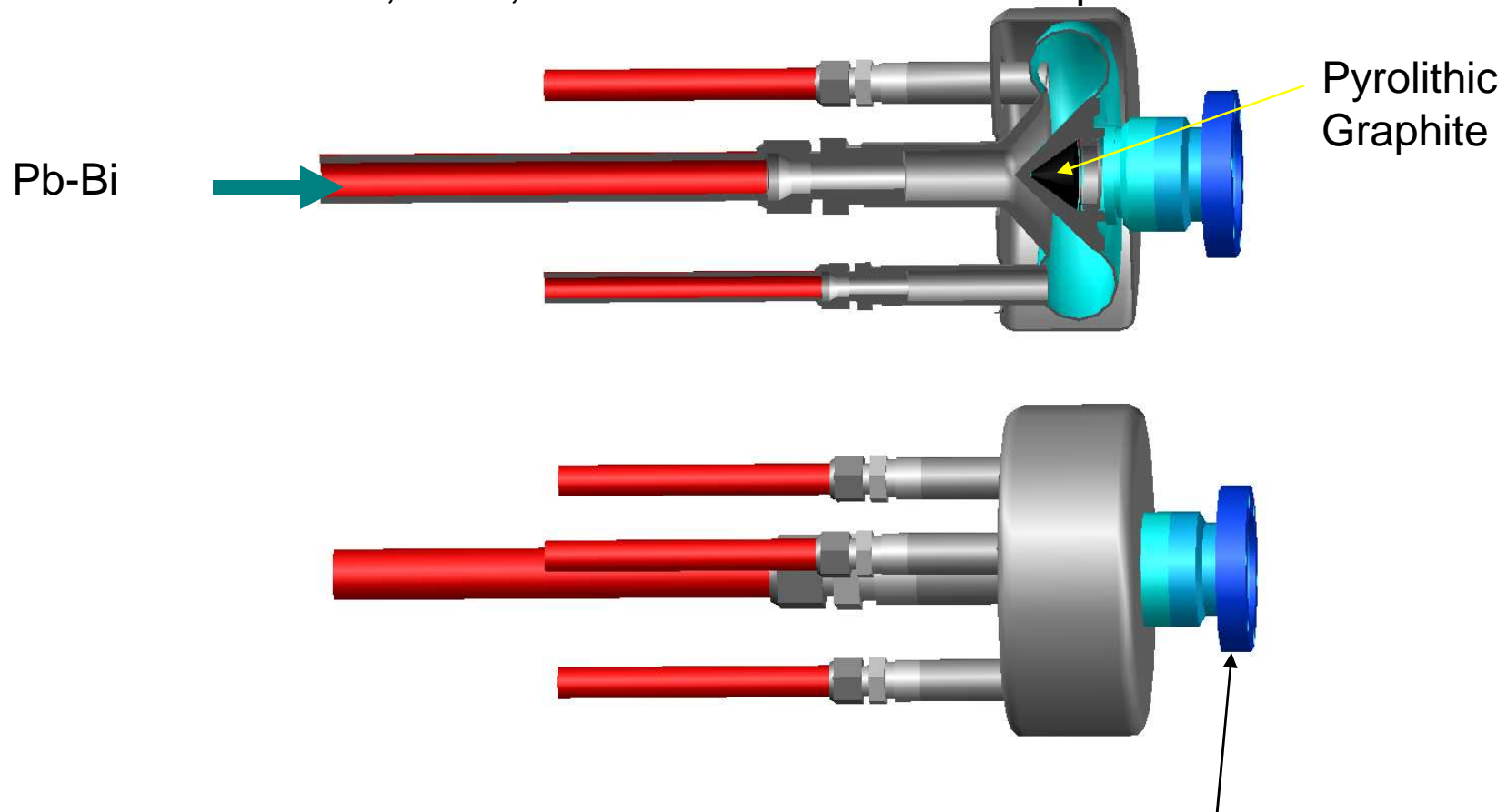
$$\dot{m} \cong \frac{E_{tot}}{\Delta T C_p} \cong \frac{2 \cdot 10^5}{20 \cdot 4.18 \cdot 10^3} \cong 2.4 L / sec$$

Threads help in thermal contact



Example of the beam dump proposed at Cornell for ERL

15 MeV beam, 0.1 A; Coolant-Pb-Bi in the first loop

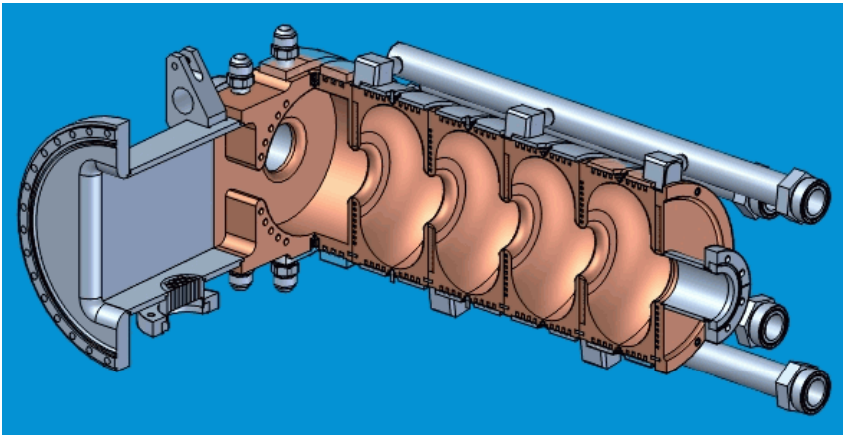


Cone keeps its shape while expanding. Diameter of the flange -4in

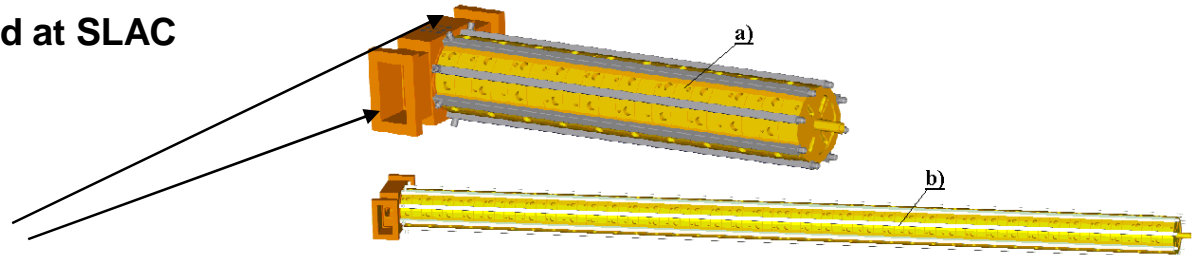
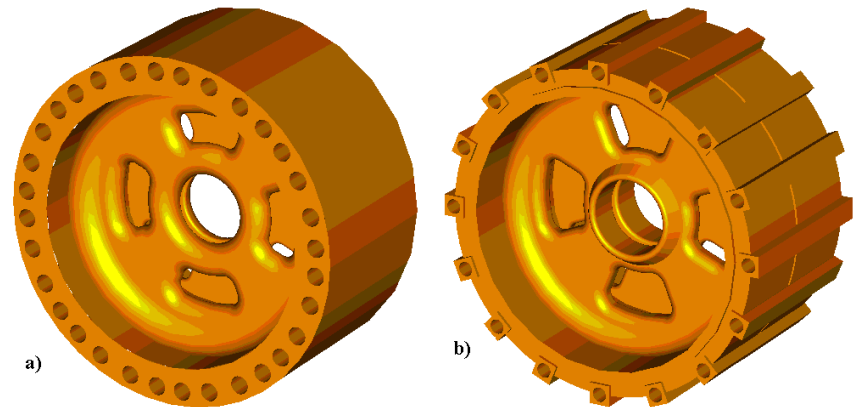
6. PRIMARY ACCELERATING STRUCTURE

RF STRUCTURES – SLAC and JNR (Dubna)

Structures located right after the target are working in strong solenoidal field (up to 3T)



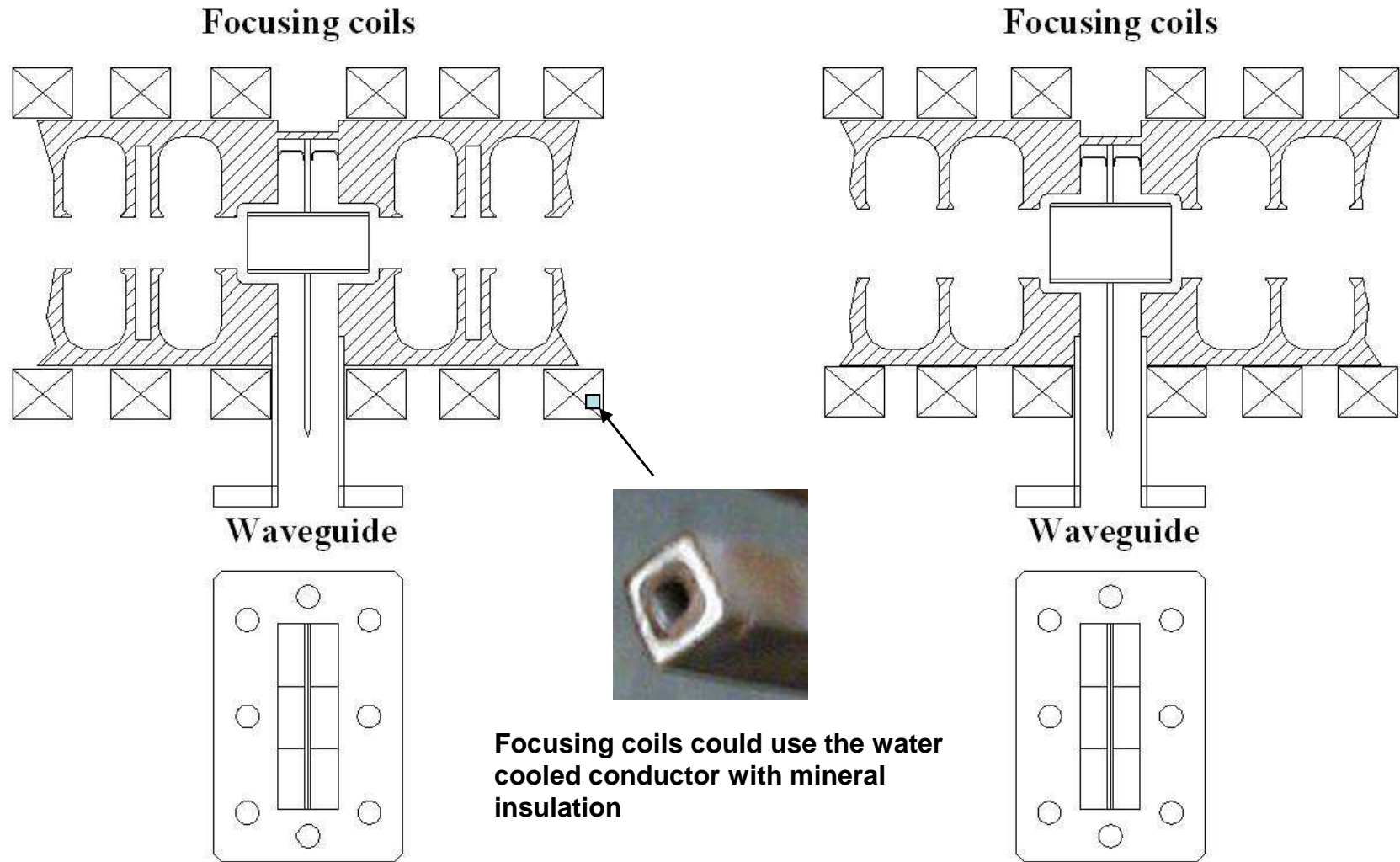
Accelerating structure, developed at SLAC



Symmetrical input at far from target end

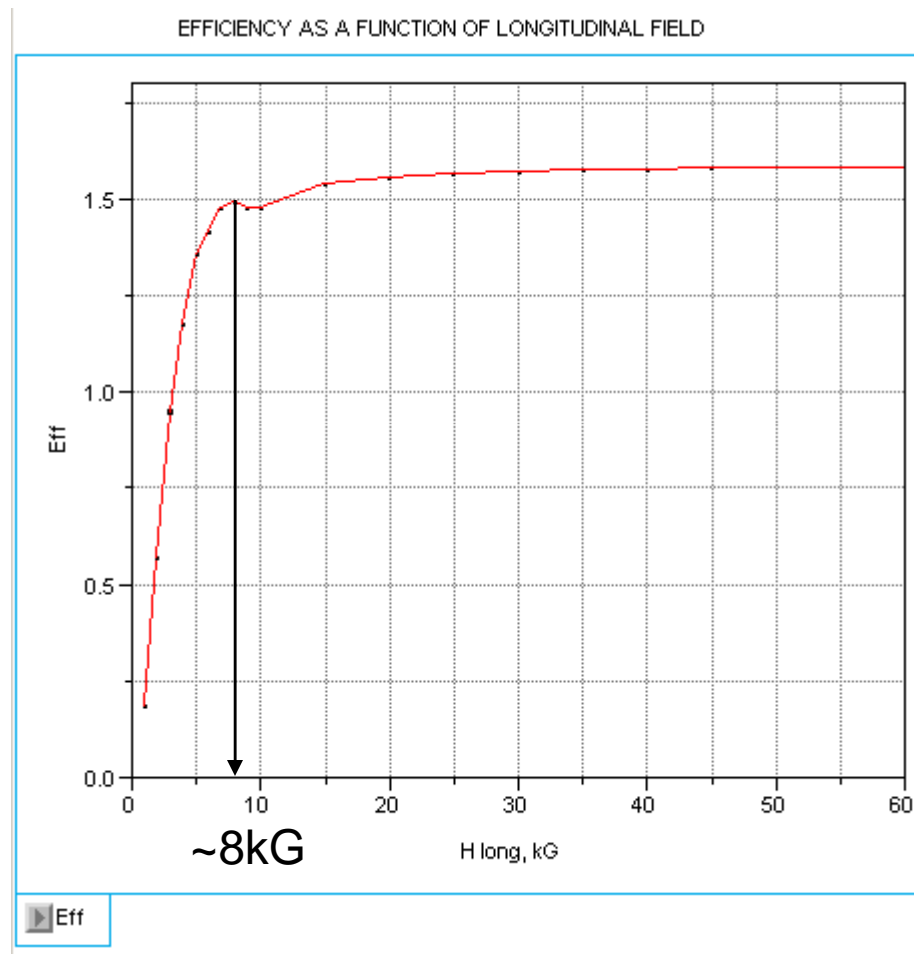
Accelerating structure developed at Dubna (under test in DESY), JINR a) –for high (19 MeV/m) gradient, b) –for moderate (8.5 MeV/m) gradient .

L.V. Kravchuk, V.A. Moiseev, A.N. Naboka, V.V. Paramonov, A.K. Skasyrskaja



Possible solutions for pulsed solenoids-longitudinal slit of structure or usage of Cu-StSteel bimetallic structure.

If all other parameters are kept fixed, then efficiency of conversion as a function of longitudinal magnetic field looks like:



Pretty moderate field indeed

7. EXPERIMENT E-166 AT SLAC

E-166:

Experimental test of polarized positron production
with gammas generated by high energy beam in
helical undulator

17 Institutions, 33 members

Just remind

$$E_{\gamma} \cong \frac{n \cdot 2.48 \cdot (\gamma / 10^5)^2}{\lambda_u [cm] (1 + K^2 + \gamma^2 \vartheta^2)} [MeV]$$

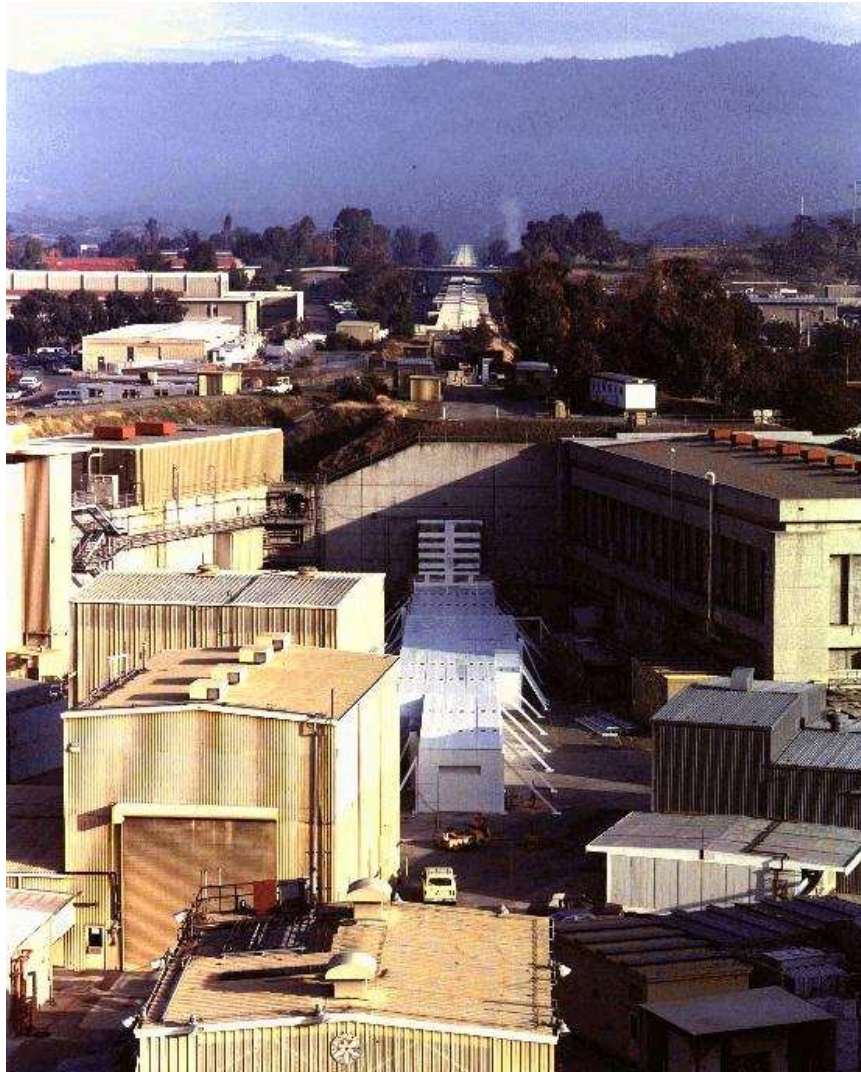
Goes to few mm period for 50 GeV beam

First suggested in 1992



Final Focus Test Beam (FFTB) → E166

First magnets delivered from Novosibirsk in 1991



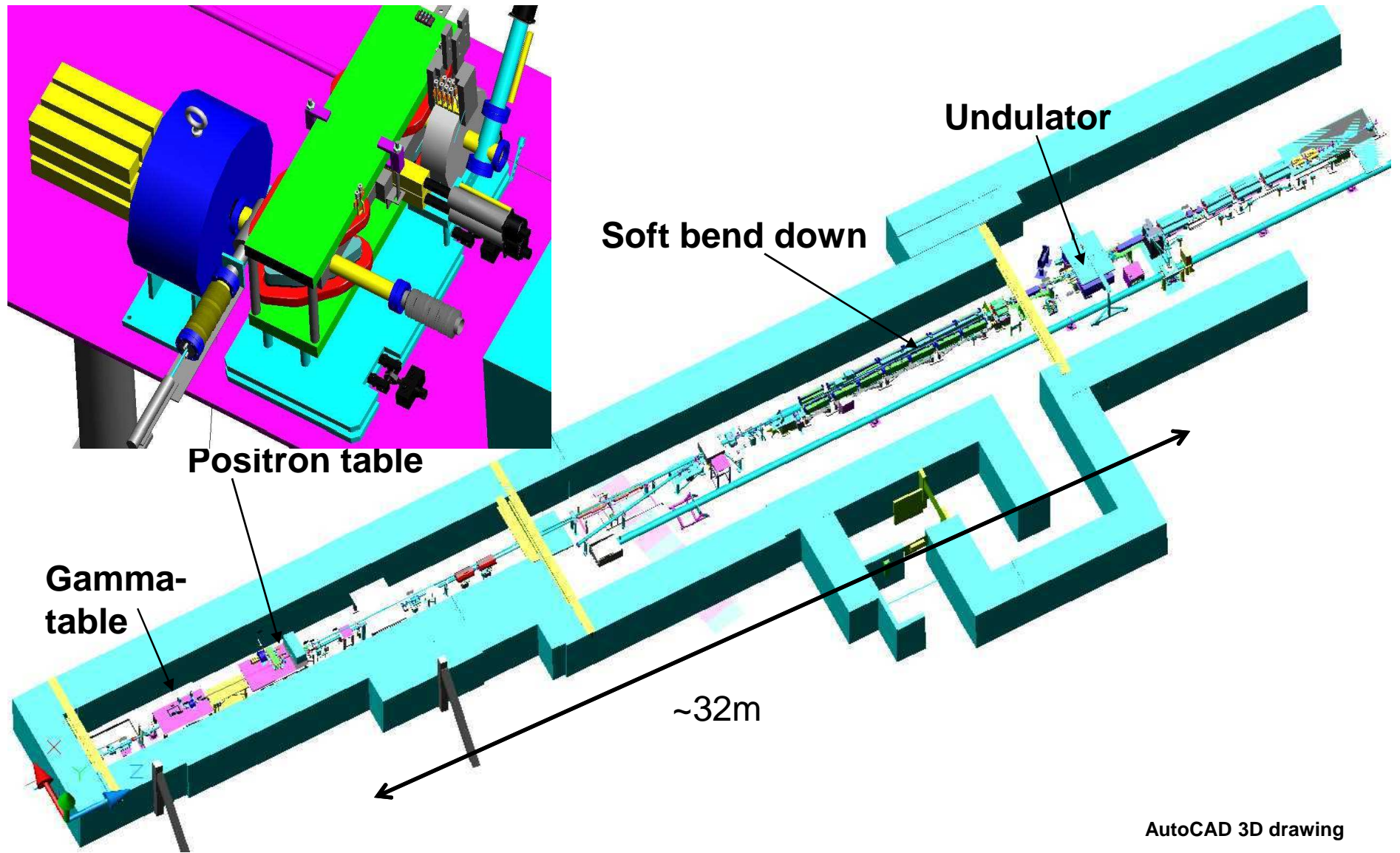
Demonstration of polarized e^+ production

FFTB at SLAC with 50 GeV, 2×10^{10} e^- /pulse, up to 30 Hz

1 m long helical undulator

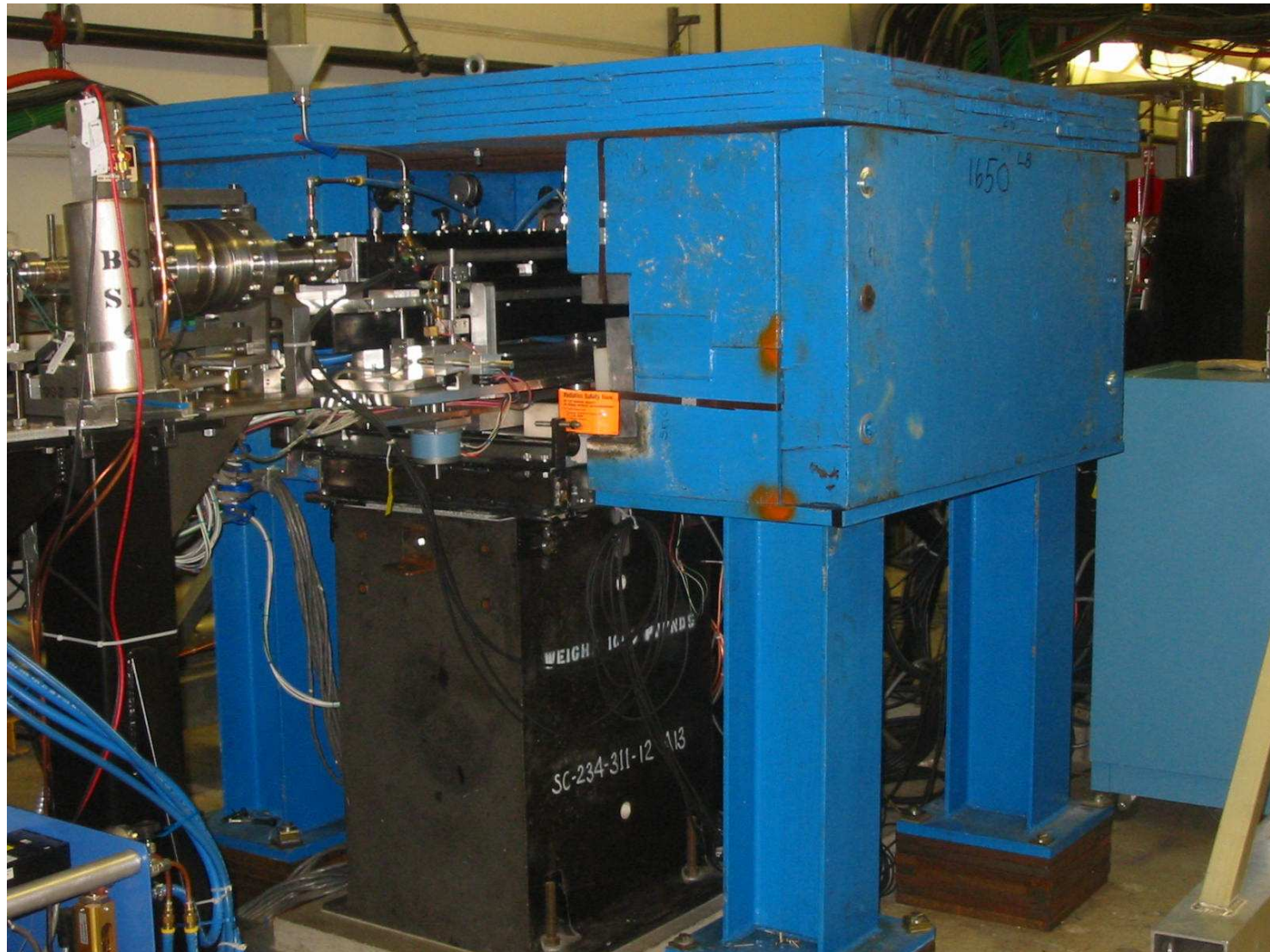
**Measurement of positron polarization by
Coverting Positrons into gamms again
and use Compton helicity-dependet
transmission attanuation**

3D scope of E-166



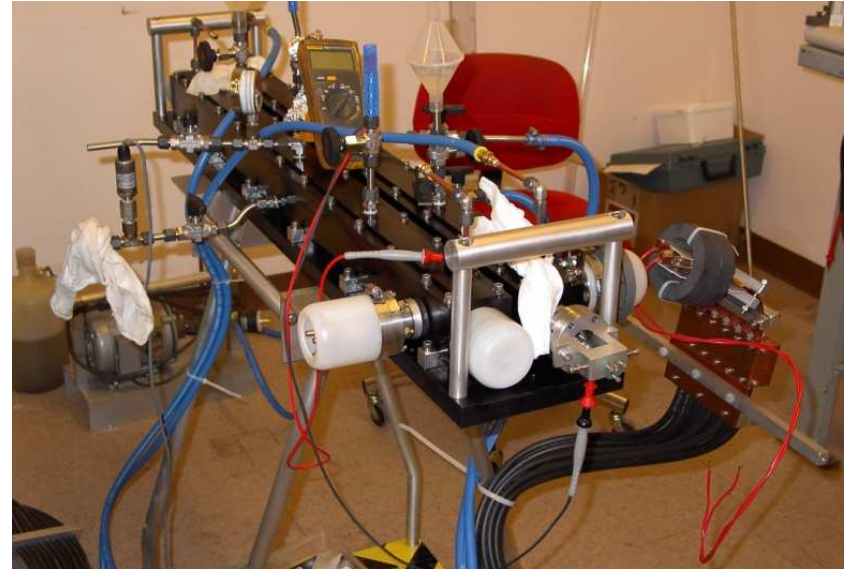
AutoCAD 3D drawing

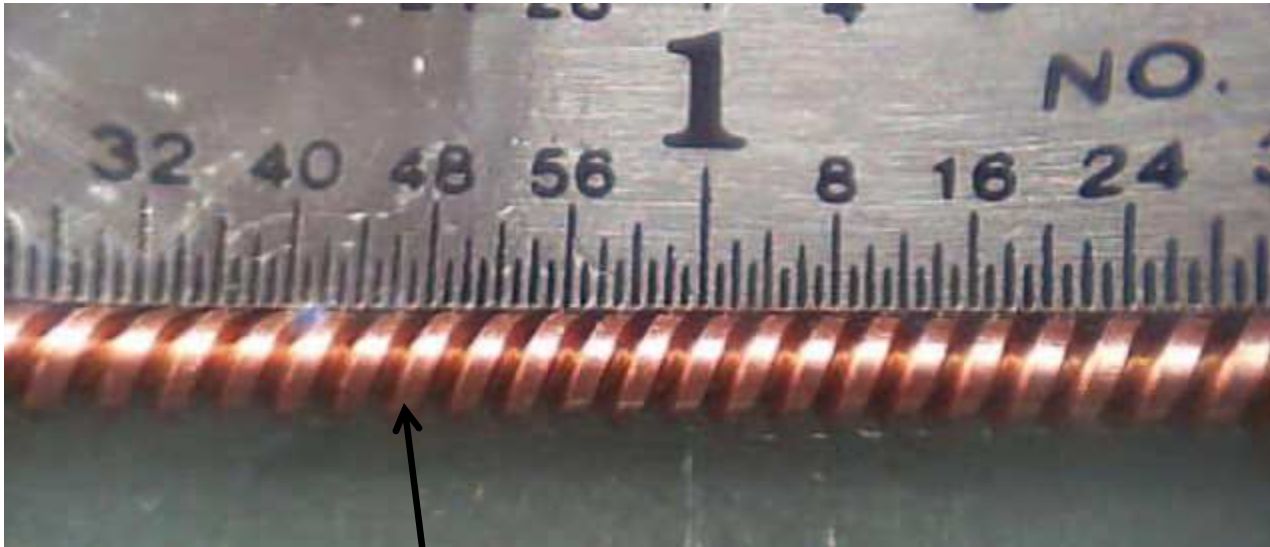
Undulator covered by local shielding



Helical undulator (Cornell)

Coolant-Oil, Ferrofluid

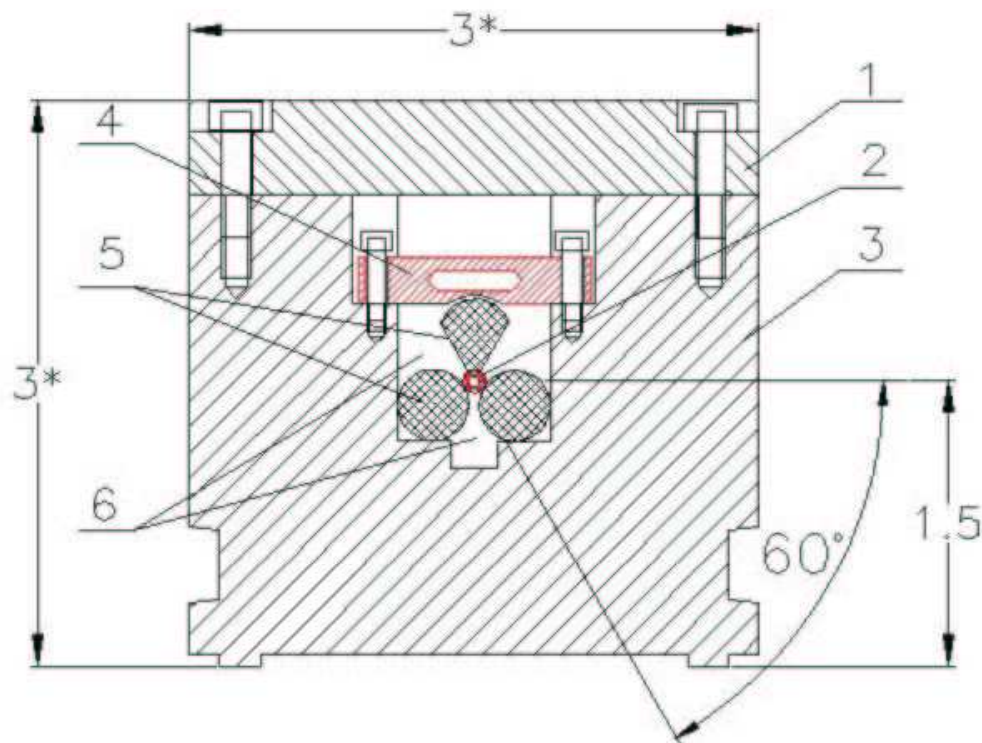




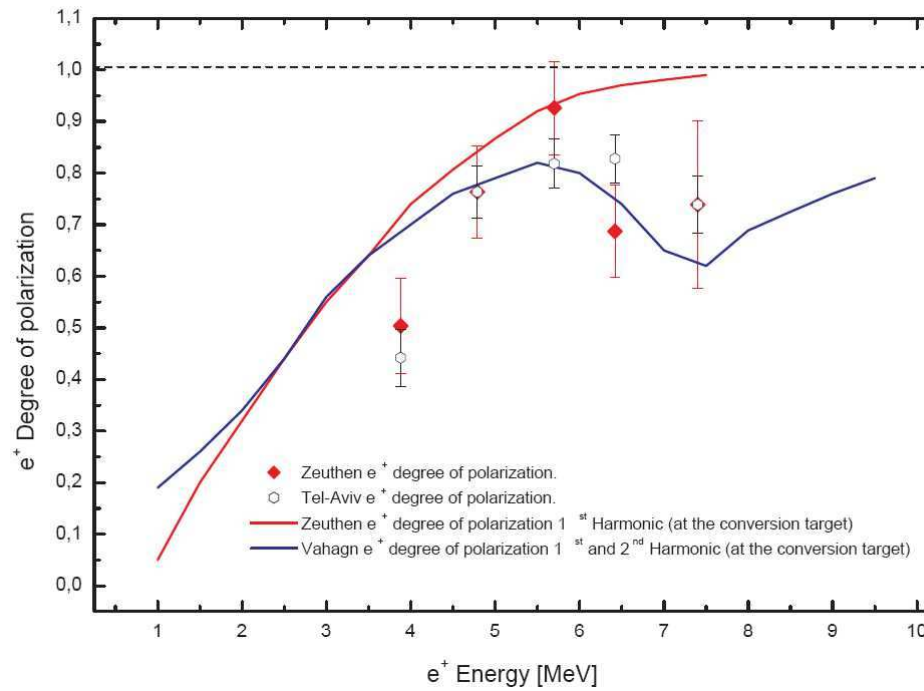
Scaled view on the undulator windings. Wire with rectangular cross-section has dimensions $0.6 \times 0.6 \text{ mm}^2$, period -2.54 mm.

Pulsed current up to 2.3 kA in a wire.

Smallest scale division is 1/64 of an inch.



Cross-section of undulator. Two G10 rods are placed in corners of long groove. Third rod with help of spring loading bars 4 compresses the windings to the other two. 1 -is a cover, 2 -is bi-helix. 3 -is a undulator mount, 5 -are G10 rods, 6 -is filled with coolant. Parts 1, 3 are made from Aluminum. Dimensions are given in inches. Undulator cover 1 is sealed with Indium gasket.

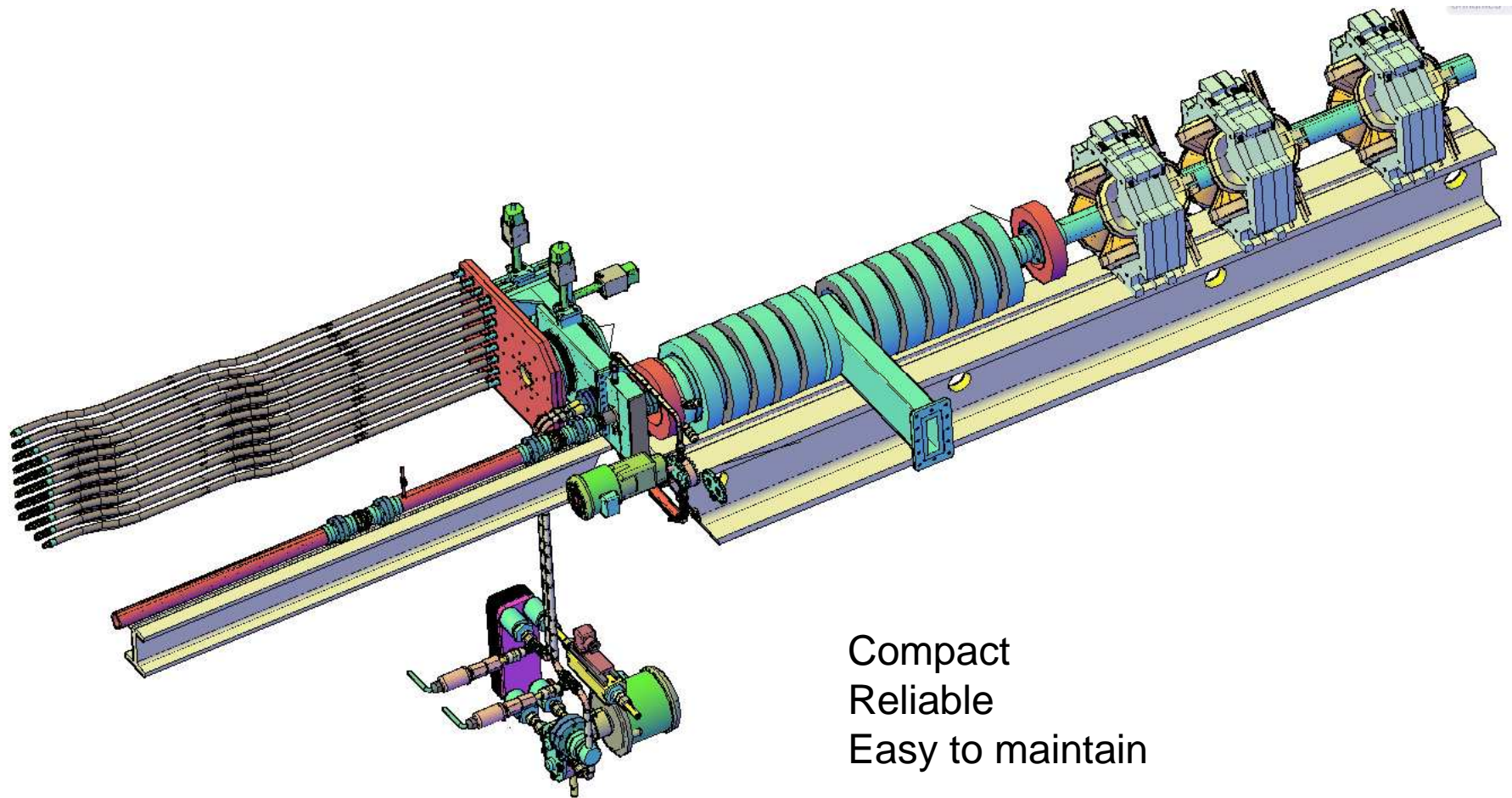


Degree of longitudinal polarization for positrons and electrons as measured by the E166 experiment.

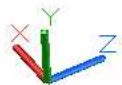
Results published in PRL, NIM

8.PERSPECTIVES

Conversion system with liquid Pb/Bi target and liquid Lithium lens

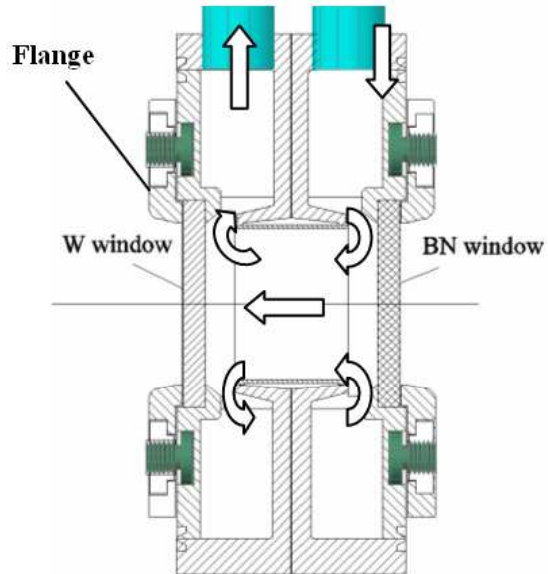


Compact
Reliable
Easy to maintain



COMBINED TARGET-COLLECTION SYSTEM FOR THE POSITRON PRODUCTION IN ILC,

A.Mikhailichenko, PAC11, THP076, NY 2011



Beam energy, GeV	100	150	250
Length of undulator, m	220	170	170
K factor	0.66	0.36	0.28
Period of undulator, cm	1	1	1
Distance to the target, m	200	350	600
Thick. of target/ X_0	0.55	0.57	0.6
Radius of lens, cm	0.6	0.6	0.6
Gradient, kG/cm	60	60	65
Length of the lens, cm	0.7	0.7	0.7
Current, kA	108	108	117
Radius of collimator, cm	0.2	0.5	0.15
Rad. of irises in RF, cm	3	3	3
Rad of coll. before RF, cm	2	2	2
Acceptance, MeVxcm	9	9	9
Energy filter $E>$, MeV	51	54	63
Energy filter $E<$, MeV	110	110	180
ΔT per train $10^{13} e^-$, °C	172	139	270
ΔT in lens from beam, °C	18	35	80
ΔT in lens from current, °C	90	90	100
Efficiency, e^+/e^-	1.52	1.57	1.52
Polarization, %	54	57	64

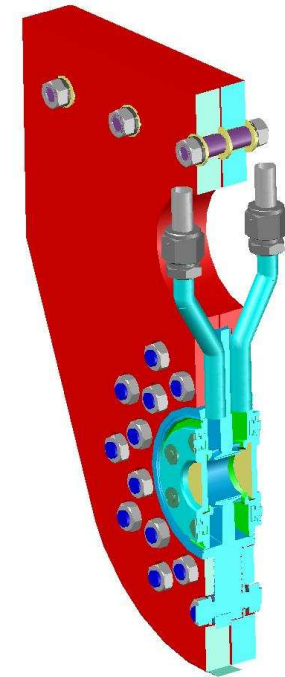
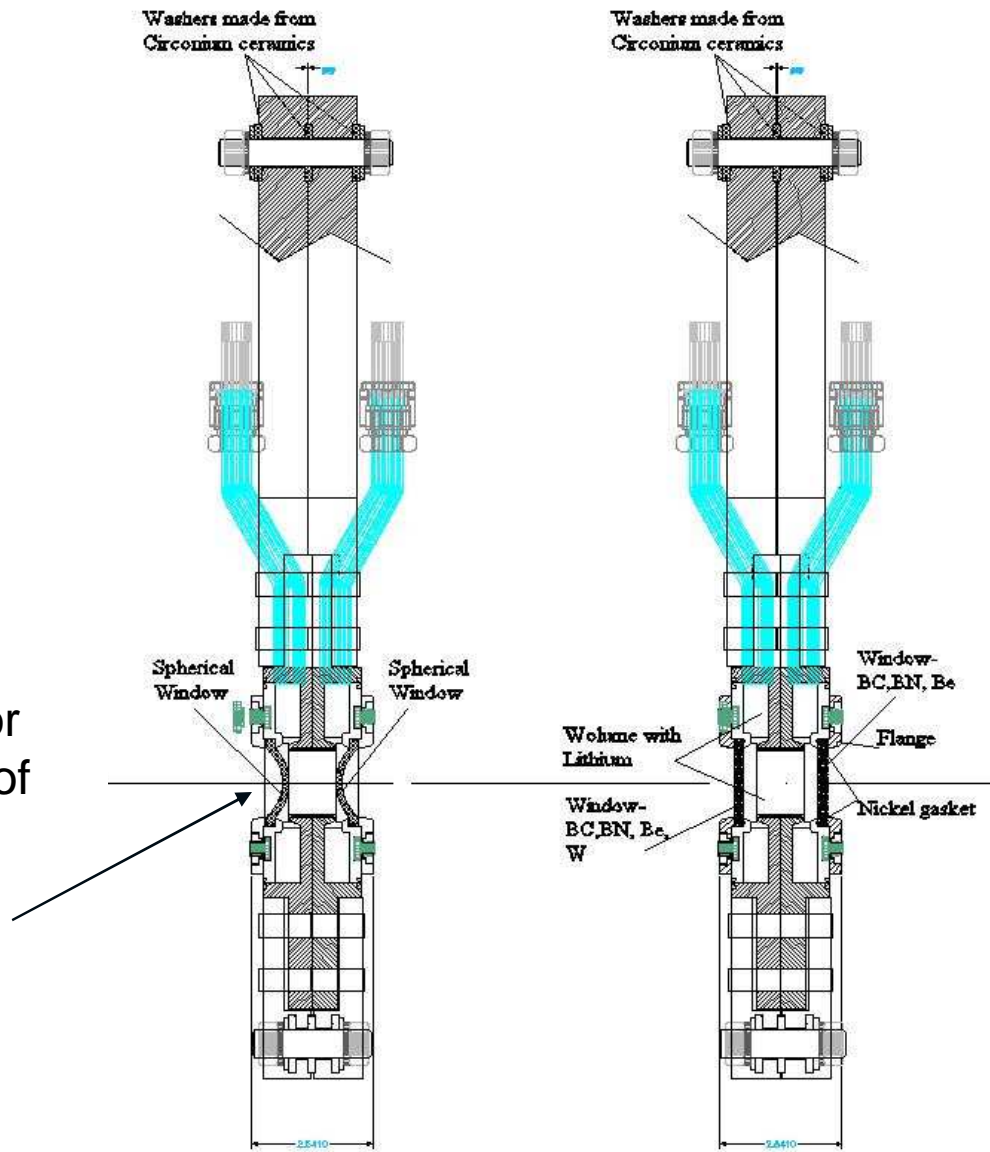
9. SUMMARY

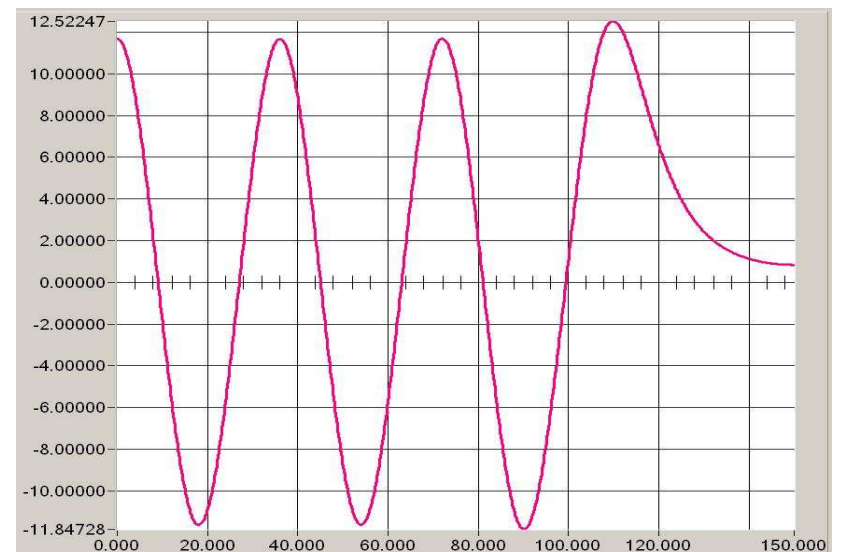
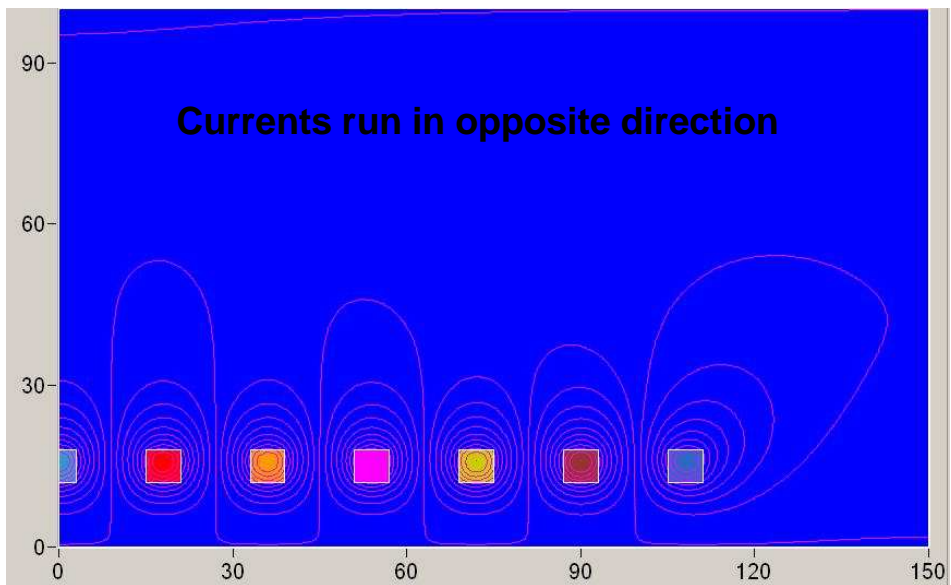
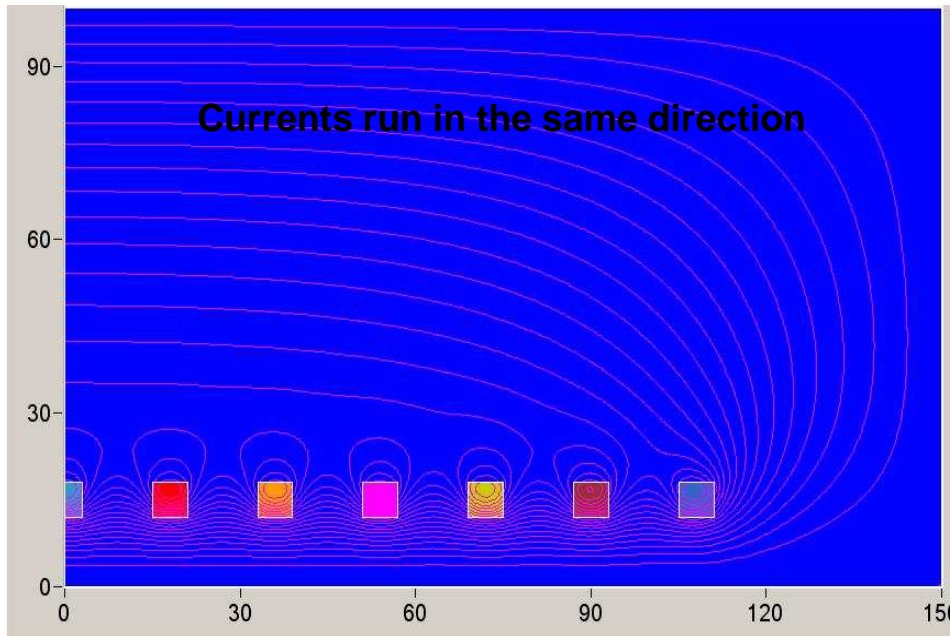
- **Liquid metals have wide area for application in ILC positron source**
- Start to end Monte-Carlo simulation code for conversion -KONN confirmed that low K factor is possible with focusing by Li lens; $K < 0.4$ –big relief for the conversion system
- Utilization of Lithium lens allows Tungsten survival under condition required by ILC with $N_e \sim 2 \times 10^{10}$ with moderate $K \sim 0.3-0.4$. Thin W target allows better functioning of collection optics (less depth of focusing).
- Lithium lens is well developed technique and the lens with parameters required for ILC is guaranteed.
- Field is strictly limited by the surface of the lens from the target side.
- Liquid metal target allows compact design and stability under dynamical load; could compete with spinning rim target.
- Combined Lithium lens with W flange can work for ILC; for CLIC all parameters are relaxed.
- E-166 confirmed the polarization $\sim 80\%$ achievable with undulator-based positron production scheme for ILC

END

Backup slides

Can be used for compensation of spherical aberrations





Current density $\sim 130\text{A/mm}^2$; coil cross section is $6\text{x}6\text{cm}^2$ Field in kG

Laser bunch as an undulator

The number of the quantas radiated by an electron by scattering on photons - real from the laser or virtual from the undulator:

$$N_\gamma \cong 4\pi\alpha \frac{L}{\lambda_u} \frac{K^2}{1+K^2} = 4\pi \frac{e^2}{\hbar c} \frac{L}{\lambda_u} \left(\frac{eH\lambda_u}{2\pi mc^2} \right)^2 \approx \left(\frac{e^2}{mc^2} \right)^2 \frac{L\lambda_u}{2\pi\hbar c} H^2 \cong r_0^2 L \frac{H^2}{\hbar\Omega} \cong \sigma_\gamma n_\gamma L$$

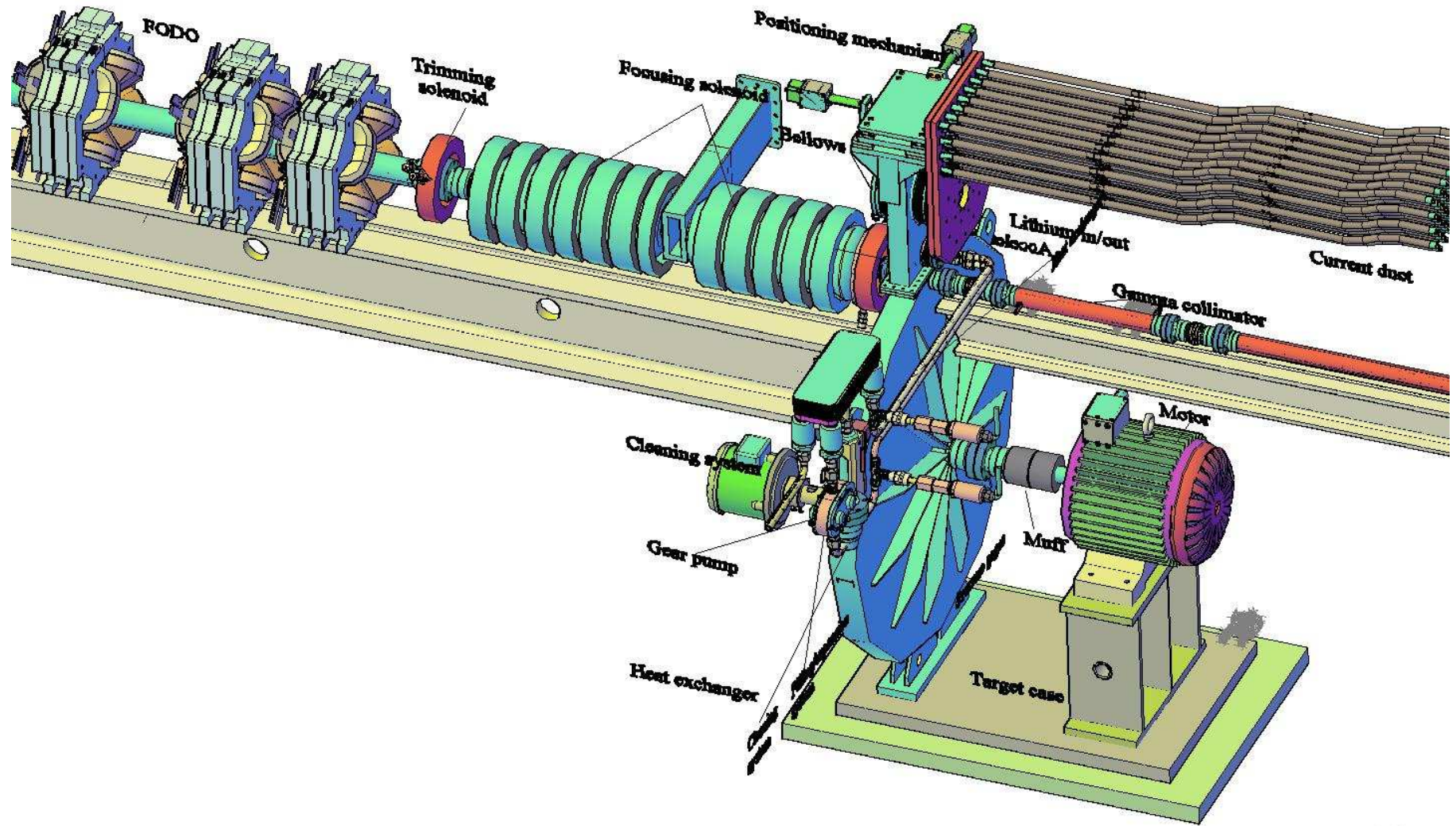
$$K = eH\lambda_u / 2\pi mc^2 \cong 0.934 \cdot H[T] \cdot \lambda_u[cm] \quad K = \beta_\perp \gamma \quad \sigma_\gamma \cong \pi r_0^2 \quad n_\gamma \cong \frac{H^2}{\hbar\Omega} \quad \Omega = \frac{2\pi c}{\lambda_u}$$

Formation length in undulator $l_f \cong \lambda_u$ L - length of undulator

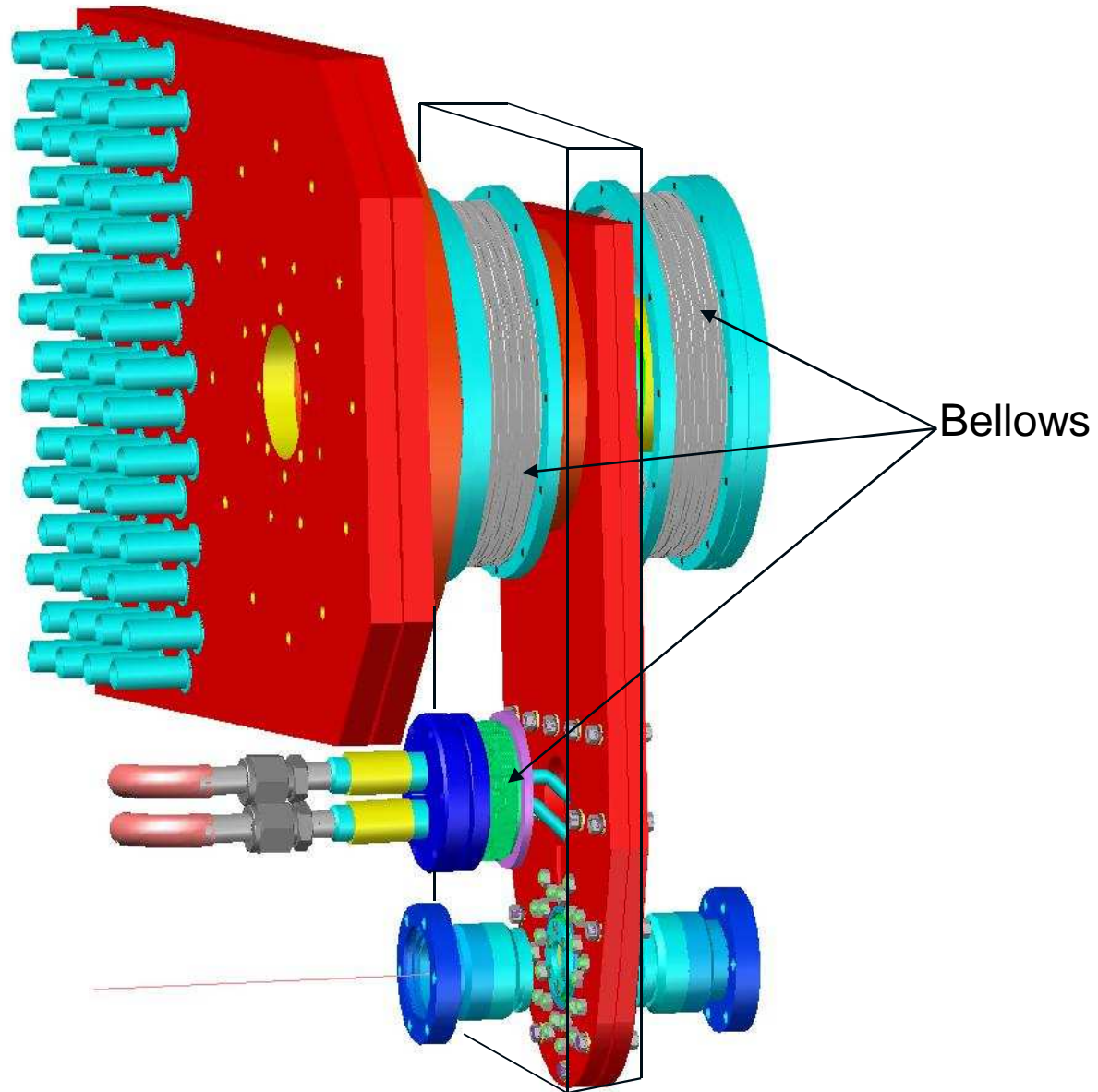
$$N_\gamma \cong L / \sigma_\gamma n_\gamma = L / l_\gamma \quad l_\gamma \cong 1 / \sigma_\gamma n_\gamma \quad \text{-- Length of interaction}$$

Written in this form it is clear that the photon back scattering (especially with 90° crossing angle) is an equivalent of radiation in an undulator (as soon as the photon energy is much less, than the energy of particle).

The ILC conversion system with rotating target and the liquid Lithium lens.

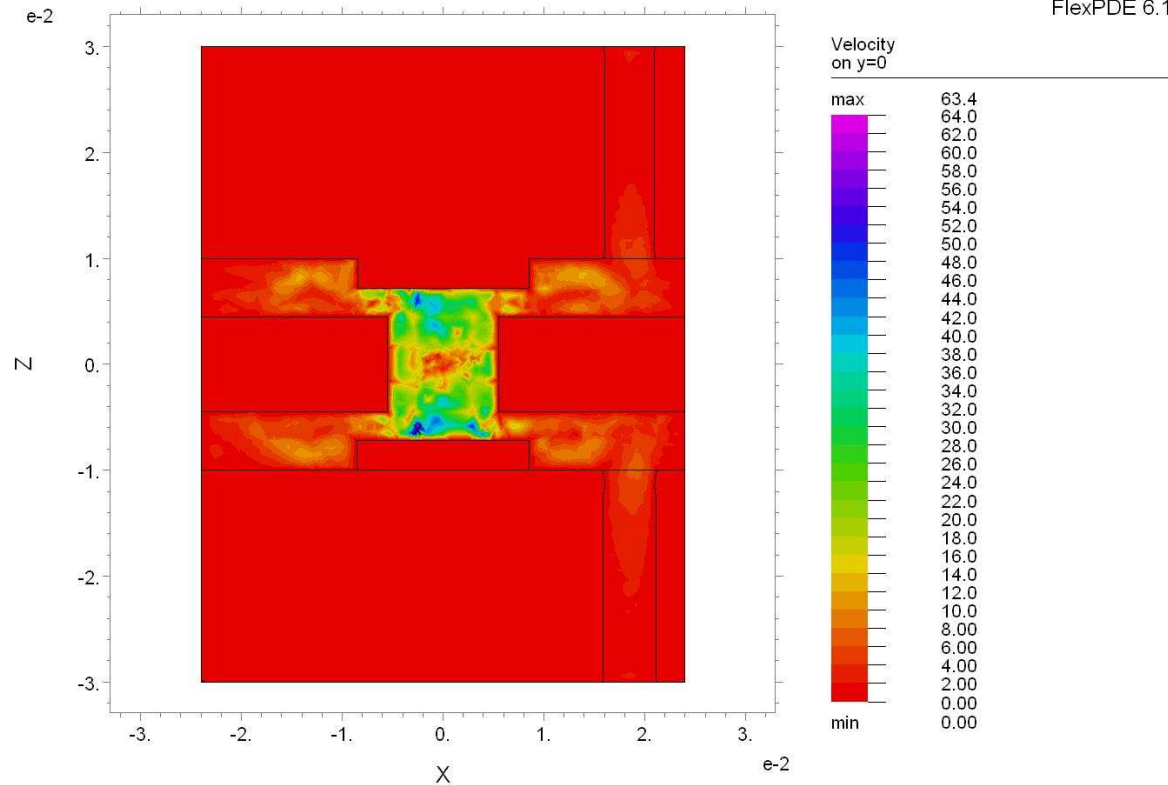


Scaled view on vacuumed feed through and lens; vacuum case not shown



Lithium Lens with Viscous Flow-3

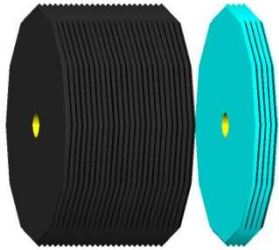
12:10:50 1/25/10
FlexPDE 6.11



Viscose flow Jan 28 2010: Cycle=205 Time= 2.3000e-3 dt= 1.0225e-5 P2 Nodes=39225 Cells=27733 RMS Err= 0.0609
Reynolds number max= 829.9611 Integral= 5.512972e-3

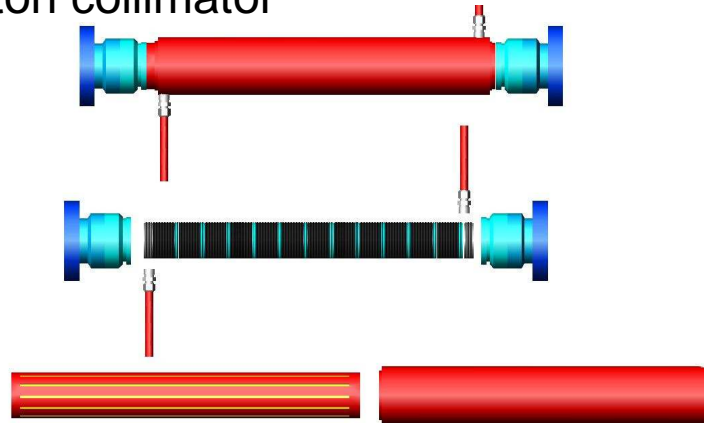
Velocity contour painted. One can see slight asymmetry induced by systematic flow. Turbulence pretty manifested.

Gamma collimator and gamma absorber (cont.)

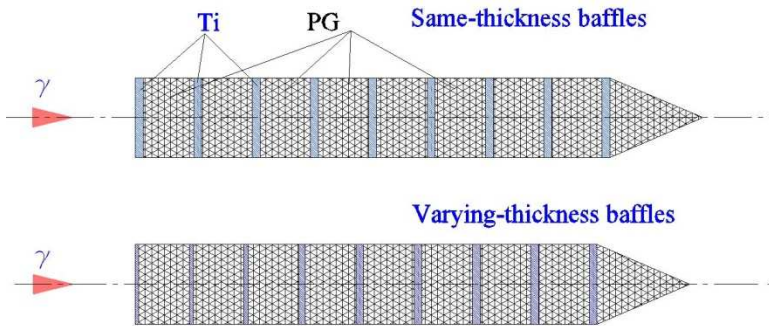
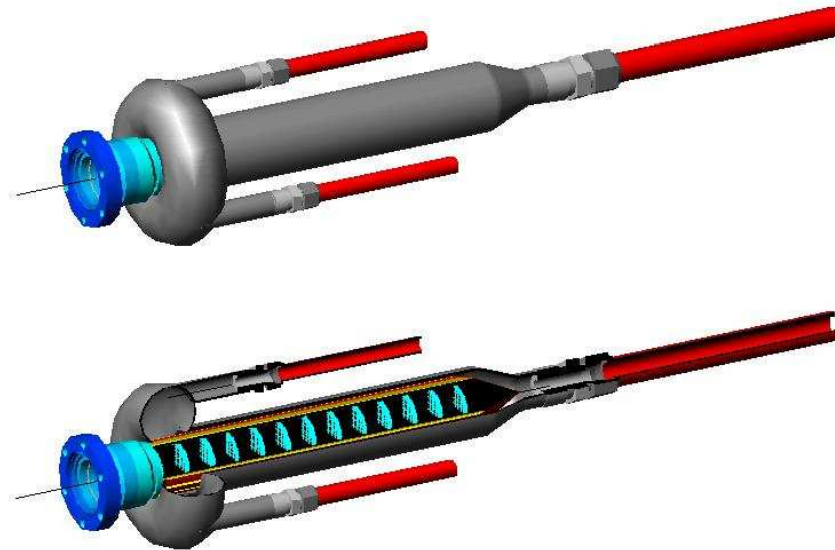


PG and Ti spoilers

Photon collimator



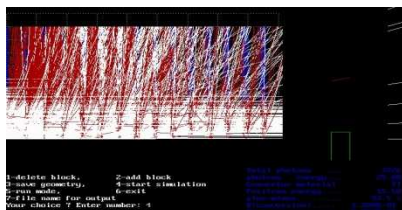
Photon beam absorber



Ti -Titanium

PG-Pyrolytic Graphite with transversely oriented A plane

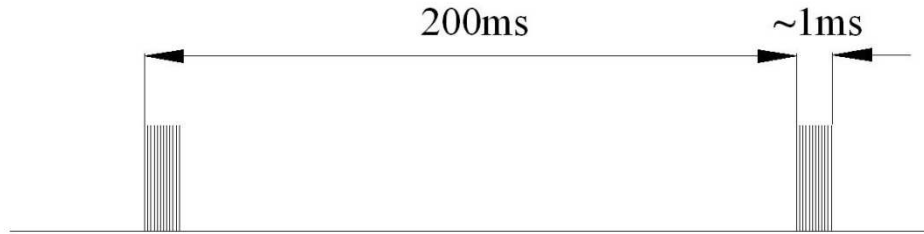
Spoilers with different thickness



Modeling

For ERL Ti spoilers not required

Beam pattern



Equation for thermal diffusion in window

$$\nabla(k\nabla T) + \dot{Q} = \rho c_V \dot{T}$$

defines time of relaxation from its characteristic

For Be: $k=2 \text{ W/cm}^\circ\text{K}$, $\rho=1.84\text{g/cm}^3$, $c_V=1.82 \text{ J/g}^\circ\text{K}$

$$\frac{dx^2}{dt} = \frac{k}{\rho c_V} \rightarrow \delta^2 = \frac{k}{\rho c_V} \tau \rightarrow \tau = \frac{\rho c_V}{k} \delta^2$$

If $\delta=0.05\text{cm}$

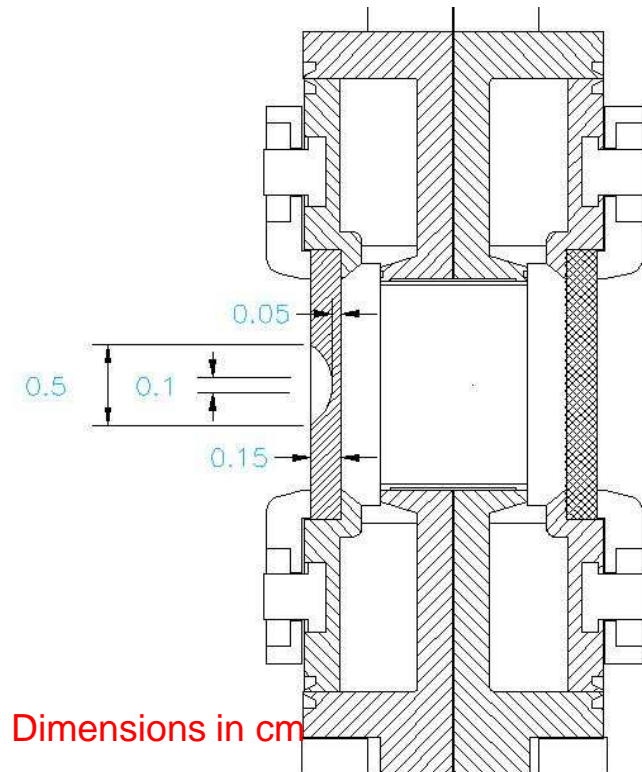
$$\tau = \frac{1.84 \cdot 1.82}{2} 2.5 \cdot 10^{-3} \cong 4.2\text{ms}$$

This gives ~20% temperature drop within train for Be

For Li thermal skin-layer for 1 msec time goes to

$$\delta = \sqrt{\frac{k}{\rho c_V} \tau} = \sqrt{\frac{0.848}{0.533 \times 3.6} 0.001} = 0.021\text{cm}$$

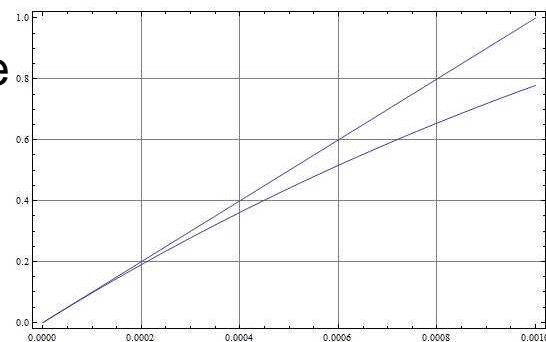
Flange with recession has faster relaxation time



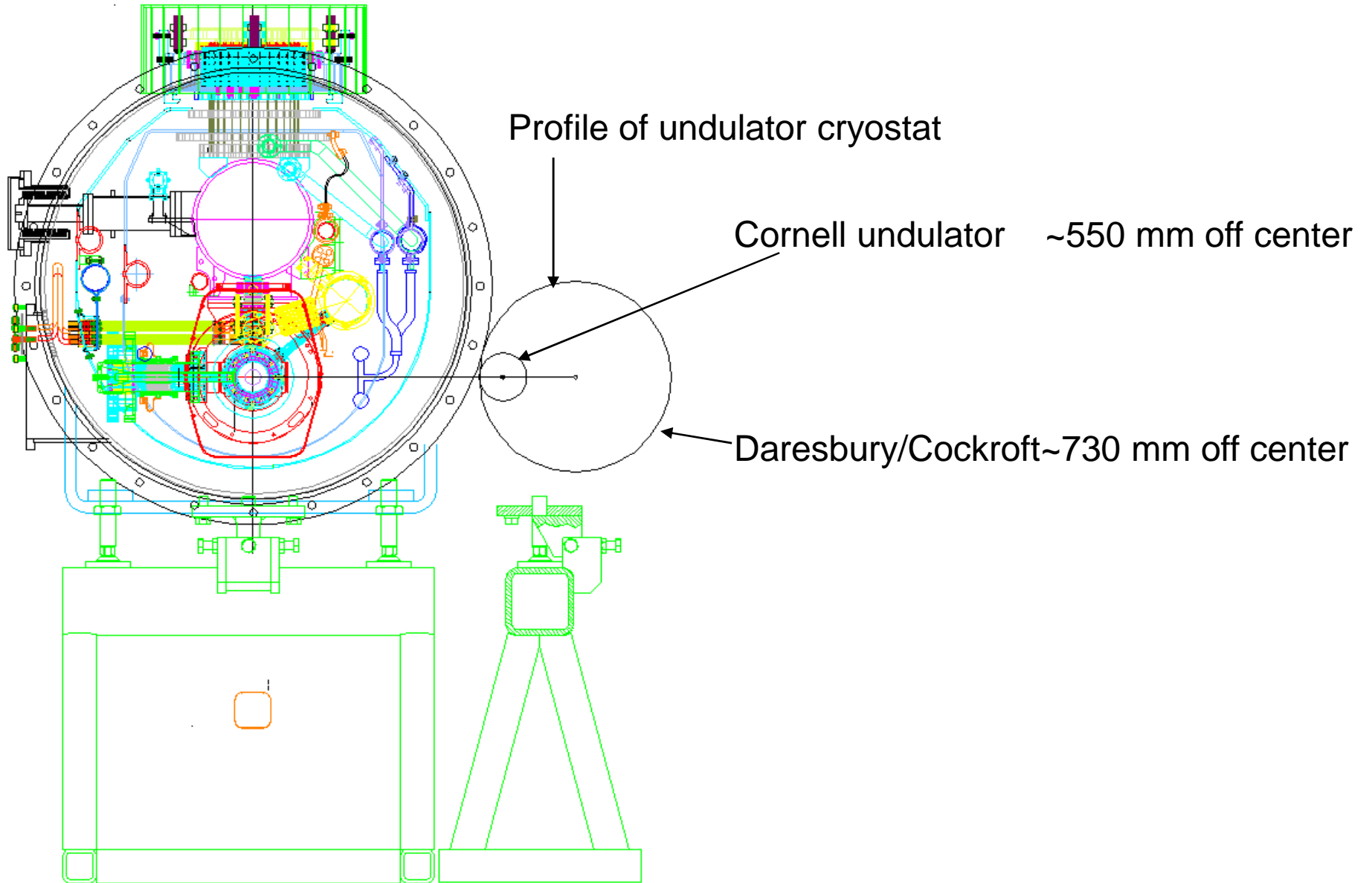
```

τ = 0.001
m = 4.
Plot[ $\frac{T}{T_0} = e^{-\frac{t}{\tau}}$ , {t, 0, τ}, Frame → True, GridLines → Automatic]
Plot[ $\frac{T}{T_0}$ , {t, 0, τ}, Frame → True, GridLines → Automatic]
Show[%, %]

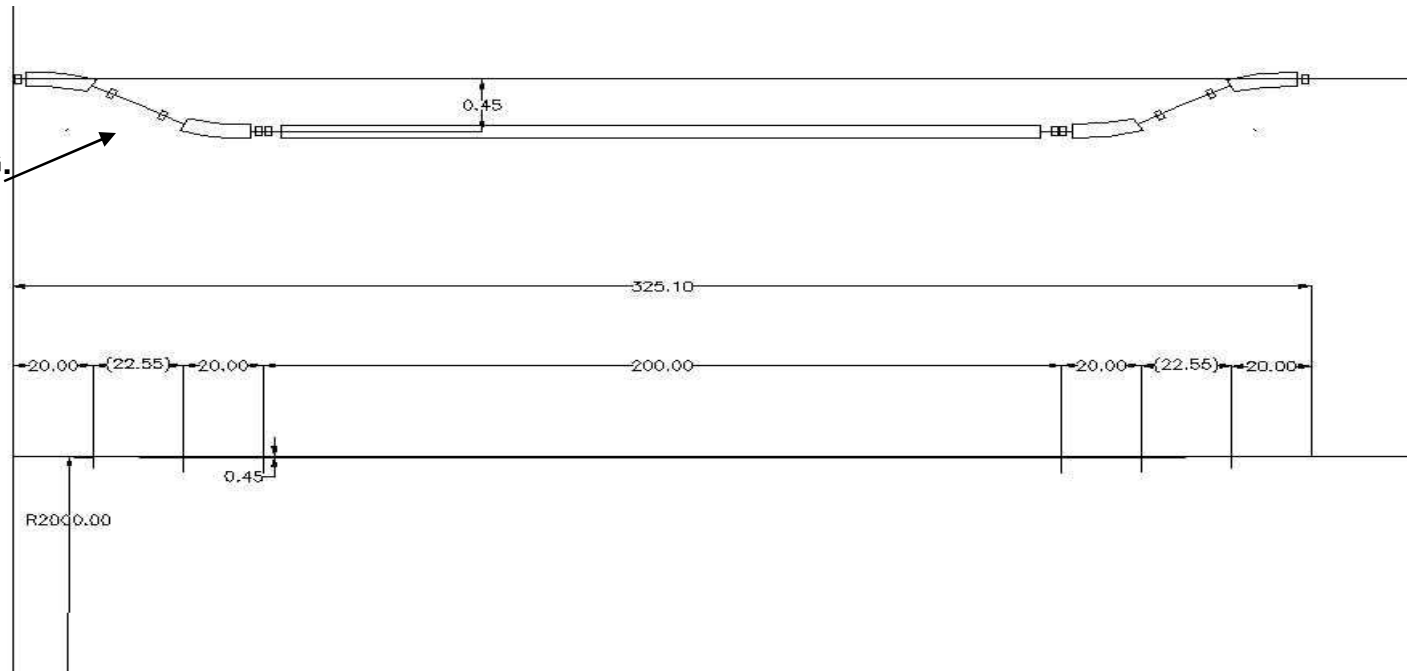
```



WHAT IS THE MINIMAL SPACING?



V.V. Vladimirsky, D.G.
Koshkarev, 1958



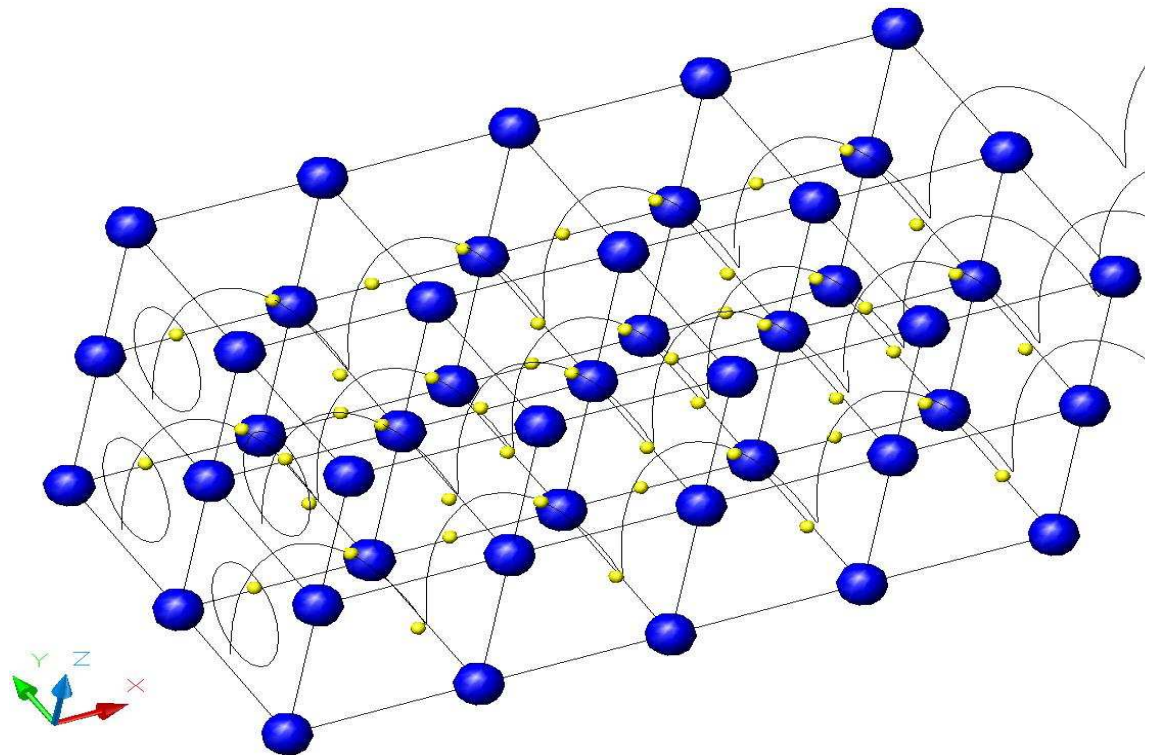
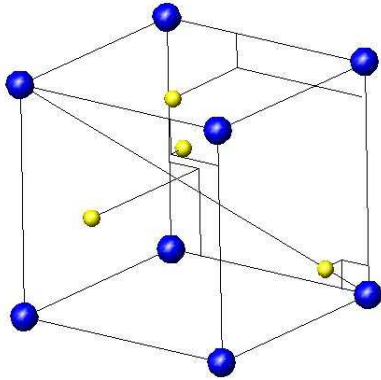
Very high density of SR in any bending magnet, as emittance is extremely small

T.A.Vsevoljskaya, A.A.Mikhailichenko, G.I Silvestrov, A.N. Cherniakin, “*To the Project of Conversion System for Obtaining Polarized Beams at VLEPP Complex*”, internal report BINP, Novosibirsk, 1986.

Helical (chiral) crystals

Crystal structure MnSi and FeGe

P.Bak, M.H.Jensen, J.Phys.C: Solid St.Physics, 13,(1980) L881-5

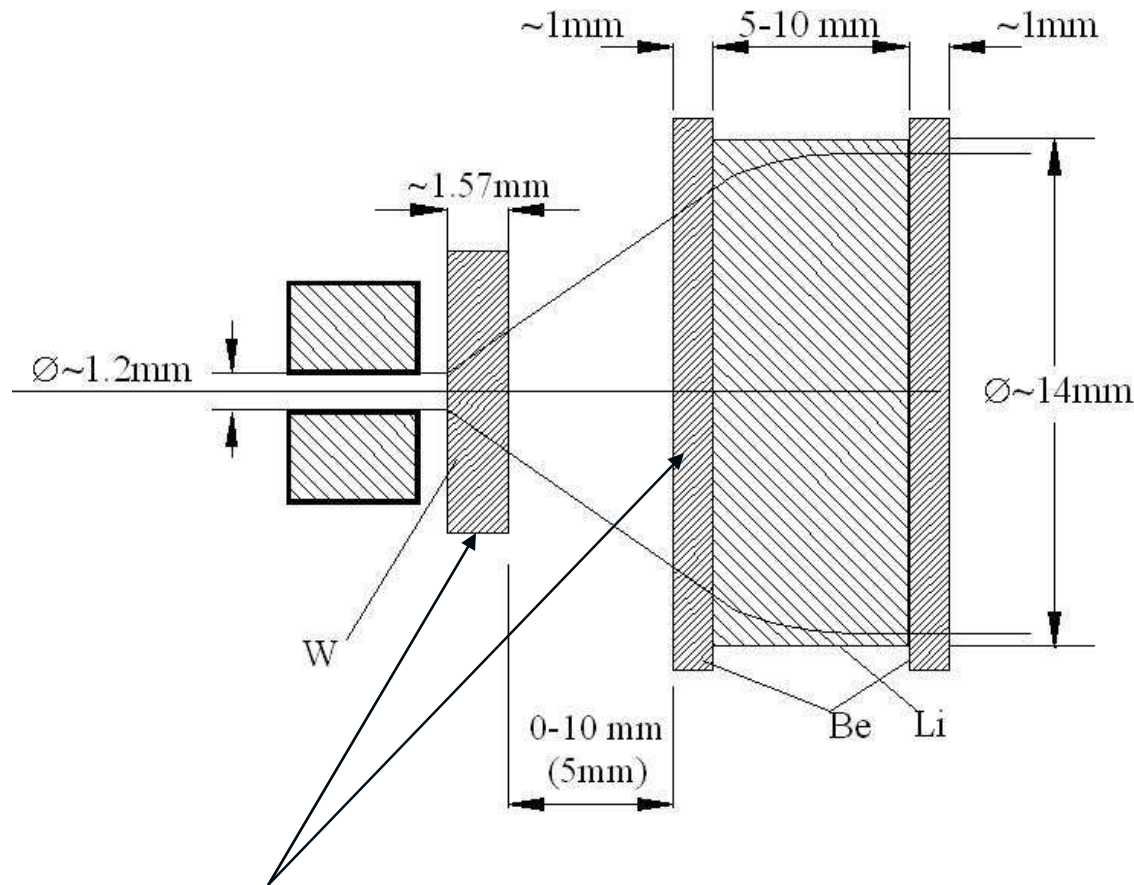


Helical structure demonstrates also CsCuCl_3 , $\text{Ba}_2\text{CuGe}_2\text{O}_7$, MnS_2

KONN –Monte-Carlo code for positron production starting from undulator

KONN can calculate now the energy deposition and temperature rise in target and in Li lens at any point.

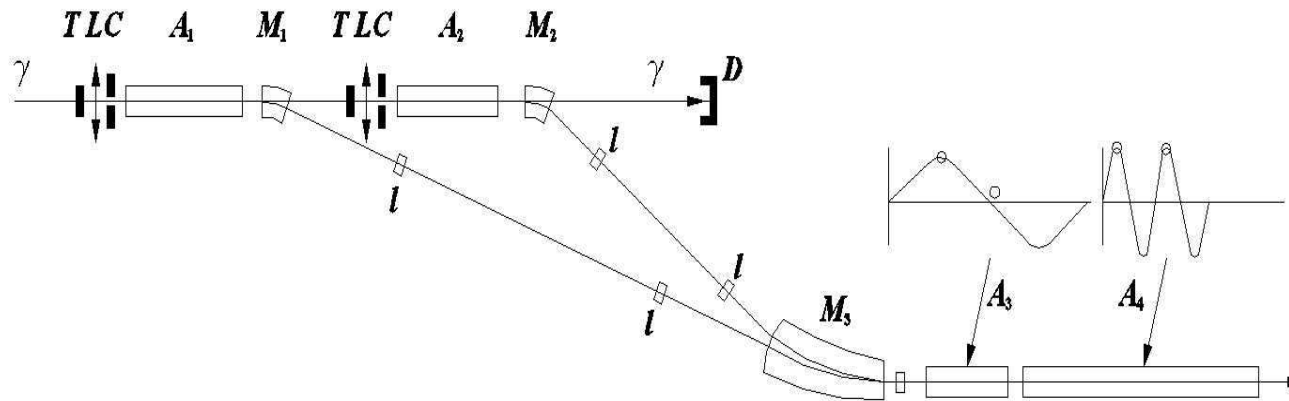
Distance between target and the lens serves for enlargement the spot size on the entrance



← Typical parameters

Target could be combined with entrance flange

COMBINING SCHEME



Energy provided by acceleration structures A_1 and A_2 are slightly different, $A_1 > A_2$.

After the first target only 13% of photons are lost. So it is possible to install second target and collect positrons from this second target.

Combining in longitudinal phase space could be arranged easily in the same RF separatrix in damping ring.

Additional feed back system required for fast dump of coherent motion.

Combining scheme allows ~double positron yield and cut in half the length of undulator → increase of polarization

TESTED UNDULATORS

**For aperture available for the beam 8 mm in Ø clear
OFC vacuum chamber, RF smoothness**

SC wire	54 filaments	56 filaments	56 filaments	56 filaments
# layers	5	6	11	9 (12) +sectioning
$\lambda=10$ mm @300°K	K=0.36 tested	K=0.42 tested	K=0.467 tested	K≈0.5 (calculated)
$\lambda=12$ mm @300°K	K=0.72 tested	K=0.83 tested		K≈1 (calculated)

**For aperture available for the beam 6.35 mm (1/4") in Ø clear
OFC vacuum chamber, RF smoothness**

# layers	11			12+sectioning
$\lambda=13.5$ mm @300°K	K=1.48 tested			K≈1.6 calculated
$\lambda=10.0$ mm @300°K	K≈0.7calculated			K≈0.72 calculated